UNIVERSITÀ DI PISA

Department of Information Engineering

Master's Thesis in Telecommunication Engineering

Design and implementation of a software predistorter for amplifier linearization in OFDM-based SDR systems

Candidate:

Emanuele Tolomei

Supervisors:

Prof. Filippo Giannetti

Ing. Vincenzo Pellegrini

Anno Accademico: 2015/2016

ACRONYMS AND ABBREVIATIONS

In the present dissertation, the following abbreviations are applied:

ACPR	Adjacent Channel Power Ratio
AM	Amplitude Modulation
AM-AM	Amplitude-to-Amplitude distortion
AM-PM	Amplitude-to-Phase distortion
AWGN	Additive White Gaussian Noise
BER	Bit Error Rate
DAC	Digital to Analog Converter
DSP	Digital Signal Processor
DVB-T	Digital Video Broadcasting – Terrestrial
EER	Envelope Elimination and Restoration
EVM	Error Vector Magnitude
FFT	Fast Fourier Transform
FPGA	Field Programmable Gate Array
HPA	High Power Amplifier
IBO	Input Backoff
IF	Intermediate Frequency
IFFT	Inverse Fast Fourier Transform
IMD	Intermodulation Product
LINC	Linear amplification using non-linear components
LUT	Lookup Table
MER	Modulation Error Rate
MPM	Memory Polynomial Model
OBO	Output Backoff
OFDM	Orthogonal Frequency Division Multiplexing
PA	Power Amplifier
PAPR	Peak to Average Power Ratio
PDF	Probability Density Function
PGA	Programmable Gain Amplifier

PM	Phase Modulation
PSD	Power Spectral Density
QAM	Quadrature Amplitude Modulation
QPSK	Quadrature Phase Shift Keying
RF	Radio Frequency
SDR	Software Defined Radio
SNR	Signal to Noise Ratio
SSPA	Solid State Power Amplifier
TWT	Travelling Wave Tube

CONTENTS

1 INTRODUCTION

In modern wireless communication systems, an important role is played by the amplifier in the RF transmitter. It controls the maximum distance covered, the battery consumption for mobile devices, heating, etc. Nowadays RF transmitter has a lot of uses, starting from old FM stations, and arriving, in the recent period, to piloting of drones. Simplifying as much as possible, what this device accomplishes is to convert the baseband signal containing the data to be transmitted into a radio frequency signal able to travel through the ether. This can be done directly, or in two distinct phases before passing to an intermediate frequency (IF). In both cases, the signal after conversion must be amplified with a power amplifier and then transmitted on the channel.

This thesis will focus on the amplifier part of the transmitter. In particular, existing predistortion techniques, used to improve the linearity of the power amplifier, and a software, non-real time, predistorter developed for the thesis will be described.

1.1 OUTLOOK OF THIS THESIS

The RF transmitter has, as written before, a lot of applications. One possible application for the present thesis is the particular case where we have to develop the link between a drone (UAV) and its ground station. In these links, the most important result to achieve is to improve the maximum attenuation the signal can tolerate before the link breaks. This means both improving the distance that the drone can cover without losing signal from the ground station and strengthening the link from interferences or bad weather conditions. To obtain this, we can examine the link budget equation which defines the received power in a radio frequency link.

$$Pr = \frac{Pt\ Gt\ Gr}{A} * \left[\frac{\lambda}{4\pi R}\right] \tag{1.1}$$

It can be seen from (1.1) that to improve the received power two parameters can be easily controlled, the antenna gain and the transmitted power. The first one is related to the antenna design, and it is strictly connected to the directivity obtained by the antenna. However, for a mobile device like a drone it is not easy to design a directive antenna, because of the continuous movement of the drone. So it is better to work on the transmitted power, and consequently it is necessary to use power amplifiers both in the ground station and on board, on the drone; however, on a drone there are constraints like battery duration and dimensions of the equipment to be considered.

The aim of this thesis is to solve these problematics, not only for drone applications but in a more general view, so they will be further discussed in the next chapters, together with possible solutions.

1.2 CHAPTER OUTLINE

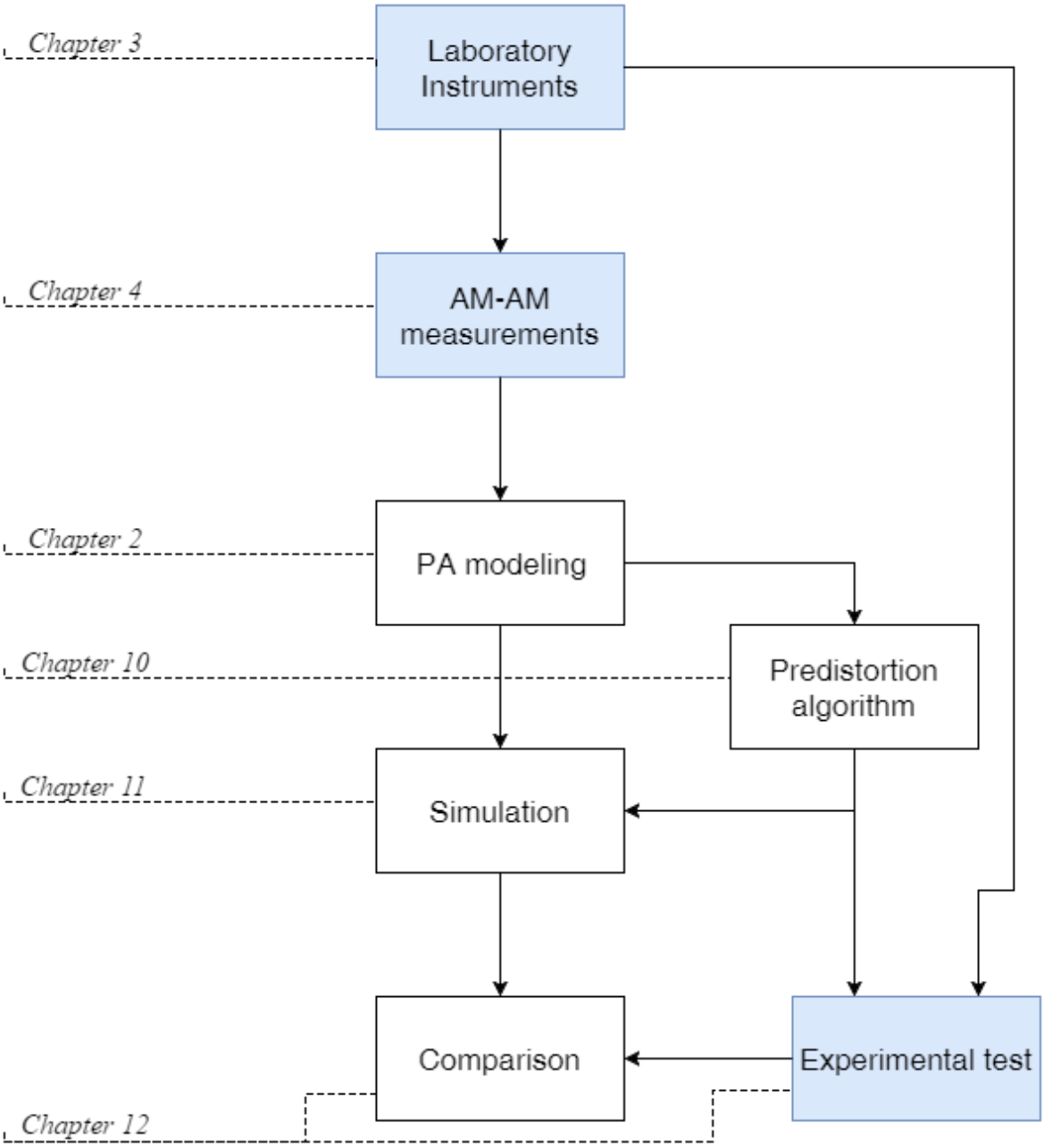

Figure 1 - Structure of the thesis. Blue blocks are relevant to hardware work or description, white blocks are software developing and theoretic explanation.

The dissertation is structured in 11 chapters, which now will be summarized.

In the first two chapters, generalities about power amplifiers will be given, discussing modeling, problems deriving from non-linearities and possible solutions.

Chapter 3 will describe the instruments used for measurements and experimental tests, giving characteristics and explaining the setup for the tests.

Chapter 4 will focus on the experimental procedure followed to obtain the desired data measurements from amplifiers and other devices, giving and explaining results.

In the following chapter the most important performance metrics for general predistortion systems are given.

The following two chapters will focus on linearization techniques and, specifically, predistortion definition and classification of predistortion systems. Also adaptive predistortion will be introduced, explaining advantages and disadvantages.

In Chapters 8 and 9 the chosen predistortion scheme, the digital baseband predistortion, will be explained and the reason of this choice will be presented.

Chapter 10 is dedicated to the presentation of the predistortion system developed for this thesis, together with the description of modifications and possible improvements.

The final two chapters present the experimental work done both with simulation and with laboratory instrumentation, describing the procedure followed and the measurement results.

Finally, the last chapter summarizes all the results obtained with this work, giving possible future development and concluding the thesis.

2 POWER AMPLIFIERS

The first signal modulation technologies consisted of simple amplitude modulations. These modulations produced extremely variable RF signal envelope, and therefore it was necessary to choose an amplifier operating point that was far enough away from saturation, so as to avoid non-linear distortions arising from the loss of linearity of the characteristic of these amplifiers. Subsequently, the frequency or phase modulations took over, thanks to their main characteristic, that is to generate a constant envelope signal. This has allowed to choose a working point closer to saturation than it was possible with amplitude modulations.

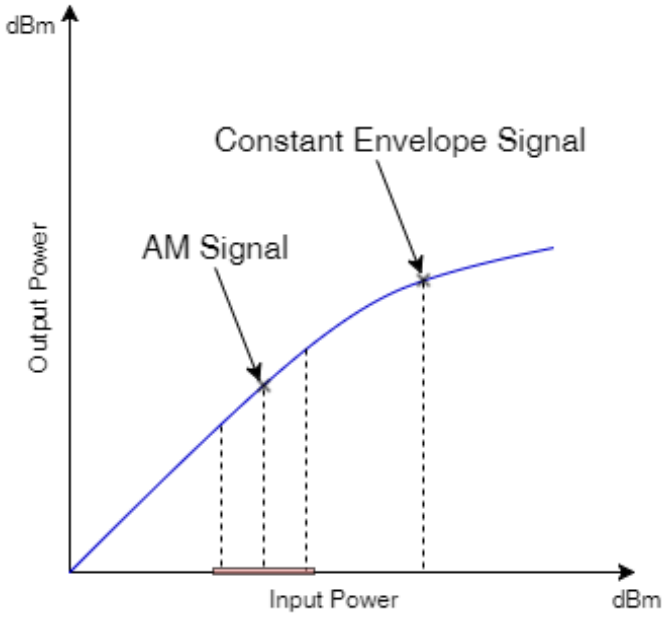

Figure 2 - Output power gain with C.E. vs AM input signal

However, recently the amplitude modulations are back again predominant in telecommunications systems through improved spectral efficiency compared to the phase and angle modulation. The new amplitude modulations typically utilize both the phase and amplitude to transmit information. Because of this, these modulations are very sensitive to disturbances affecting the signal amplitude. This also includes the non-linear distortion introduced by the power amplifier. Nonlinearities cause data errors, but also broaden the bandwidth of the signal, potentially disturbing the adjacent channels, and this is unacceptable given the increasingly insistent crowding of the frequency spectrum. To eliminate these non-linear distortions, specific amplifiers could be used, but these, on the other hand, have low **energy efficiency**. This parameter, η, is defined as follows:

$$\eta = \frac{RF\ Output\ Power}{DC\ Input\ Power} \tag{2.1}$$

Energy efficiency is a very important parameter when the reference implementation of the communication system covers mobile devices, because it affects power consumption and therefore battery life. When piloting a power amplifier, the more input power we send, the more efficiency of the power amplifier we obtain, but also we get more distortion from non-linearities on output signal, so it is necessary to find a trade-off, or try to reduce these non-linearities.

In this chapter power amplifiers will be further discussed and classified; then the characterization of a power amplifier is explained, given the definitions of the most important parameters that give an idea of the amplifier's behavior; the effects of nonlinearities mentioned above will be presented and possible solutions will be hinted; finally, different power amplifier models to consider non-linear distortions will be listed and discussed in detail, together with the explanation of the memory effect.

2.1 CHARACTERIZATION OF POWER AMPLIFIERS

To find an analytic model for a power amplifier, from now on shortened as PA, first it is necessary to describe properly its non-linearity. To do this there are some parameters typically given by the amplifier manufacturer. These parameters do not provide a complete description of the PA behavior, giving a high level characterization of the amplifier, but they are a good starting point.

2.1.1 AM-AM / AM-PM characteristics

A very common and the most immediate way to model the behavior of power amplifiers is to plot the AM-AM and AM-PM characteristics. The first one relates the amplitude of the amplifier input signal (baseband) with the amplitude of the corresponding output signal (baseband). This feature is useful to show the effect of compression of the envelope of the output signal, which is typically caused by the cut-off region of the transistors. The second represents the relationship between the phase of the output signal and the input signal amplitude.

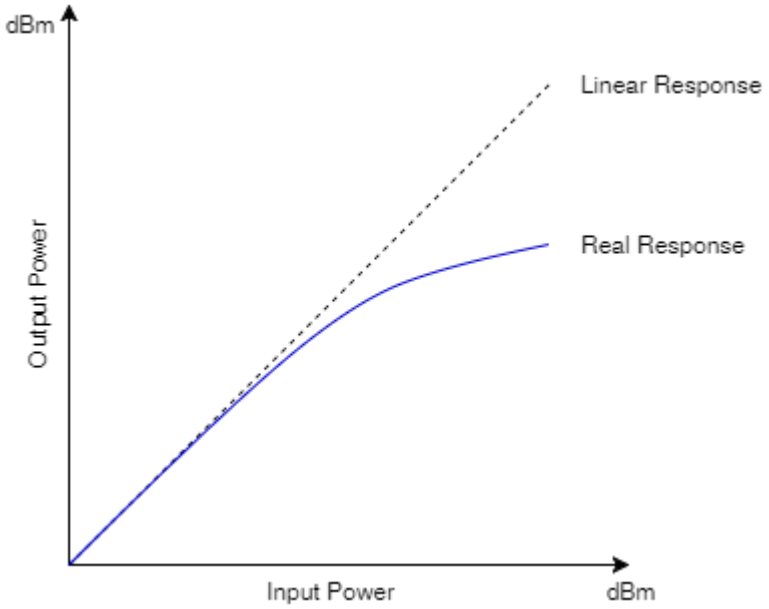

Figure 3 – Example of AM-AM characteristic

Other useful parameters are typically given by the power amplifier manufacturer, like the ones listed below.

2.1.2 1 dB Compression point

Another simple way to characterize the nonlinear behavior of a power amplifier is the 1 dB compression point, defined as the point at which the amplifier gain is reduced by 1 dB relevant to the gain that provides in its linear region.

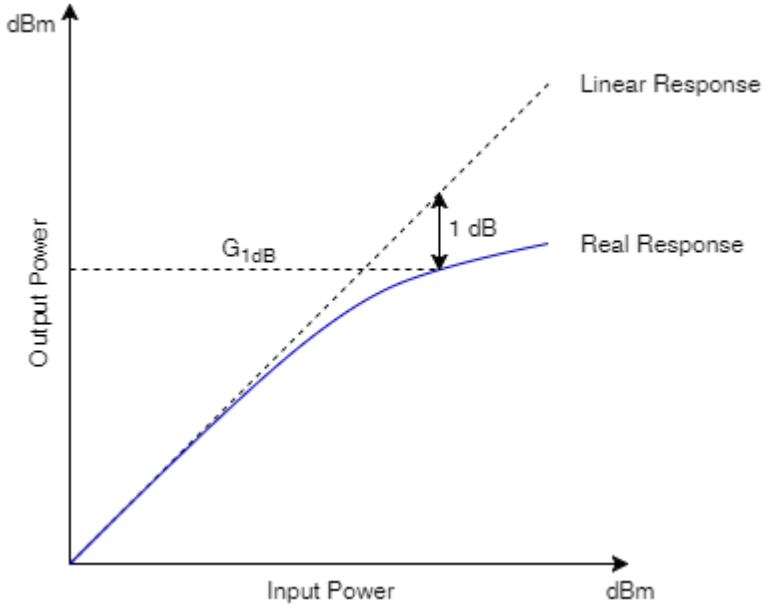

Figure 4 - 1 dB compression point

2.1.3 Third Order Intercept Point

The n-th order intercept point of a PA is defined as the intersection of two lines in the AM-AM plot; the fundamental component power versus the input power and the n-th order intermodulation product power again versus the input power.

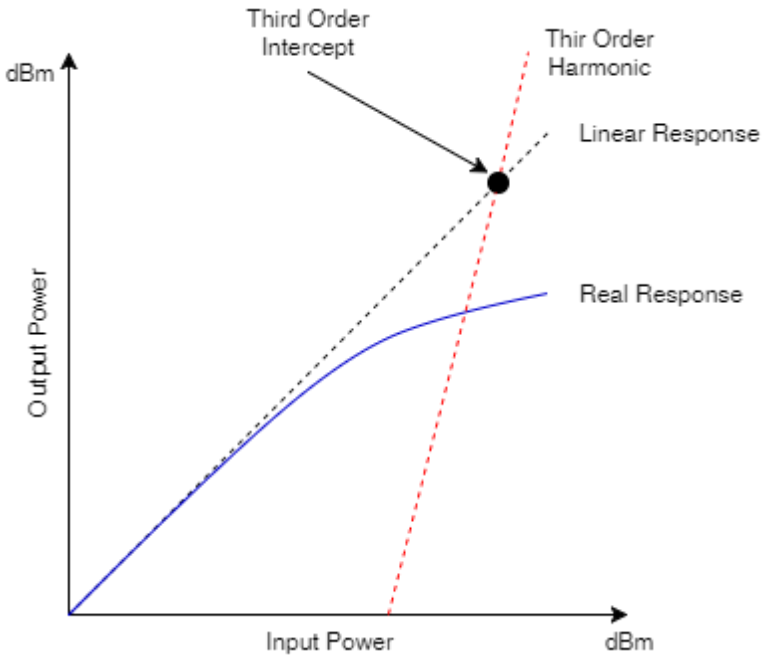

Figure 5 - Third Order Intercept Point

The intermodulation components derive from non-linearities, and they are particularly problematic because their frequencies are in-band. In particular, even order intermodulation products are not so harmful because they are out-of-band; but odd order ones, and the 3rd order (IMD3) especially, are in-band.

The 3rd order intercept point is usually provided by the amplifier manufacturer, but if this is not the case, it can be easily obtained performing a two-tone test. In this test, a signal which is a sum of two tones at different frequencies is sent to the amplifier, so as to measure the power of the third order harmonic component.

2.2 NON-LINEAR DISTORTION EFFECTS

Ideally, a PA in a communication system is perfectly linear and its effect consists only in a power gain for the transmitted signal. As we have explained before, in a real scenario this is not the case, and PAs present a nonlinear transfer function that alters the expected results. Non-linearities in the PA characteristics produce undesired effects on the transmitted signal that have to be taken into account in the design of a communication system. In the following sections these effects will be explained, with a particular focus on consequences for wideband signals, such as OFDM.

2.2.1 Constellation distortion

In the case of single-carrier amplitude-modulated signals, the effect of the power amplifier's non-linearity causes a **compression or an expansion** of the baseband symbols constellation, and a **phase rotation** that depends on the amplitude of the symbol. In particular, the more external the symbols of the constellation are, the more they are compressed and moved closer to the origin, and the more they are differently phase-rotated from the symbols with smaller amplitude.

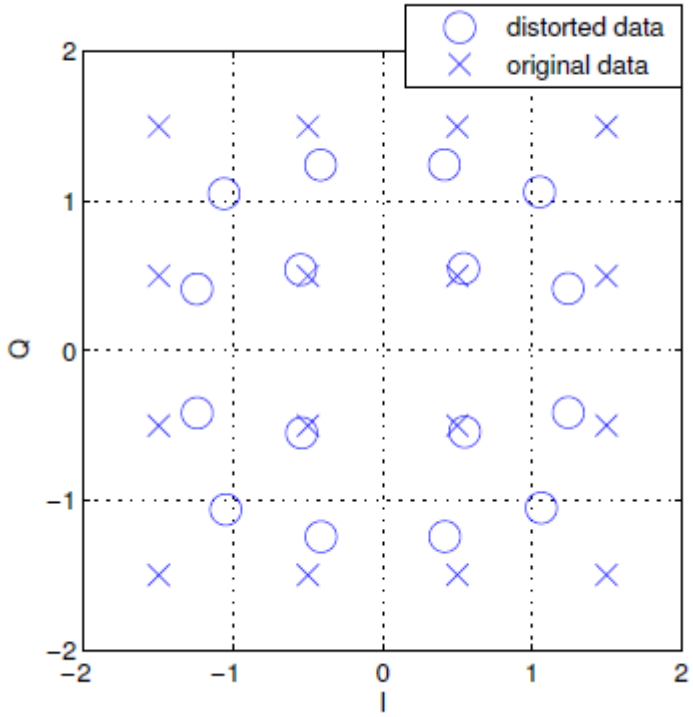

Figure 6 - Distorted 16QAM constellation

This alters the constellation with the effect of increasing the BER, since it increases the likelihood that these received symbols fall in an adjacent symbol's decision region.

For multicarrier signals, such as the OFDM one, the situation is more complicated, since the M-QAM symbols are subjected to an inverse Fourier transform in the transmission before switching to radio frequency and thus be amplified. The result is that the time-domain signal's amplitude varies very abruptly; one speaks in this case of high **PAPR** signals (Peak to Average Power Ratio). PAPR is an important parameter of the input signal for amplifier linearization. It will be further described in Chapter 5.

In the case of OFDM input signal, it can be observed that the effect of the gain compression on the constellation is different from single carrier signals: the symbols are dispersed around their real value, while the phase distortion has the same effect observed in the case of single carrier signal. As it will be explained later, the principal performance parameter that takes this effect into account is the MER (Modulation Error Rate).

2.2.2 Spectral regrowth

Another very annoying effect introduced by the amplifier nonlinearity is the spectral regrowth. This occurs especially for broadband signals, as in the case of OFDM modulation, and causes it to generate unintended spectral components, at frequencies outside the bandwidth of the original signal, broadening its spectral width.

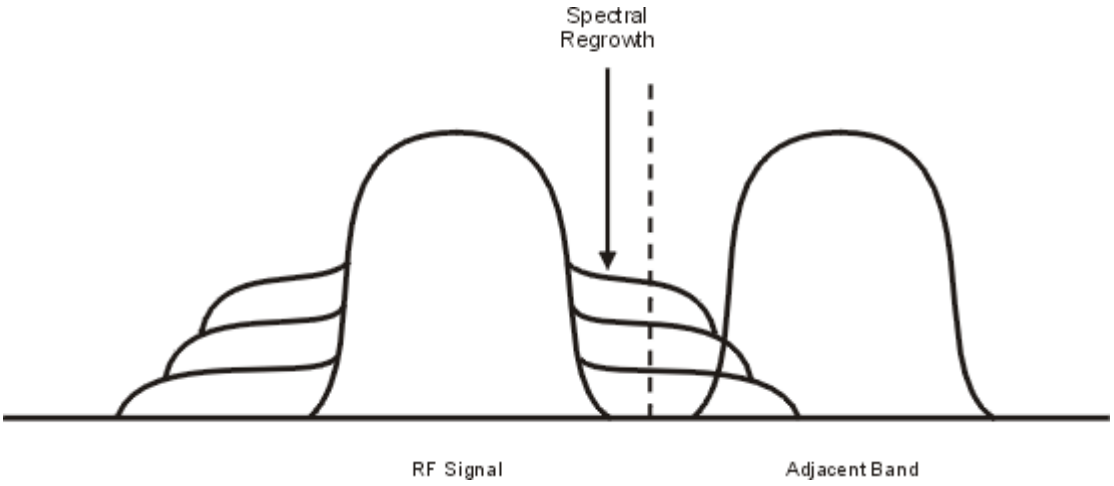

Figure 7 - Interfering channel due to spectral regrowth

The effect can be seen easily inserting a two tone input signal

$$f(t) = \cos\big((\omega + \Delta\omega)t\big) + \cos((\omega - \Delta\omega)t) \tag{2.2}$$

with $\omega = 2\pi f_c$, into a third order non-linearity, represented by the following equation:

$$f_{out}(t) = f(t) + af(t)^3 \tag{2.3}$$

Putting together equations (3.2) and (3.3) gives as output signal:

$$\begin{aligned} f_{out}(t) = \left(1 + \frac{9a}{4}\right) f(t) + \frac{a}{4}\cos(3\omega t - 3\Delta\omega t) + \frac{a}{4}\cos(3\omega t + 3\Delta\omega t) + \\ + \frac{3a}{4}(\cos(3\omega t - \Delta\omega t) + \cos(3\omega t + \Delta\omega t) + \cos(\omega t - 3\Delta\omega t) + \\ + \cos(\omega t + 3\Delta\omega t)) \end{aligned} \tag{2.4}$$

Undesired components of the output signal can be seen around the frequency of the original signal and around the third harmonic of the carrier frequency. This effect is summarized in Figure 8, with f1 and f2 instead of $\omega - \Delta\omega$, $\omega + \Delta\omega$.

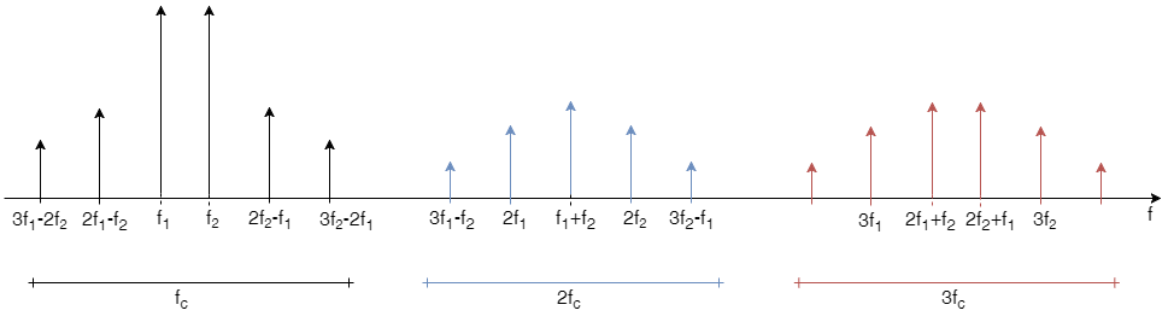

Figure 8 - Undesired spectrum components when using two tone input signal

This result could be generalized to amplification of broadband signals, where we can consider the signal as an infinite number of tones in the signal bandwidth.

This is a big problem if the portion of the electromagnetic spectrum in which we are transmitting is divided into channels, because you are likely to create interference to other signals transmitted on adjacent channels. Indeed, for this reason the frequency spectrum is regulated by precise rules on the bandwidth of the signal and the maximum power that can issue out of band. In this case the parameter that has to be monitored is the ACPR (Adjacent Channel Power Ratio).

2.2.3 Distortion in OFDM systems

In [1], the output signal from a modeled PA with an OFDM modulated input signal is analytically calculated to give more detailed information on EVM. In particular, a PA input OFDM signal $z(t)$ with N subcarriers, with T the symbol time duration, passed through a low pass filter $g(t)$, which we consider as root raise cosine filter, is expressed as:

$$z(t) = \sum_{m=-\infty}^{+\infty} \sum_{n=0}^{N-1} z_n^m g(t - nT - mNT) \tag{2.5}$$

with:

$$z_n^m = \frac{1}{N} \sum_{k=0}^{N-1} A_k^m \, e^{j2\pi nk/N} \tag{2.6}$$

where A_k^m are the complex symbols of the specific chosen M-QAM constellation. The input signal $z(t)$ can be also expressed with is amplitude and phase complex representation:

$$z(t) = r(t)e^{j\phi(t)} \tag{2.7}$$

We can note that $z(t)$ is obtained as a sum of N independent variables with the same stochastic law. This means that for sufficiently large N, as the case of 2048 subcarriers OFDM, it can be approximated by a complex Gaussian process, according to the central limit theorem, with average equal to zero and variance expressed by:

$$\sigma^2(t) = E[|z(t)|^2] = \frac{P}{N}\sum_{m=-\infty}^{+\infty}\sum_{n=0}^{N-1} g^2(t - nT - mNT) \tag{2.8}$$

where P is the energy of the symbols of the constellation. Now, we consider a PA model given by its AM-AM and AM-PM characteristics, F_a and F_p respectively. The resulting output signal $z_a(t)$ from the PA is given by:

$$z_a(t) = F_a[r(t)]e^{jF_p[r(t)]}e^{j\phi(t)} \tag{2.9}$$

Using an extension of the Bussgangs theorem, Dardari has shown that the output signal of the PA driven with the gaussian input $z(t)$ can be decomposed in a sum of 2 components: a signal component proportional to input signal and a complex zero mean noise component $d(t)$ uncorrelated with $z(t)$:

$$z_a(t) = K(t)z(t) + d(t) \tag{2.10}$$

Being $K(t)$ the proportional factor. It can be demonstrated [1] that, when the mean of the input gaussian process is null, the PA gain component $K(t)$ can be expressed as:

$$K(t) = \frac{1}{2}E\left[S'[r(t)] + \frac{S[r(t)]}{r(t)}\right] \tag{2.11}$$

where

$$S\big(r(t)\big) = F_a[r(t)]e^{jF_p[r(t)]} \tag{2.12}$$

So the amplifier gain depends on $\sigma^2(t)$. If $\sigma^2(t)$ is constant, $K(t)$ is constant. This condition is true if $g(t)$ is rectangular or the Fourier transform of $g^2(t)$ is null outside of the bandwidth $\left[-\frac{1}{2T}, \frac{1}{2T}\right]$.

At the receiver side, the signal is filtered by root raised cosine low pass filter, adapted to $g(t)$, and the resulting signal $v(t)$ is sampled at the instants $t_n^m = nT + mNT$, giving the samples v_n^m. If the amplifier gain $K(t)$ is a constant K_0, the obtained samples can be expressed as:

$$v_n^m = K_0 z_{\tilde{g}n}^m + d_{\tilde{g}n}^m \tag{2.13}$$

with $z_{\tilde{g}n}^m$ and $d_{\tilde{g}n}^m$ that correspond respectively to $z(t)$ and $d(t)$ filtered by receiver adapted filter and sampled. Every frame of N samples is transformed by Fast Fourier Transform giving N output decision variables B_k^m that ideally should be linearly proportional to the N original symbols A_k^m. The decision variables B_k^m, obtained by *FFT* on v_n^m, are thus equal to:

$$B_k^m = K_0 A_k^m + D_k^m = K_0 A_k^m + \sum_{n=0}^{N-1} d_{\tilde{g}n}^m e^{-j2\pi nk/N} \tag{2.14}$$

From this relation, it can be noted that the received constellation points B_k^m are equal to the original points A_k^m multiplied by a complex gain introducing attenuation and rotation of symbols plus a noise term representing the dispersion of the constellation points. Furthermore, when N is large enough the noise component D_k^m can be approximated by a zero mean complex gaussian noise (central limit theorem) with variance σ_D^2. Calculating this variance for a general case is complicated, but if we consider the special case of a rectangular shaping filter $g(t)$, σ_D^2 is equal to:

$$\sigma_D^2 = NE[|S(r)|^2 - |K|^2 r^2] \tag{2.15}$$

And obviously, for a linear PA with $|S(r)|=|K|$, is equal to zero.

2.2.4 Countermeasures

The solutions of problems arising from power amplifiers non-linearities are different. One possibility is to use an almost linear amplifier, but this will inevitably have low energy efficiency, and this creates problems of overheating and power consumption that are critical in battery-powered devices such as drones. Another possibility is to use different, more robust, modulation schemes, but these typically also have lower spectral efficiency, resulting in lower data rate. Finally, to limit the consequences of the spectral regrowth, a frequency spacing between the signals could be introduced, but also this solution is hardly practicable because these parameters are typically set by the telecommunications standards.

In conclusion, to solve these problems the developer has only the possibility of introducing a signal processing block, which acts on the signal to be transmitted, that can reduce the non-linearities of the power amplifier in use.

2.3 POWER AMPLIFIER MODELING

The commercial power amplifiers in circulation are basically of two types: the **TWT** amplifiers (Travelling Wave Tube) and the solid-state **SSPA** (Solid State Power Amplifier). The first ones are an older technology, they have poor linearity characteristics but they can handle much output power. Often they are still used onboard in satellite communications. The SSPA are more recent, they can deliver less power but they have good linearity properties.

The most accurate method to model the behavior of an amplifier is undoubtedly to use its transistor level representation. However, there are many problems arising from this choice. The first is that usually the amplifier manufacturer does not provide this representation with the documentation, because it requires very slow and complex simulations, also it has to be taken into account the difficulty in achieving analytical calculations with this model. For this reason, it is preferred to use representations at a higher level, that require a low number of parameters to obtain the measures.

We can divide power amplifiers models into two main categories: those without memory, and those with memory. With the firsts, AM-AM and AM-PM characteristics can be used to fully describe the behavior of the power amplifiers; for the seconds these two curves are not sufficient. In amplifiers with memory, in fact, the amplitude of the output signal at a given instant depends not only on the amplitude of the input signal at that same instant, but also from that at the previous instants. Therefore, it is necessary to use mathematical models that take this effect into account.

2.3.1 Memoryless models

The first type of PA models are the memoryless ones. A memoryless characterization does not take into account memory effects, that will be explained in the next section. These models assume that PA characteristics do not change with time, and are easier to implement compared to models with

memory. On the other side, they can't completely describe every type of power amplifier, or power amplifiers with particular input signals.

2.3.1.1 Polynomial model

In this model the PA output V_{out} is expressed as [2]:

$$V_{out} = \sum_{n=1}^{N} a_n V_{in} |V_{in}|^{n-1} \tag{2.16}$$

Where V_{in} is the PA input voltage and a_n are the polynomial coefficients.

This is the simplest method to describe the behavior of a power amplifier. The polynomial coefficients can be calculated by least squares approximation of the measurements performed on the amplitude and phase of the amplifier output signal. A low degree polynomial model is an excellent model for already quite linear amplifiers (such as Class A). Often only the odd coefficients are used since the distortion due to the second degree does not generate components around the carrier frequency. For this reason, the most used polynomial model, and also simplest, is the third-order polynomial model, which depends on a single parameter.

The problem of this method is that a high degree polynomial is needed to model the non-linearity in proximity of the saturation, and generally strong non-linearities, thus increasing the computational complexity of the representation.

2.3.1.2 Saleh model

The amplifier gain and phase deviation are described by this model as the following [3]:

$$G(|V_{in}|) = \frac{a_A |V_{in}|}{1 + b_A |V_{in}|^2} \quad , \quad \Phi(|V_{in}|) = \frac{a_\Phi |V_{in}|^2}{1 + b_\Phi |V_{in}|^2} \tag{2.17}$$

where a_A, b_A, a_Φ, b_Φ are the parameters used to model the nonlinearity. Saleh Model is commonly used to model various power amplifiers, and fits very well especially TWT ones, because of their poor linearity and the particular behavior after the saturation point, which is taken into account by this model. It is also recommended as the standard model for high power amplifiers by IEEE broadband wireless access group. Both AM-AM and AM-PM characteristics are described. However, this method does not fit very well solid state power amplifiers (SSPA).

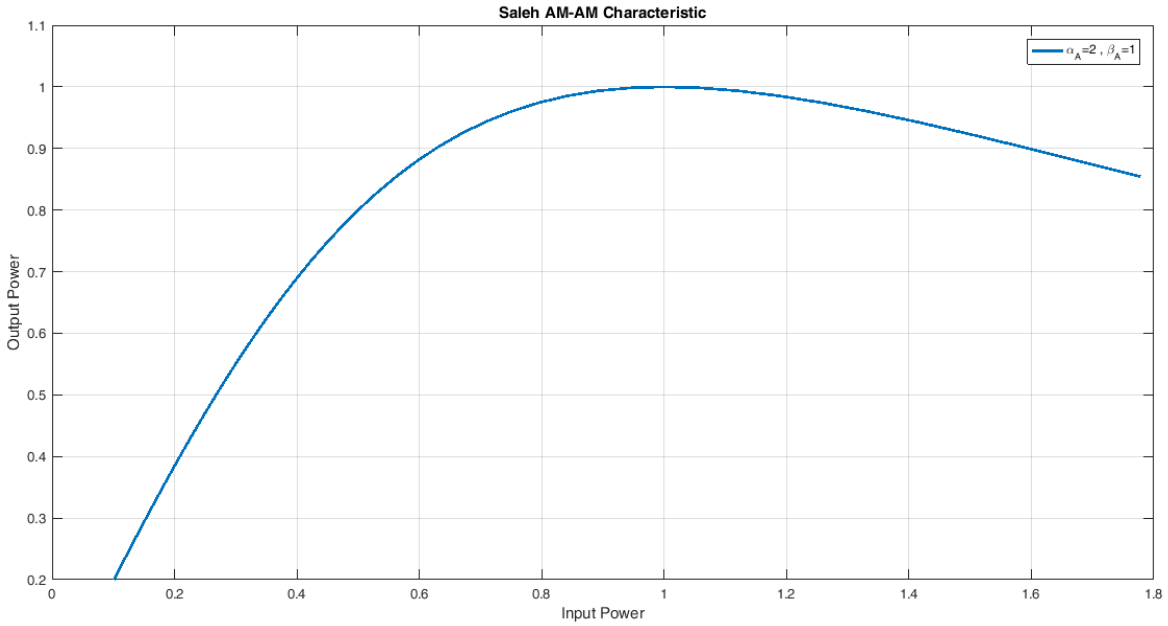

Figure 9 - Example of Saleh Model with $a_A = 2$, $b_A = 1$

2.3.1.3 Rapp model

The gain of the amplifier is described by Rapp model as [4]:

$$G(|V_{in}|) = \frac{1}{\left(1 + \left(\frac{|V_{in}|}{a_A}\right)^{2\rho}\right)^{\frac{1}{2\rho}}} \tag{2.18}$$

Where a_A is the output saturation amplitude value and ρ, called **smoothness factor**, gives an idea of the shape of the non-linearity and represents the most important parameter of this model. Rapp model has been developed for SSPA, and presents a very linear behavior for small values of the input signal amplitude.

This model provides only the output versus input amplitude characterization (AM-AM characteristic), since solid-state amplifiers typically introduce a very small phase shift on the input signal, which in first approximation can be neglected. In addition, given the gain and the output saturation amplitude of the amplifier, it has the advantage of depending on a single parameter, the smoothness factor, which gives a measure of the distortion introduced immediately before the saturation. The disadvantage is the inability to precisely characterize the non-linearity present at low amplitude values.

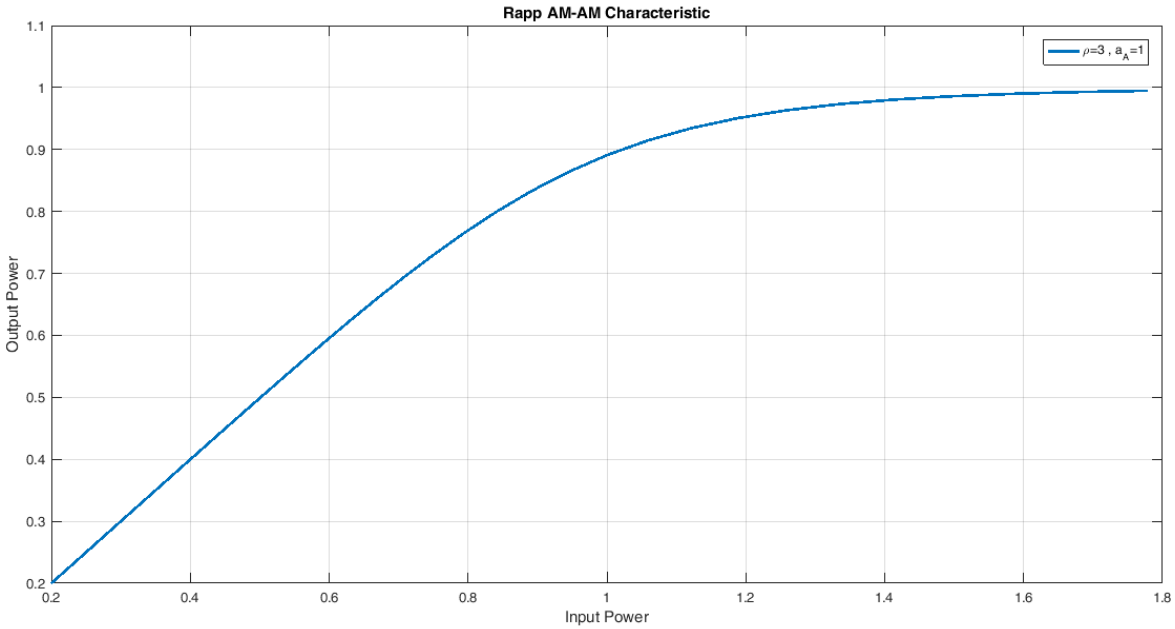

Figure 10 - Example of Rapp model with $\rho = 3$, $a_A = 1$

2.3.1.4 Ghorbani model

Ghorbani's model describes gain and phase variation as [5]:

$$G(|V_{in}|) = \frac{a_A |V_{in}{}^{c_A}|}{1 + b_A |V_{in}{}^{c_A}|} + d_A |V_{in}| \,, \quad \Phi(|V_{in}|) = \frac{a_\Phi |V_{in}{}^{c_\Phi}|}{1 + b_\Phi |V_{in}{}^{c_\Phi}|} + d_\Phi |V_{in}| \tag{2.19}$$

where $a_A, a_\Phi, b_A, b_\Phi, c_A, c_\Phi, d_A, d_\Phi$ are the parameters of the non-linearity.

This model also is thought for solid state power amplifiers, but this time also the characterization of phase distortion is introduced. It adapts very well to FET amplifiers, and can also model the non-linearity at low amplitudes. However, it requires four parameters for the AM-AM characteristic and four others for the AM-PM characteristic, thus increasing the computational complexity to extrapolate the model.

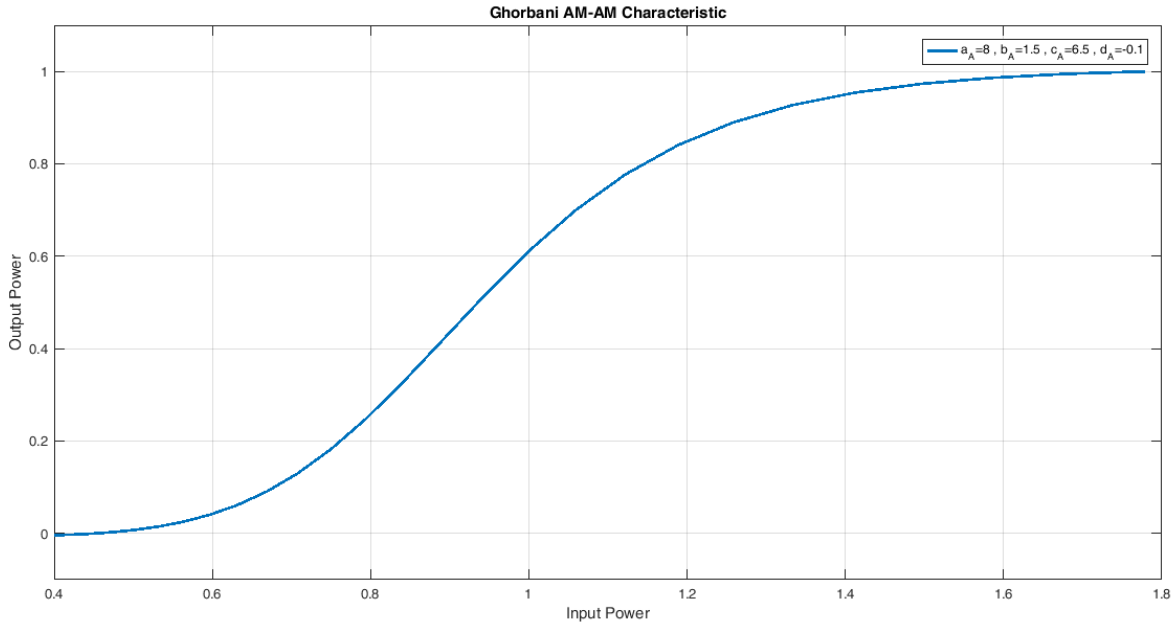

Figure 11 - Example of Ghorbani model with $a_A = 8, b_A = 1.5, c_A = 6.5, d_A = -0.1$

2.3.1.5 Variations and modified models

The ones listed above are the main models in the literature, however many variants that typically add complexity and accuracy to the original models have been developed. Among the many we can cite the modified Rapp model, that introduces the characterization of phase distortion, and the Saleh model with memory that introduces the frequency dependence of the parameters to be estimated.

2.3.2 Models with memory

Those models seen above are memoryless, but in wideband and high-power systems typically the effect produced by HPAs with memory has to be considered. Practically, effects deriving from memory are frequency-domain fluctuations in the transfer function of the power amplifier, or time dependence of the transfer function. This means, for a two tones input signal, intermodulation products are different, in power and phase, depending on the frequency separation between the two tones.

These effects are typically generated by capacitances and inductances in the amplifier chain or by frequency dependent impedances in the PA chain. The source of these effects can be the bias networks that are not infinitely wideband (**electrical memory effects**), thus generating variable impedances, or thermal fluctuations of the power amplifier due to signal level (**thermal memory effects**). The slowness of the heating process of the thermal feedback has the same effect of a low pass filter for signal with bandwidth up to 1 MHz.

Consequence of these effects is that the output value of the PA at a given instant depends not only on the input value at the same instant but also on previous input values. To include the memory

effects in PA models so it is necessary to introduce a time dependence in the output signal. Different memory models will be described.

2.3.2.1 Volterra series

This is probably the most accurate model to describe the relationship between input and output complex envelopes of the signal passing through a power amplifier. The relation [6] is the following:

$$z_a(n) = \sum_{i=0}^{N} h_1(i)z(n-i) + \sum_{i=0}^{N}\sum_{j=0}^{N}\sum_{k=0}^{N} h_3(i,j,k)z(n-i)z(n-j)z^*(n-k) \ldots + \epsilon(n) \quad (2.20)$$

where h_1 and h_3 are called **lowpass equivalent Volterra kernels**, n denotes discrete time, N the memory length and ϵ the modeling error. The coefficients h_1 and h_3 are also called respectively the linear and cubic kernel.

The complete Volterra Series based description needs on order of $(N+1)K$ coefficients of Volterra kernels, where K is the order of non-linearity. This may be sometimes too much for practical purposes. That's why some others memory models, which can be regarded like some special cases of Volterra model, have been proposed.

2.3.2.2 Wiener-Hammerstein model

This model is based on the concatenation of linear dynamic systems and static non-linearities. Basically, we can define the Wiener and the Hammerstein systems as the concatenation of two blocks. In the Wiener system a linear filter is followed by a memoryless non-linearity, while in the Hammerstein model the two are reversed [7].

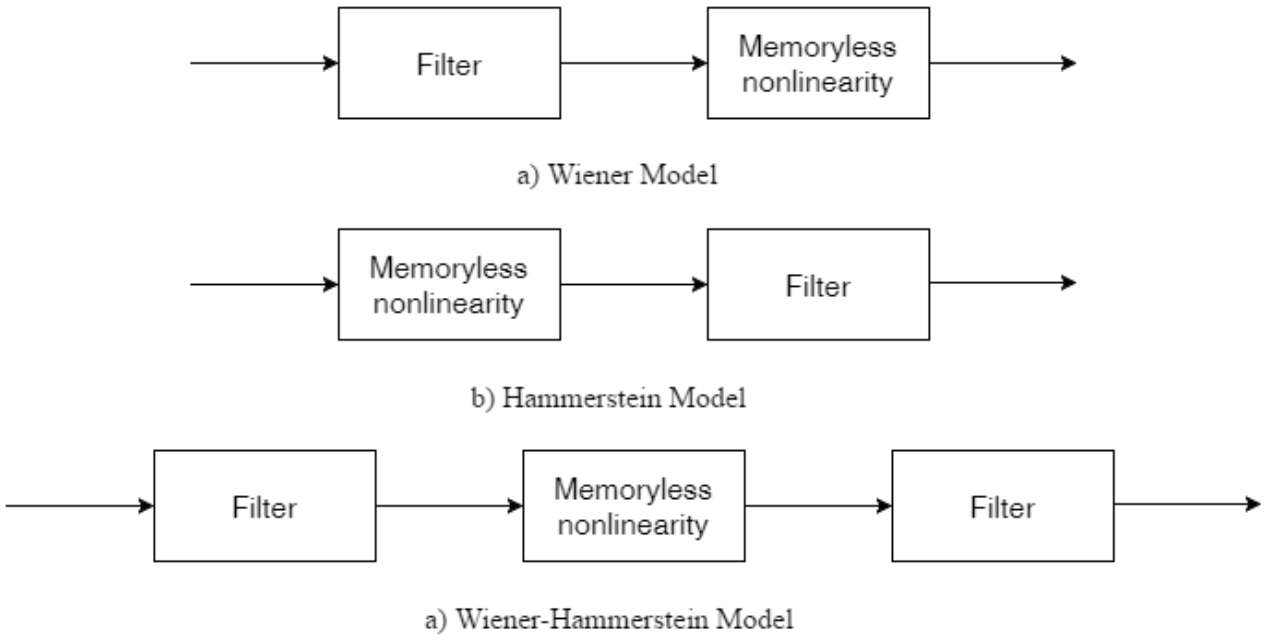

Figure 12 - PA models based on filtering

2.3.2.3 Memory Polynomial Model (MPM)

The memory polynomial model is a simplified version of the Volterra Series. To simplify that model, MPM exploits the fact that PA non-linearities are almost phase independent. The output signal can be written as [8]:

$$V_{out} = \sum_{k=0}^{K-1} \sum_{l=0}^{M-1} a_{kl} V_{in}(t - m_l t_s) |V_{in}(t - m_l t_s)|^k \tag{2.21}$$

with, K the degree of nonlinearity, M the memory length of modeled amplifier, and m_l is the elementary delay of memory, identified to best fit the experimentally measured data.

An important advantage of MPM is that it can be easily implemented on hardware. It can be described by a number of parallel Wiener filters and time delays to take into account the memory effect.

3 SETUP

3.1 INPUT SIGNAL

The amplifier's input signal is generated from the Ettus Research's USRP platform B100. In particular, it has been written with MATLAB a constant file, with all the same numerical values, such as to have the desired power at the amplifier's input. Passing through the USRP this signal will become a sinusoid centered at the set carrier frequency, which is equal to 2450 MHz. This is a typical working frequency for drone-ground communications. After the upconversion, the signal is sent to the first stage of amplification in the transmission chain, represented by the USRP adjustable gain (**PGA**).

This gain has not been used to perform the power sweep, since even the USRP suffers from the problem of amplitude compression of the transmitted signal. In fact, it has been observed experimentally that if we use the USRP PGA a 1 dB increase in the power gain value corresponds to an effective 0.8-0.9 dB output power increase. This would not be a significant compression for low PAPR signals, but for OFDM signals, which have typically 10-12 dB PAPR, it could compromise the predistorter development. For this reason, a number of files with fixed and different amplitude values have been generated via MATLAB, and sent to the device to test through USRP with a fixed PGA gain. The amplitude chosen for these files spans from the average amplitude of the OFDM file to be transmitted less 10 dB, and the same amplitude plus 10 dB, to cover the entire dynamic of the input file.

3.2 USRP B100

The first step done with the measurement tools is a full characterization of the Ettus Research USRP B100, the device used in this thesis that performs digital to analog conversion, upconversion to 2.45 GHz and finally transmission of the signal. According to manufacturer datasheet [41], this device has a bandwidth up to 16 MHz, a DAC resolution of 14 bits and a maximum output power of 15 dBm.

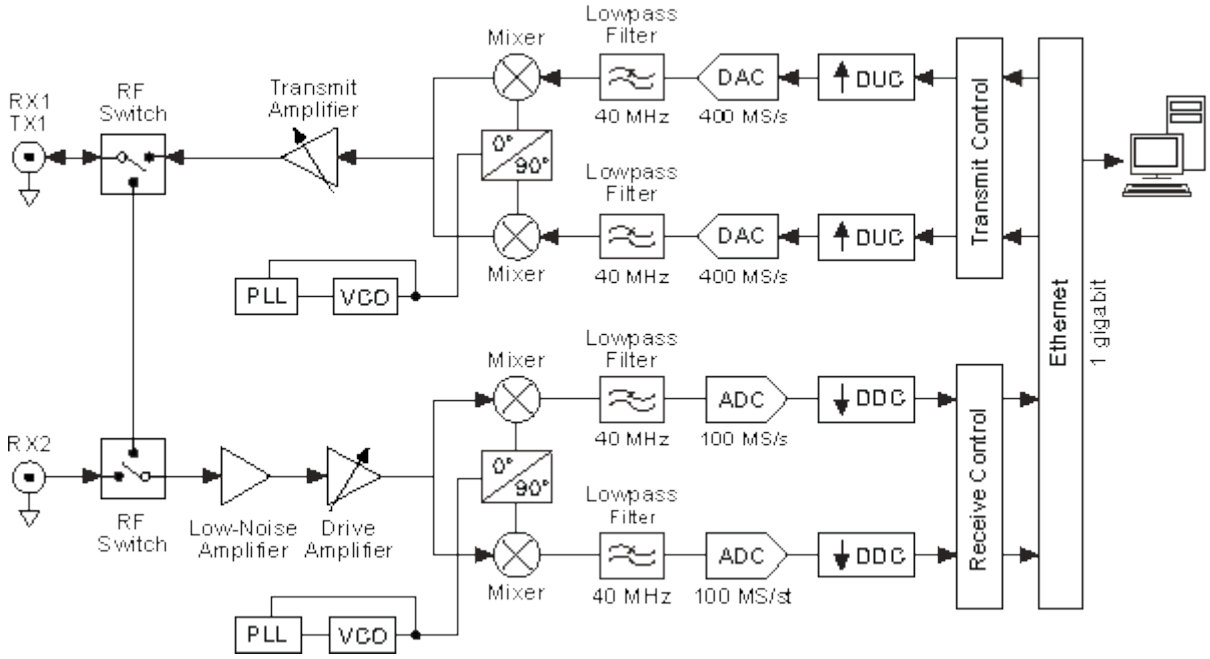

Figure 13 - Logic block scheme of USRP

The characterization of this device was necessary because also the USRP has an integrated amplifier with a variable gain (PGA), and if we wanted to predistort only the amplifier connected to USRP, we needed to be sure the USRP's PGA was working in the linear region.

3.3 TESTED AMPLIFIERS

To completely test the developed algorithm, more than a single amplifier have been linearized. In particular, the experimental results obtained by measurements are relevant to three different power amplifiers:

- Kuhne KU PA 242 TX
- Fujitsu FMC1616L1015
- OvisLink Airlive WPA-2400IG

3.3.1 Kuhne KU PA 242 TX

The first amplifier used is the Kuhne KU PA 242 TX [42]. It is a class A solid state power amplifier, which thus already presents a high linearity. The working frequency range is 2300-2500 MHz, the gain in the linear zone is 20 dB, the 1 dB compression point is relevant to an input power of 17 dBm, and the maximum value of the input power is 19 dBm. The amplifier is based on GaAs-FET transistors. Finally, the power supply for the amplifier is provided by the ISO-Tech IPS303A tool, which is set on a 12 Volt output voltage, that is the voltage required by the amplifier.

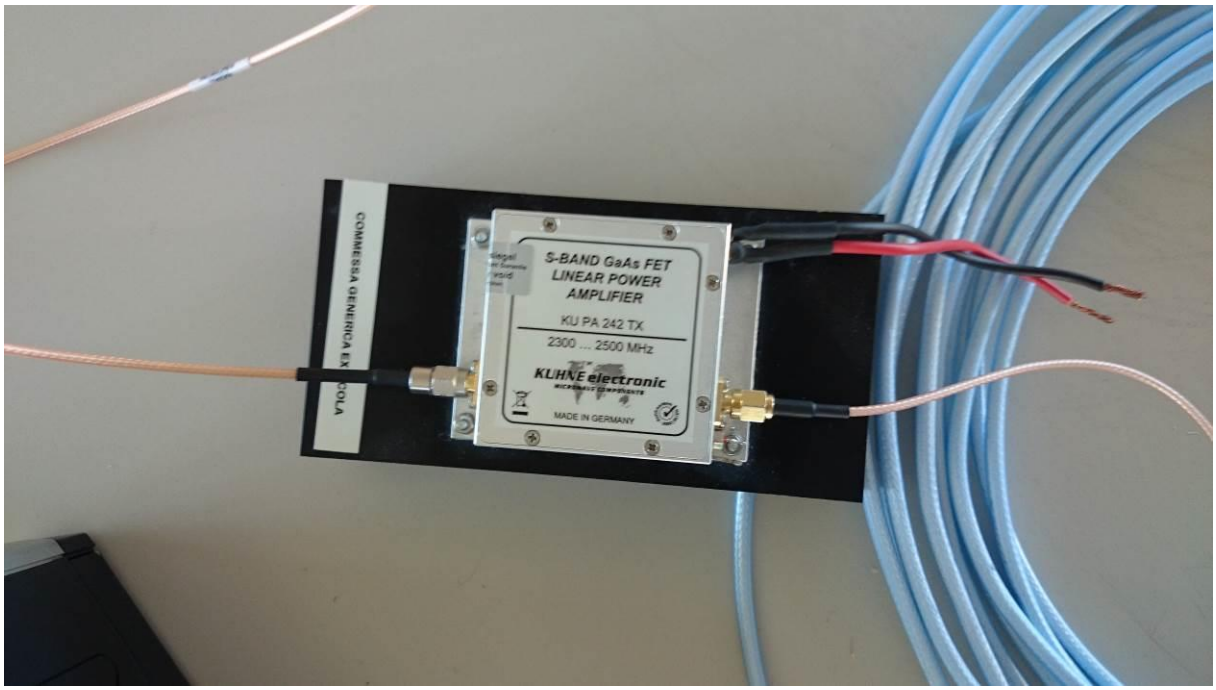

Figure 14 - Amplifier under Test

3.3.2 Fujitsu FMC1616L1015

A different type of power amplifier has also been used. In particular, a FUJITSU FMC1616L1015 [43]. This PA is a Solid State Amplifier too, but it presents low linearity properties since it is a class B amplifier. This second amplifier has also a different working bandwidth, from 1.2 to 1.4 GHz, so in order to make measurements with it, the substitution of the USRP daughterboard (frontend) was necessary. This is because USRP B100 has different frontends which can work at different frequencies. For Kuhne and OvisLink, the 2.4 GHz frontend has been used, for Fujitsu the 1.2 GHz frontend was necessary.

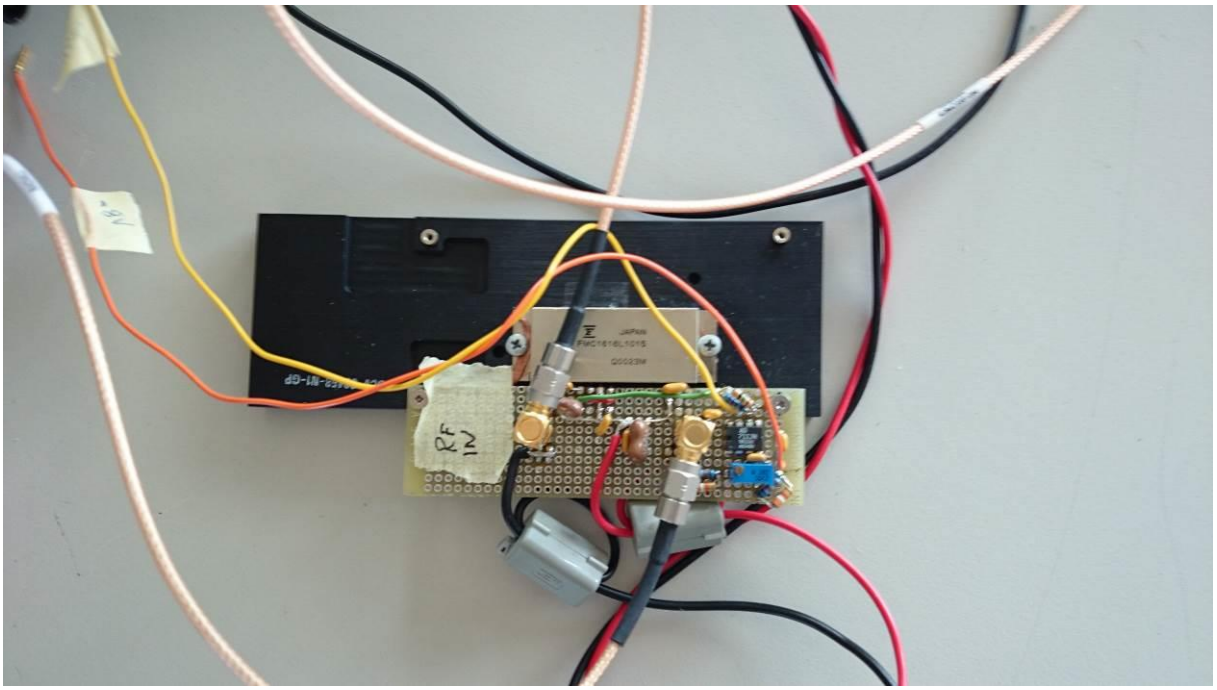

Figure 15 - Fujitsu PA

3.3.3 OvisLink Airlive WPA-2400IG

The last amplifier to be tested was the OvisLink Airlive WPA-2400IG [44]. It is a commercial PA used typically for Wireless LAN applications, thus working with 2.4 GHz carrier frequency. Again, this device is a SSPA, and its characteristics are similar to the Kuhne amplifier. It has a power gain equal to 12 dB, a maximum output power equal to 27 dBm (500mW).

Figure 16 - OvisLink Airlive PA

3.4 ANTENNA

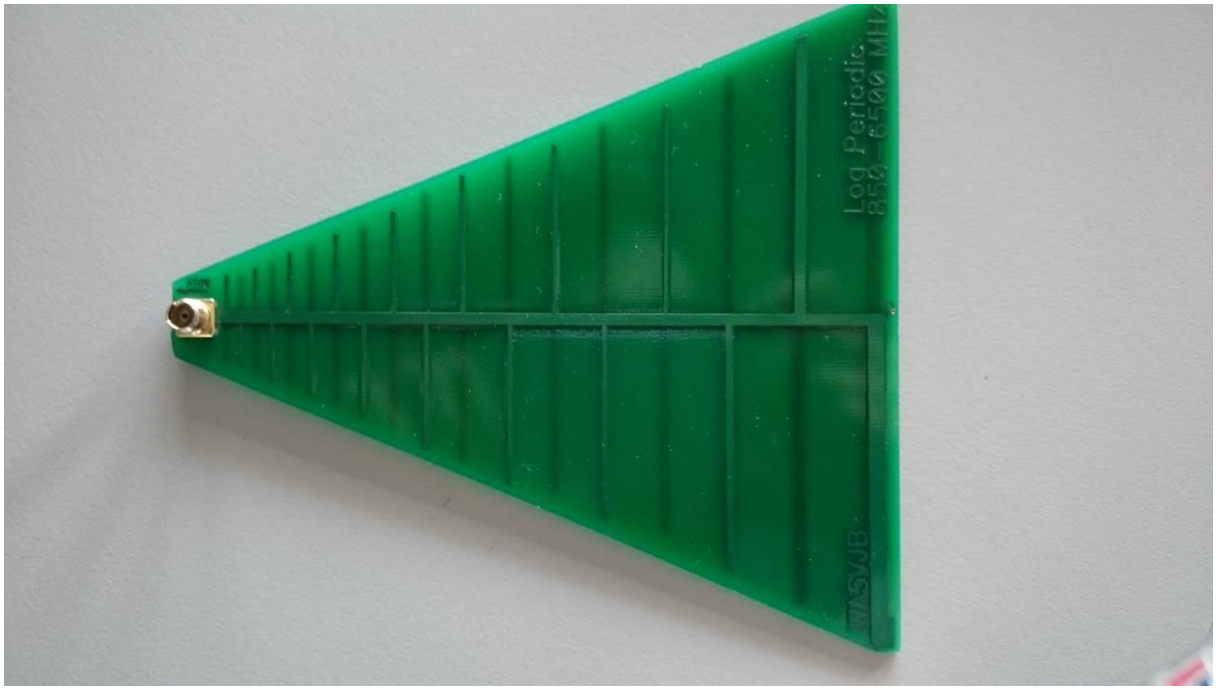

Figure 17 –Antenna

The antennas used at the transmitter and receiver are identical. They are PCB printed logperiodic antennas, developed to work in the 850-6500 MHz frequency region. According to datasheet [40], the antenna gain is equal to 6 dBi.

3.5 DOWNCONVERTER

In order to demodulate the OFDM signal and calculate parameters such as MER and BER, the signal carrier frequency needs to be translated. This is necessary because of the input frequency range of the modulation analyzer, which does not cover the carrier frequency of 2450 MHz. Thus, a downconverter is placed before the measurement tool, working also as a Low Noise Amplifier (LNA). In details, the model of the downconverter is Kuhne KU LNC 2227 B PRO 2000, whose local oscillator frequency is 1833 MHz. The RF input signal carrier is 2450 MHz, so the downconverter output is centered at 617 MHz.

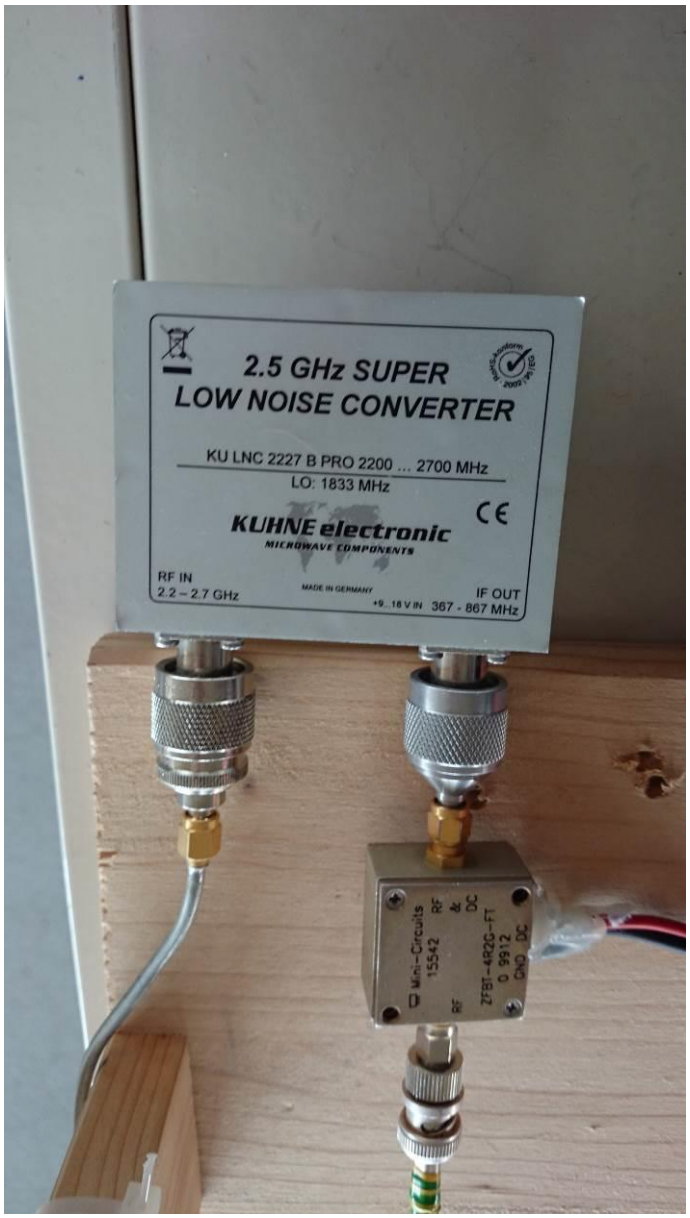

Figure 18 - Low Noise Downconverter

The downconverter power supply is supposed to be given through the RF input, so a coupler to insert the power supply is needed before the signal is fed through the downconverter.

3.6 POWER MEASUREMENT TOOL

To measure the output power, when characterizing HPAs, the amplifier output has been passed through two attenuators before arriving to the measurement tool. The two attenuators values are 40 dB and 10 dB, and they are connected in series. The measurement tool consists of an Anritsu MS2724B, a spectrum analyzer, set to a center frequency of 2.450 GHz, with a 14 MHz frequency span, and a bandwidth of 8 MHz.

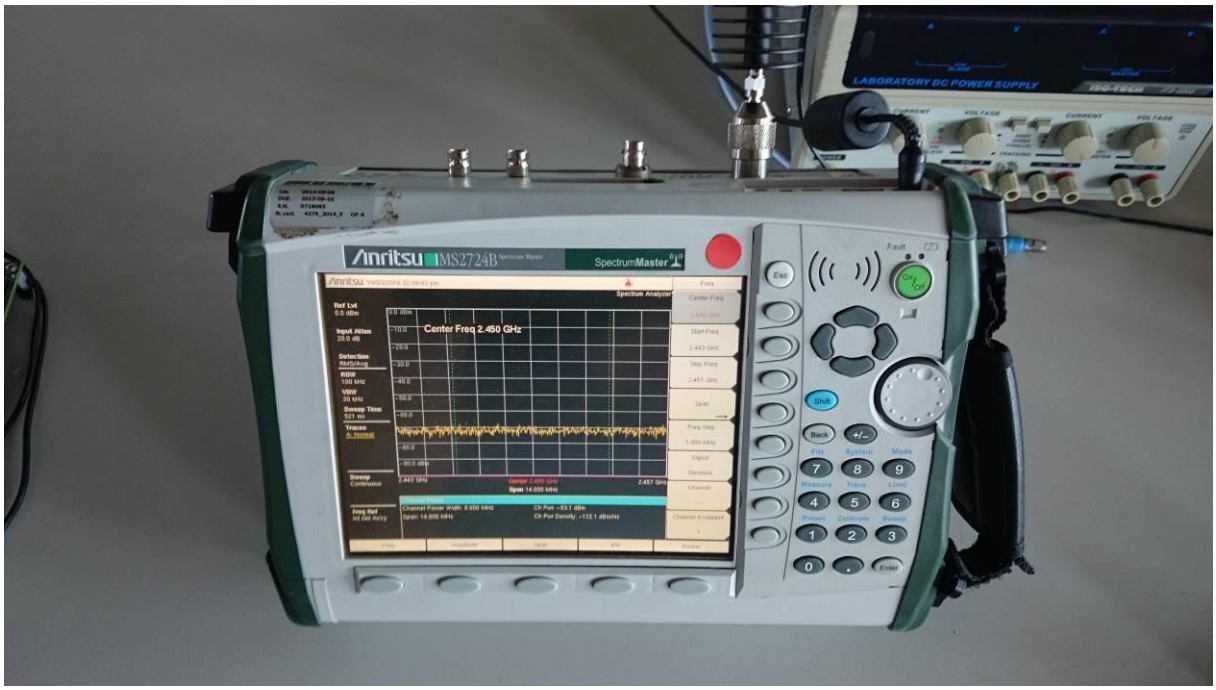

Figure 19 - Spectrum analyzer

The two attenuators are indispensable because without them the very high power at the amplifier output would damage the spectrum analyzer. To further protect it, the measurement tool has also an internal attenuator, that has been set to 10 dB. Given those attenuators, measurements taken has been corrected by summing 50 dB to take into account external attenuation. Internal attenuation has been taken into account by the spectrum analyzer itself.

When measuring USRP and Limiter output power, the 50 dB attenuator is excessive, because the power we are giving to the spectrum analyzer is limited. In these cases, no attenuation or just the 10 dB attenuator have been used.

This tool has been used also to measure the input power of the PA. This was necessary because the USRP itself is not perfectly linear. So to have a good approximation of the AM-AM characteristic, for every value of the input sinusoid amplitude, two measurements has been made: the input power, with USRP output connected directly to the spectrum analyzer; and the output power with the amplifier between USRP and the measurement tool.

With this instrument it is also possible to obtain the Adjacent Channel Power Ratio (ACPR), simply visualizing the spectrum of the signal. ACPR is the difference, in dB, between the signal level and the noise level.

3.7 MER MEASUREMENT TOOL

For the MER measurement, another instrument has been used. It consists of a **modulation analyzer**, the Rover HD Touch, which is capable of OFDM signal demodulation and shows important

parameters such as MER, BER, received power. It can also show the baseband symbols constellation, to better understand the distortion introduced by the amplifier.

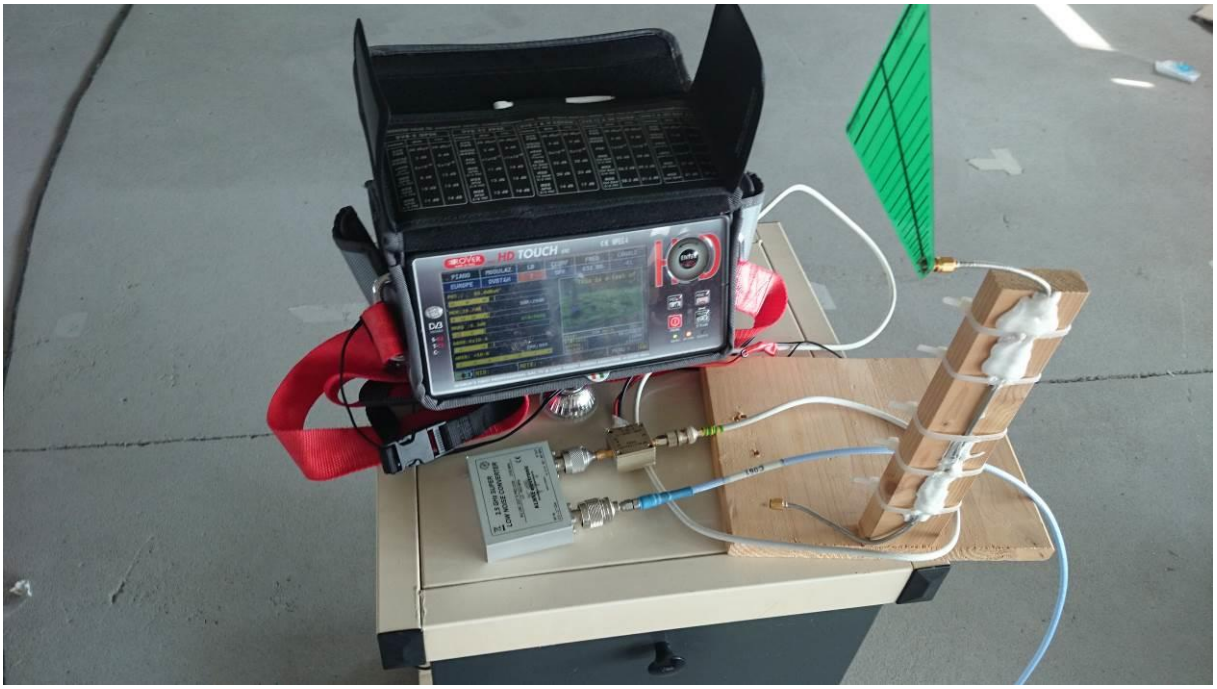

Figure 20 - Receiver implementation

The important settings for the MER measurements for this instrument are the center frequency, set to 617 MHz as explained above, and the LB, set to 7.

3.8 LIMITER

The first linearized device was a limiter, in particular the Mini-Circuits ZFLM-252-1WL+ model. This choice was made to make sure the predistortion algorithm works properly, since the limiter has typically very poor linearity properties. In order to linearize the limiter, of course we needed a measured AM-AM characteristic. Basically, this device has a transfer function similar to amplifiers' one, except for the unitary gain until the saturation.

Figure 21 – Limiter Mini-Circuits

4 AM-AM CHARACTERISTIC MEASUREMENT

In this chapter first the instruments used in this thesis will be presented, not only the amplifier used for the experimental tests but also measurement tools and other devices, then it will be described the procedure with which the AM-AM characteristic has been extrapolated from every device with an input-output power relation, and finally the results of these measurements will be presented and discussed, focusing on those relevant to amplifiers.

4.1 DEVICE CHARACTERIZATION

4.1.1 USRP B100 characterization

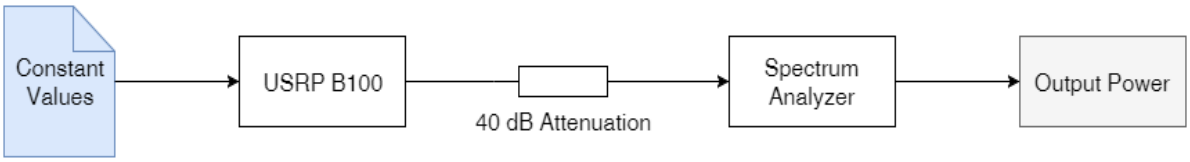

Figure 22 - Block scheme for USRP characterization

From the measurement results, presented in Figure 23, obtained with a linear interpolation between measured points, it can be noted that the USRP presents very high linearity characteristics, also near its saturation power and for low amplitude values. Knowing the PAPR of the input signal, about 11 dB, we could choose the best operational point for the USRP, so as to ensure the linear behavior of the device.

However, another problem was found characterizing this device. The dynamic range of the DAC can only accept integer values from about -1000 to 1000. This was found because using higher values as constant input signal, the USRP output power had an apparently casual behavior. This was not related to non-linearities of the amplifier stage of USRP, the PGA, because varying the USRP gain did not produce the same effect on the output power, giving the expected linear behavior until saturation. The cause of the problem is that, as it will be described later, the OFDM input signal we are using is already filling completely this dynamic. The consequence is that when the file is predistorted, high amplitude samples are scaled by a positive dB factor, incrementing the power of the signal, therefore breaking the URSP DAC dynamic. This problem, together with the adopted solution, will be further described in the next sections.

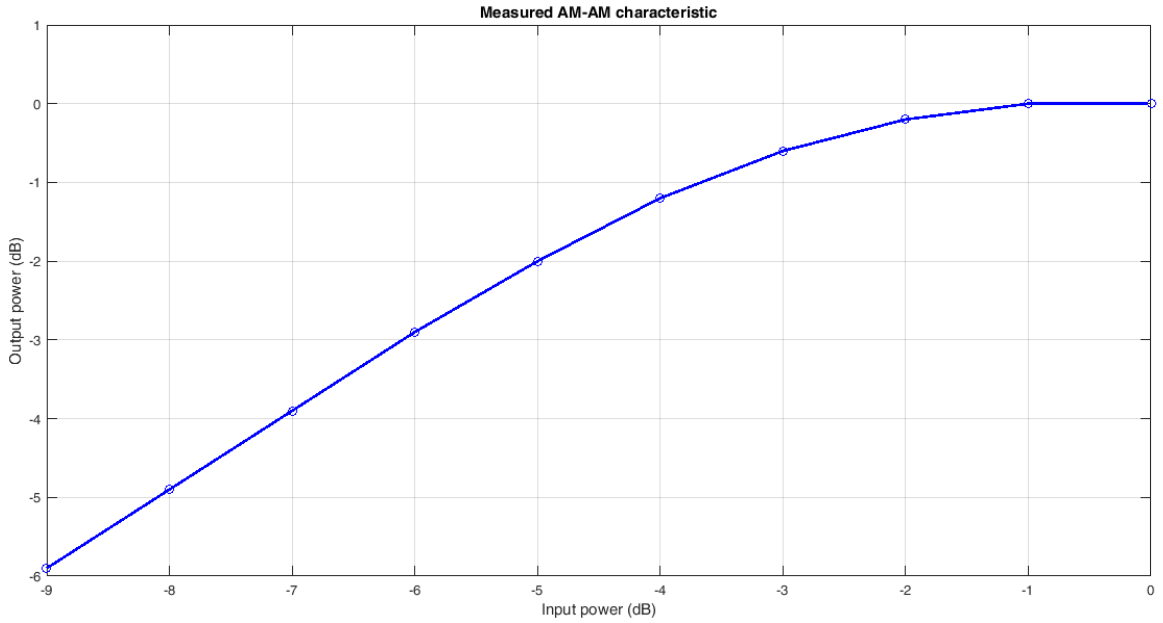

Figure 23 - USRP measured AM-AM characteristic

4.1.2 Limiter

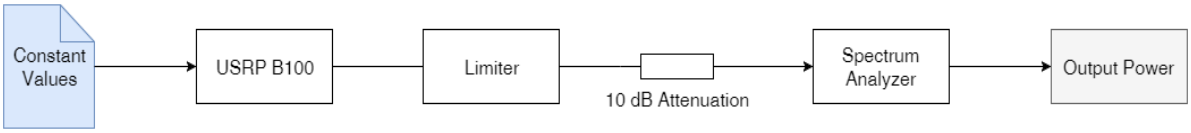

Figure 24 - Block scheme for limiter characterization

Measurements of the limiter confirms the poor linearity of this type of devices. The saturation is really far in the input power range, and is reached very slowly.

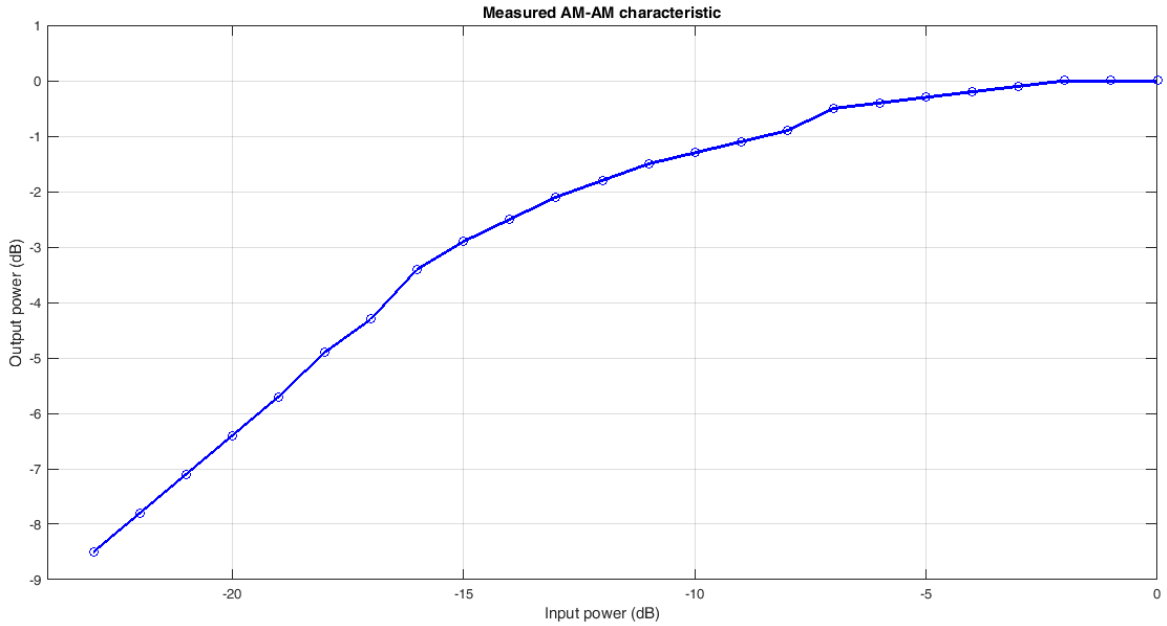

Figure 25 - Limiter measured AM-AM characteristic

Regarding the AM-PM characteristic, using the MER measurement tool described before, that is able to show the received symbol constellation, it was found that this can be considered as constant and equal to zero. This confirms what it was supposed to be, because theory suggested the low phase distortion given by Solid State Power Amplifiers.

4.2 MEASUREMENT RESULTS

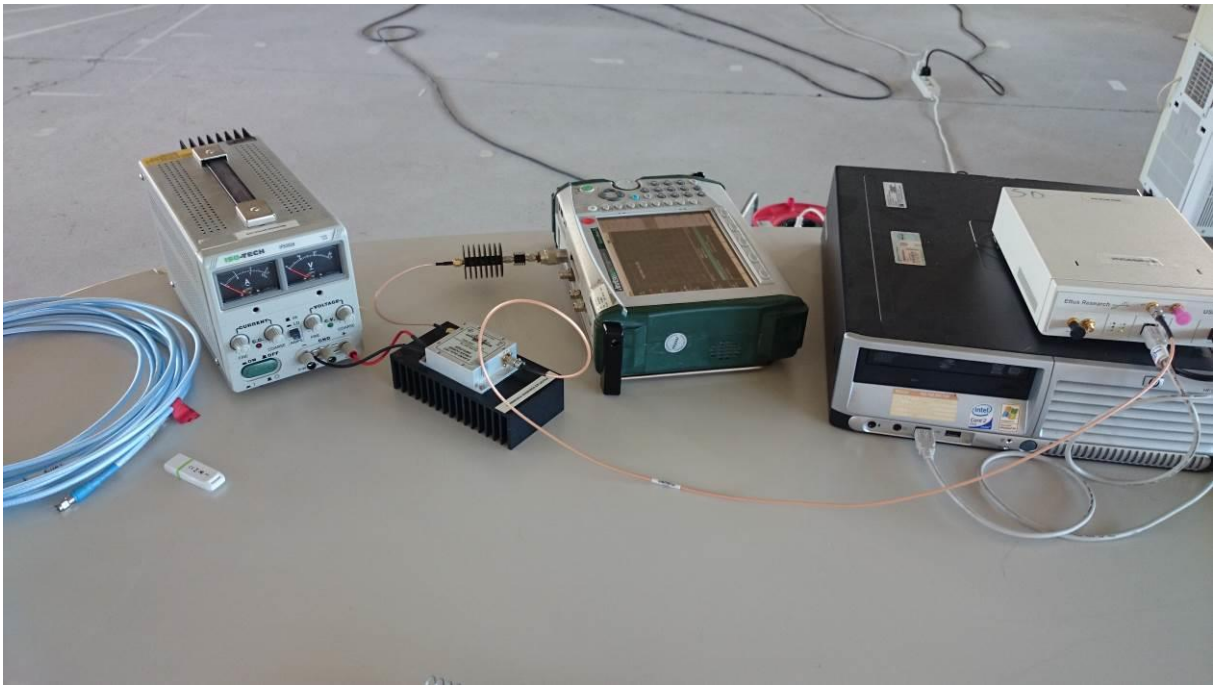

Figure 26 - Measurement instrumentation

Measurements aimed to extrapolate the PA's AM-AM characteristic, then comparing it with the theoretical data given by the datasheet, to develop the best predistorter for these specific power amplifiers.

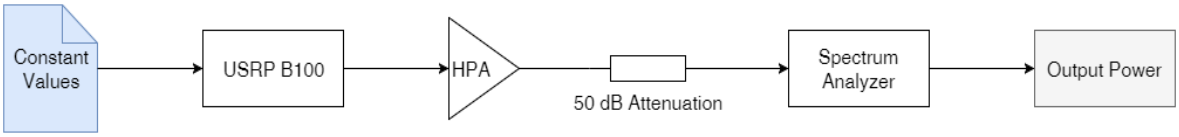

Figure 27 - Block scheme for HPAs characterization

In Figure 27 the setup used for amplifiers characterization is shown. In these cases also the power needs to be provided. This was done by the power supply providing the correct voltage to the HPAs.

The AM-AM characteristics extrapolated by these measurements will be presented later in this document, together with the model chosen to approximate them. For the measurements setup, it is important to note that for the Fujitsu amplifier the input signal used to make the measurements is a sinusoid at 1.2 GHz, instead of 2.4 GHZ like the input signal used for Kuhne and OvisLink. This generated a problem with the downconverter, because it is not designed to work with a RF signal centered at 1.2 GHz, however we found experimentally that this leads to a MER degradation equal to 1.4 dB only. This loss of performance is acceptable, since the most important parameter for our experiment it is the MER gain between non-predistorted and predistorted file, not the absolute MER value.

From the measurements results emerged the high linearity of Kuhne, which presents distortion practically only near the saturation (Figure 46), and the strong non-linearity of the Fujitsu (Figure 48), which also presents a very irregular characteristic. This is probably given by the memory effect of this amplifier, that does not consent to extrapolate correctly the AM-AM characteristic. Regarding the OvisLink, the measurements underlined a behavior similar to the one obtained with the Kuhne amplifier (Figure 47).

In general, the results confirmed the theoretical data provided by datasheets and amplifier documents released by manufacturers.

5 PERFORMANCE METRICS

In this chapter, the principal metrics to measure the distortion level generated by a power amplifier are described. These parameters are also useful to compare different types of linearization systems and then choose the most effective scheme for a particular application. Attention will be given particularly to the special case of an OFDM input signal.

5.1 PEAK TO AVERAGE POWER RATIO (PAPR)

The PAPR is an important parameter, very useful to know when it has to be decided how the power amplifier has to be piloted. This parameter typically is not measured on the amplifier output signal, being more useful when measured for the input signal. PAPR is defined as follows [9]:

$$PAPR_{dB} = 10 * log_{10} \frac{{A_{peak}}^2}{{A_{RMS}}^2} \tag{5.1}$$

Where A_{peak} is the peak amplitude of the input signal and A_{RMS} is the root mean square of the amplitude. High PAPR signal are more sensitive to gain compression because of their higher dynamic with respect to low PAPR signals. Ideally, a perfectly constant envelope signal has a PAPR equal to 0 dB, because the peak amplitude is equal to the average amplitude, and it does not suffer from gain compression.

In [10], the maximum PAPR for OFDM signals has been analytically obtained:

$$PAPR_{dB\ max} = 10 * log_{10} N \tag{5.2}$$

With N the number of subcarriers. This results in an enormous PAPR for a 2048 subcarriers signal (33 dB), thus being quite pessimistic, however it was found experimentally that a real DVB-T 2K transmission, with 2048 subcarriers OFDM modulation, has a PAPR equal to 12 dB, which however is a high value.

5.2 ADJACENT CHANNEL POWER RATIO (ACPR)

One of the most important performance metrics is the Adjacent Channel Power Ratio (ACPR).

$$ACPR_{dB} = 10 * log_{10}\left(\frac{P_{adj}}{P_{ref}}\right) \quad (5.3)$$

It is defined as the ratio between the power of the amplified signal calculated on the bandwidth of the signal itself, P_{ref}, and the out-of-band power P_{adj}, which will potentially cause interference with adjacent channels. This parameter monitors the phenomenon of spectral regrowth.

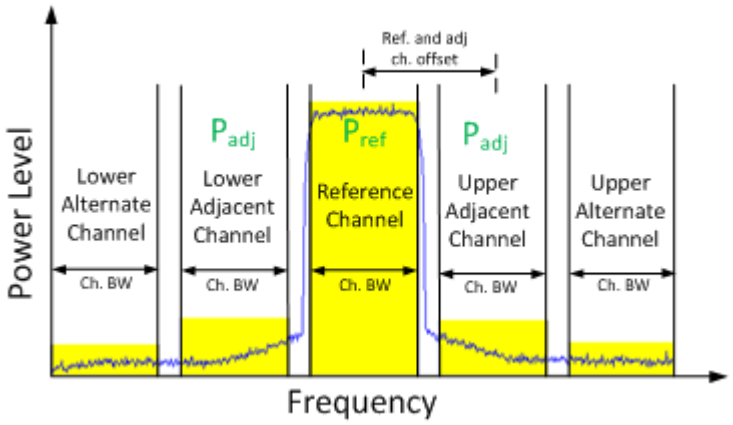

Figure 28 – ACPR definition

5.3 MODULATION ERROR RATE (MER)

The MER gives an indication of how dispersed is the symbols' constellation in relation to the ideal values.

$$MER_{db} = 10 * log_{10}\left(\frac{Average\ Symbol\ Power}{Average\ Error\ Power}\right) \quad (5.4)$$

It is defined as the ratio between the average power of the ideal symbols and the average power of the error vector between these symbols and those actually received. In the case of OFDM signal it has even more importance given that the constellation is not compressed, instead, due to the Fourier transform, it is dispersed around the ideal symbols.

In fact, the MER is equivalent to the SNR for digitally modulated signals, and assumes the same meaning.

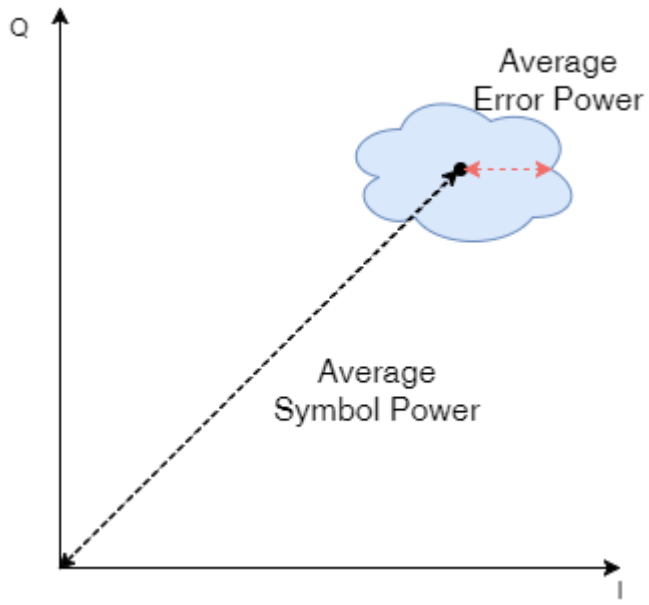

Figure 29 – MER definition

5.4 ERROR VECTOR MAGNITUDE (EVM)

$$EVM_{\%} = \sqrt{\frac{P_{error}}{P_{reference}}} * 100 \tag{5.5}$$

This metric is very similar to the MER, with the difference that in this case the power of the error vector is placed at numerator and at denominator there is the power of the reference symbols. Another difference is that in this case the numerical value is typically expressed as a percentage instead in dB, for which a 0% value indicates an ideal constellation with zero error.

If we consider the special case of OFDM system, the EVM can be expressed as following:

$$EVM = \sqrt{\frac{E\left[\left|cB_k^m - A_k^m\right|^2\right]}{E\left[\left|A_k^m\right|^2\right]}} \tag{5.6}$$

where B_k^m and A_k^m are respectively the received and the transmitted constellation symbols, previously calculated for an OFDM signal distorted by a non-linear PA, and c is a constant value

that compensates the complex attenuation introduced by the PA, and is equal to $\frac{1}{K_0}$, with K_0 the linear gain of the PA. If we use equation (2.14) and substitute *c* in (5.6), we obtain:

$$EVM = \sqrt{\frac{\sigma_D^2}{P|K_0|^2 + \sigma_D^2}} \tag{5.7}$$

with σ_D^2 representing the distortion noise caused by the nonlinearity of the PA, and previously calculated for OFDM systems with rectangular shaping in (2.15), and P the energy of the transmitted symbols.

From this last expression it can be noted that the EVM is proportional to the distortion noise variance, and that it is independent on the size M of the M-QAM modulation used on the subcarriers. Instead, it depends on the IBO (Input Back-Off) used when driving the PA, because σ_D^2 depends on this value, increasing as the IBO decreases.

It is also important to note that the equation (5.7) is calculated under the condition of only non-linear distortion and without thermal noise. However, the effect of thermal noise can be easily taken into account, since it is represented by a white gaussian noise, like the distortion noise with N sufficiently large. Since they are both white gaussian processes and uncorrelated, they can be simply added in power.

5.5 BER IN DISTORTED OFDM SYSTEMS

It has been explained that the EVM is an important parameter when studying distortion effects on OFDM signal, but sometimes it is useful to have also a BER value, which is another important quality parameter. Thus, a useful relation to find would be the BER-EVM relation for OFDM systems.

First, for an OFDM signal the BER is, in general, different for each subcarrier. This means the average BER should be considered, obtained by averaging on every subcarrier. If we consider the same thermal noise on every subcarrier, the equation for the total BER can be expressed as:

$$BER = \frac{2\left(1 - \frac{1}{\sqrt{M}}\right)}{log_2\left(\sqrt{M}\right)} Q\left(\sqrt{\left[\frac{3log_2\left(\sqrt{M}\right)}{M-1}\right] SNR}\right) \tag{5.8}$$

With M the size of the M-QAM modulation adopted. The SNR comparing in this equation has to take into account not only the thermal noise power, but also the nonlinear distortion noise power. Assuming only the thermal noise, and without PA, SNR would be:

$$SNR = \frac{2E_s}{N_0 log_2(M)} \tag{5.9}$$

with E_s the power of the useful signal and N_0 the thermal noise power spectral density. If we consider also the distortion noise, giving the assumption of a gaussian process uncorrelated with thermal noise, the expression for the SNR becomes:

$$SNR = \frac{|K_0|^2 E_s}{\sigma_W^2 log_2 M + \sigma_D^2} \tag{5.10}$$

where K_0 is the constant gain of the amplifier, deriving from (2.11) when the shaping filter has a bandwidth limited from $\left[-\frac{1}{2T}, \frac{1}{2T}\right]$, and σ_W^2 is equal to $\frac{N_0}{2}$**.** This equation represents the so called **Signal to Noise and Distortion Ratio** (**SNDR**), taking into account both the thermal noise and the nonlinear distortion noise power. It can be seen, from (30) and (28), that SNR and EVM are strictly correlated. In particular, if the number of symbols considered for EVM calculation $T \gg M$, we can give the following approximation:

$$SNR \approx \frac{1}{EVM^2} \tag{5.11}$$

Substituting this last equation in (5.8) results in the relation between BER and EVM:

$$BER = \frac{2\left(1 - \frac{1}{\sqrt{M}}\right)}{log_2\left(\sqrt{M}\right)} Q\left(\sqrt{\left[\frac{3log_2\left(\sqrt{M}\right)}{M-1}\right]\frac{1}{EVM^2}}\right) \tag{5.12}$$

6 LINEARIZATION OF A POWER AMPLIFIER

As noted previously, to solve the problem of non-linear distortion introduced by the amplifiers, the best choice, given the previously described target application, consists of some kind of signal processing, without intervening on the amplifier or on the chosen modulation. This means making the AM-AM characteristic linear and the AM-PM characteristic constant. There are many approaches that can be used to linearize the behavior of the power amplifiers.

6.1 PAPR REDUCTION TECHNIQUES

This first technique does not really linearize the power amplifier, instead it operates on the input signal aiming only to reduce the PAPR of the signal. In this way, knowing either the power amplifier characteristic or its output signal is not needed, since the linearization procedure depends only on the input signal.

Basically, with this technique the input signal is subjected to a distortion with the objective of reducing peaks in the time domain signal, or incrementing the average value of the signal power. In both cases, the PAPR decreases, allowing the system to work with a higher input power for the power amplifier, thus reducing the backoff. The easiest PAPR reduction method is the clipping technique, where the input signal is just clipped if the amplitude exceeds a certain value. This threshold is chosen in a way so that the loss of signal quality given by distortion introduced by the clipping is compensated by the gain of quality due to the less distortion given by the amplifier.

The main advantage of this approach is the easy implementation, because we completely forget of the power amplifier characterization, but, on the other hand, it achieves poor performances compared to other linearization systems.

Here are some PAPR reduction schemes that can be found in literature:

- **Amplitude Clipping**, used in system presented in [38] for an OFDM input signal.
- **Partial Transmit Sequences**, discussed in [39] also in this case with OFDM modulated signal.
- **Tone Injection**, implemented in [10].
- **Tone Reservation**, presented in [10].

6.2 FEEDBACK AND FEEDFORWARD

These are the first methods proposed for linearization. With the feedback [23] scheme the amplifier output is scaled, the sign reverted, and reported to the amplifier to change the input signal. In feedforward approach [22] the difference between the amplifier output and its input is calculated, then with this information the output of the HPA is modified. Compared to the first method, it is

more difficult to implement because of the high linearity required on the feedforward path; however, it is unconditionally stable, unlike the feedback scheme that suffers from stability problems.

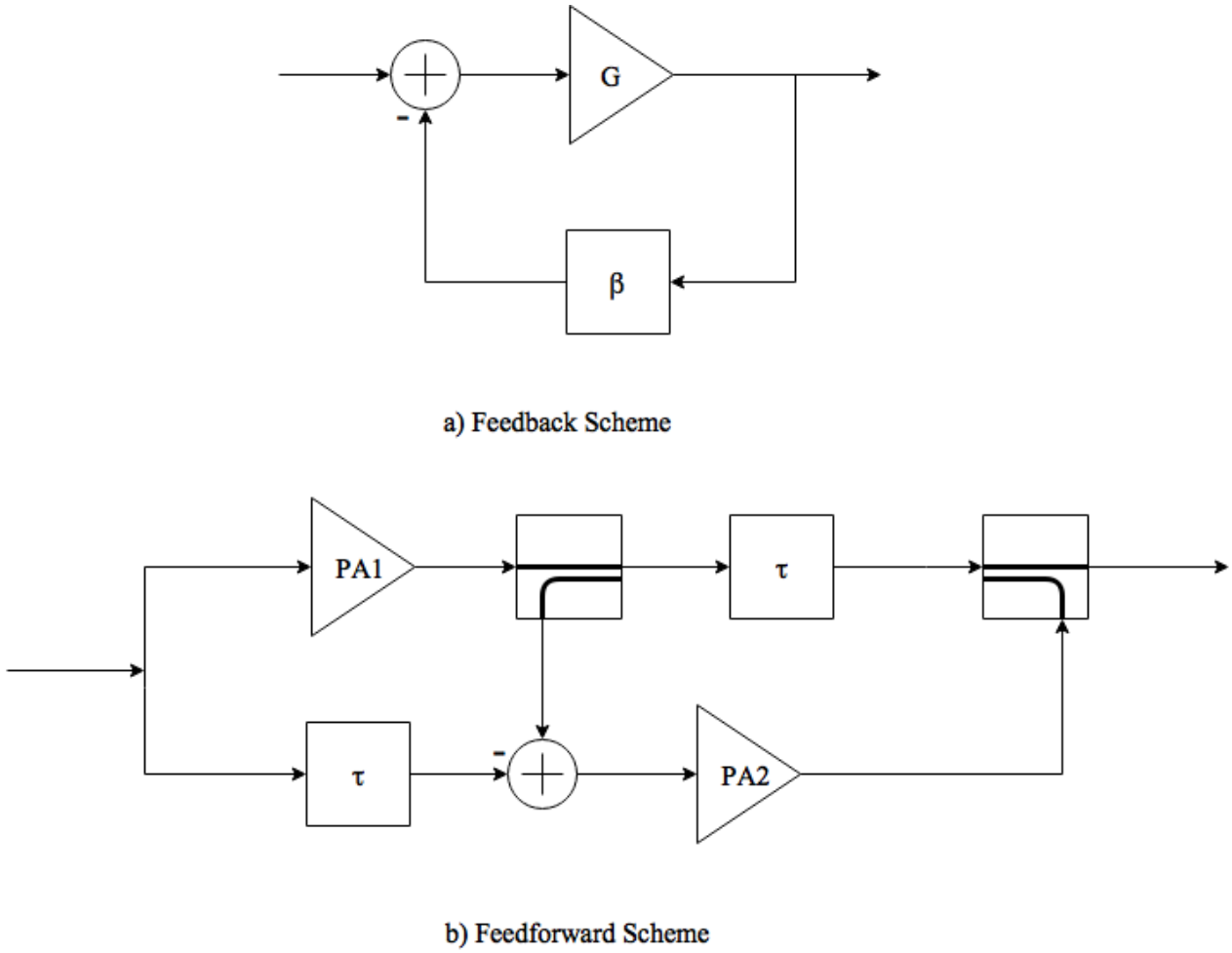

Figure 30 - Feedback and Feedforward predistortion schemes

There are several variants of feedback linearization. They can be classified into two main groups: **RF feedback** and **Modulation feedback**. The passive feedback (see [21] for an example of implementation), active RF feedback (with voltage divider replaced by an active stage) and distortion feedback (only the nonlinear distortion components remain in the feedback) are the three typical examples of RF feedback approaches. The modulation feedback approach returns the feedback from RF back to the modulation (baseband) level. In other words, the upconverters are included into forward path. Thus the feedback can compensate also for the nonlinearity of upconverters.

6.3 ENVELOPE ELIMINATION AND RESTORATION (EER)

With this technique the input signal, amplitude and phase modulated, is divided into two components; one is the envelope of the signal and the other is its phase [26]. The signal in the first path is amplified by a linear audio amplifier, in the second path, given the constant envelope of the

signal, is amplified by a nonlinear amplifier with high efficiency. The amplitude modulation is then re-applied through a further amplifier whose input is the phase modulated and amplified signal, and whose power supply is given by the amplified amplitude-modulated signal. In [27] an example of implementation for this linearization system is discussed.

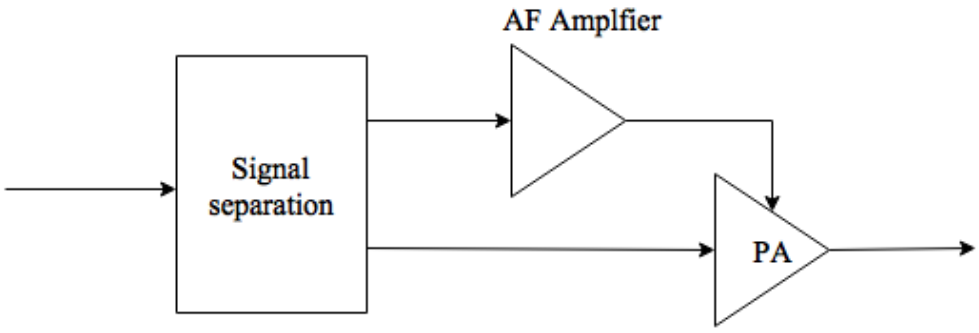

Figure 31 - EER Amplification

6.4 LINEAR AMPLIFICATION USING NONLINEAR COMPONENTS (LINC)

Also in this case the signal is divided into two components, but unlike in EER approach, both are phase only modulated, so as to have constant envelope [24]; In this way non-linear amplifiers on both paths can be used. The two signals are then recombined to form the desired signal. The disadvantage of this technique is the high complexity required by the generation of the two constant envelope signals.

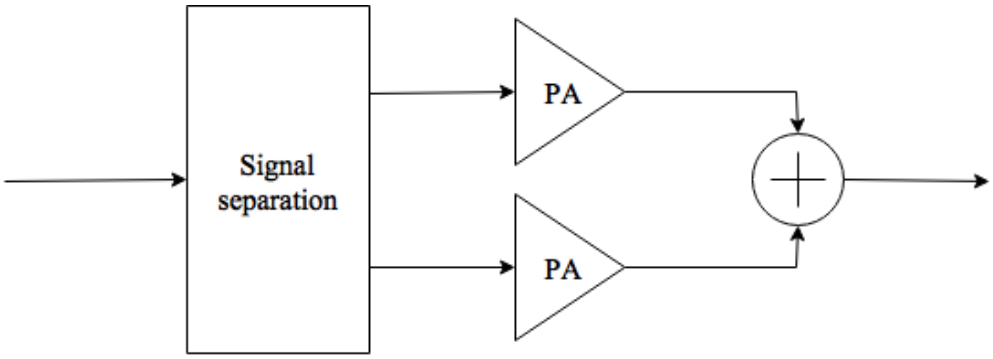

Figure 32 - LINC Scheme

An implementation of this technique for the particular case of OFDM input signal can be found in [25].

6.5 PREDISTORTION

The goal of this solution is to insert a signal processing block, before the amplifier, able to reverse the amplifier output characteristic, thus being able to obtain a linear amplification. The predistortion device is not too complex to implement in hardware, and can also be implemented so as to ensure unconditional system stability. This system, chosen as the linearization method to be used in this thesis, will be further discussed in the next chapters.

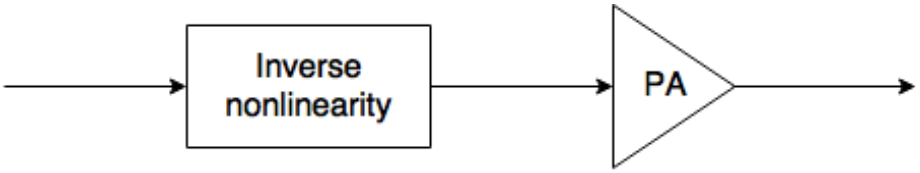

Figure 33 - Basic Predistortion Scheme

7 PREDISTORTION

Predistorting a signal means introducing a specific nonlinear distortion on the signal to be transmitted to compensate the one introduced later in the signal path from the amplifier, thereby obtaining an output signal of the latter which does not suffer from the problems arising from the nonlinearity of the HPA. The basic idea is to use a DSP block, the predistorter, capable of reversing the amplifier characteristic and then apply an inverse nonlinearity to the signal.

What a predistorter basically do is to give the PA an input which generates the desired signal at the amplifier output. To obtain this result the predistorter needs to know the behavior of the power amplifier, typically this means the AM-AM and the AM-PM characteristics must be known or extrapolated in some way.

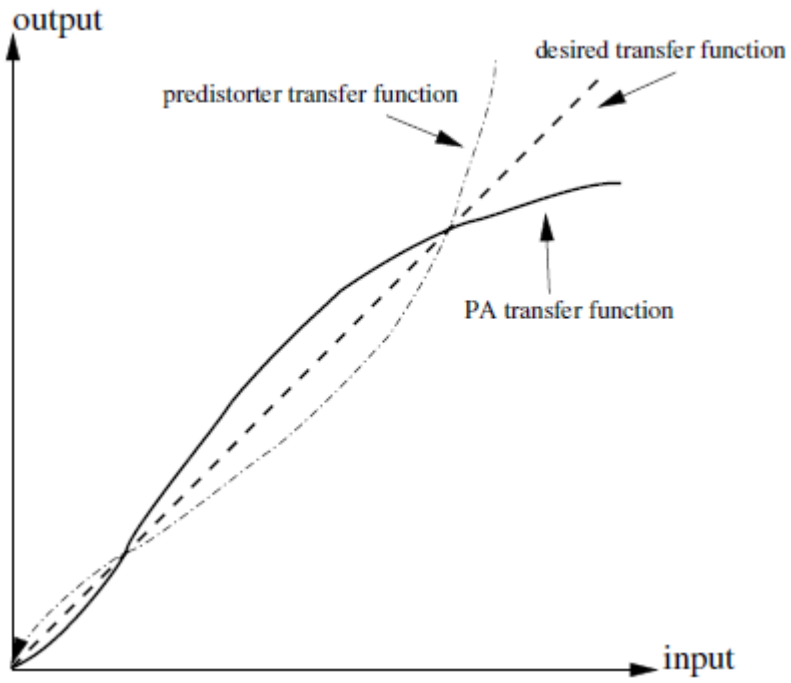

Figure 34 - PA and Predistorter Transfer Functions

According to the predistorter position within the communication system, a first classification of these systems can be given.

7.1 RF PREDISTORTION

The radiofrequency predistortion operates directly on the amplifier input signal, at the working frequency of the latter. The advantage of this approach lies in the ease of the hardware implementation, the disadvantages however are represented by the poor obtainable performance improvement and by the dependence on the operating frequency. The predistorter in fact is designed

to work in correspondence of that frequency, and consequently it can't operate for other values of the carrier frequency.

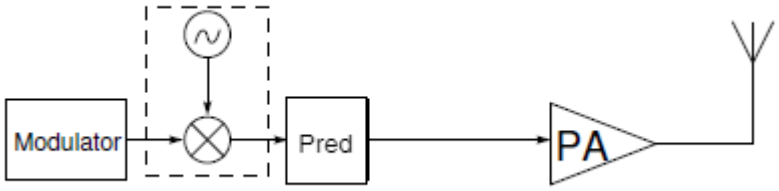

Figure 35 - RF Predistortion Scheme

A developed RF predistortion system can be found in [29].

7.2 IF PREDISTORTION

In this case the signal is predistorted prior to an intermediate frequency (IF) and then shifted to the carrier frequency before going to the amplifier. This makes the system adaptive to different values of operating frequencies, and also allows the use of elements that would not work at the carrier frequency. However, the frequencies are still very high and the use of DSP blocks is limited by the need to have a very large sampling frequency. Another problem is given by the high power consumption of the high-speed converters. One example of this technique is presented in [28].

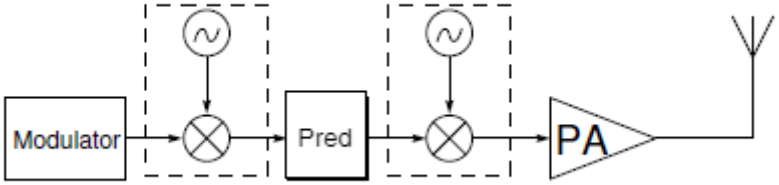

Figure 36 - IF Predistortion Scheme

7.3 BASEBAND PREDISTORTION

The baseband predistortion, sometimes defined data predistortion, is probably the most common technique for this type of processing. The signal is processed immediately at baseband, at a constellation level (with variable-amplitude modulation signals), and this allows to easily work in digital, opening the doors to the use of DSP, and consequently to complex processing of the signal to be transmitted. It is also possible to design a predistortion device of this type with analog components, but having to work both on the phase and the quadrature paths it would require two identical systems, and this is very difficult to obtain.

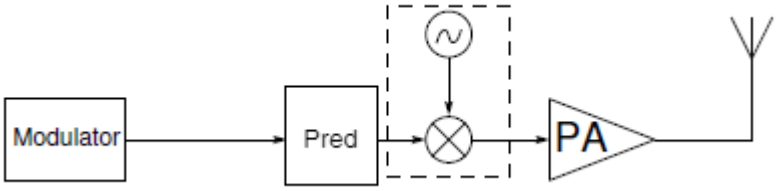

Figure 37 - Baseband Predistortion Scheme

7.4 POST-DISTORTION

The post-distortion is made typically at the receiver, so as to compensate also for the effect of the channel. In this way, however, the problem of out of band emissions is not solved. Moreover, the post-distorter has to work with the power levels present at HPA output, and this is a great disadvantage. An implementation of this technique is discussed in [32].

7.5 CLASSIFICATION

PA characteristics may vary with time, due to temperature variations or aging. For this reason, the design of a good predistorter that does not take these variations into account is not sufficient for those systems that require high-linearity PA. Thus, a feedback from the PA output to update the predistorter characteristics is needed, so that the predistortion function follows the variations of the PA transfer function. Based on the presence of this feedback, the predistortion systems can be further classified.

7.5.1 Adaptive predistortion

The predistortion system considers the amplifier characteristics changing due to temperature variations and aging. This is typically done via a feedback that takes the PA output back to the input to calculate an error and update the predistortion parameters. Stability is a crucial point for these systems.

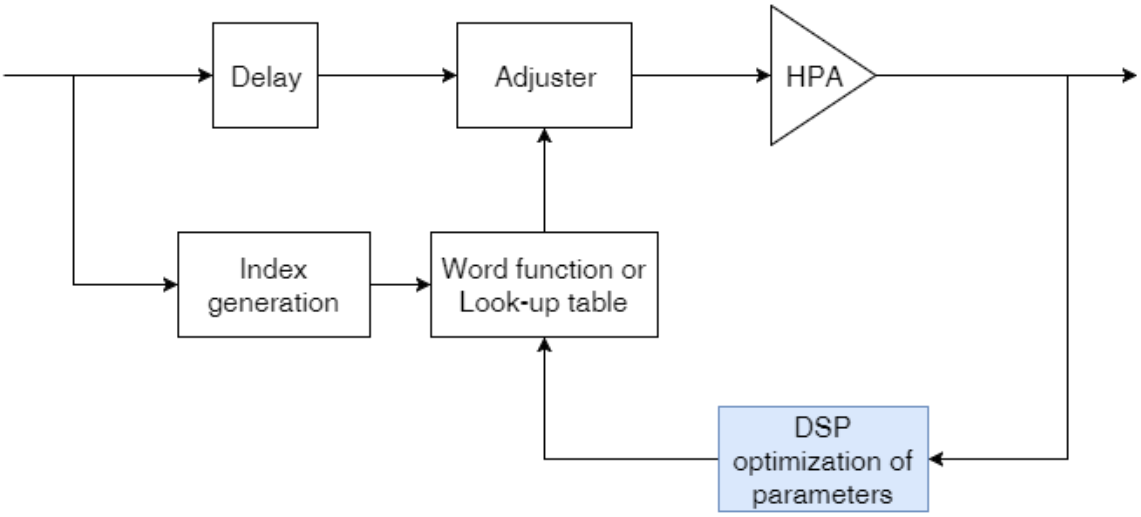

Figure 38 - Adaptive Predistortion Scheme

Knowing the PA characteristics is not necessary since, thanks to the feedback, they can be obtained using a training signal or modifying the original input signal to explore the entire amplitude scale of the PA.

A big problem for these systems is instead the necessity of a delay block in the forward path: the input signal needs to be delayed to let the adaptation algorithm calculates the error between the PA output and the associated PA input, and to update the correspondent look up table entry.

7.5.2 Non-adaptive predistortion

The system is static and does not change its characteristics with time. This means easier implementation but less precision. Also, it is necessary to know the PA behavior, typically the AM-AM and AM-PM characteristics, to design the predistorter.

If PA characteristics do not change too much with time this predistortion system can obtain nearly the same results of the adaptive one with much less computational complexity.

8 BASEBAND PREDISTORTION

Baseband predistortion is the most used technique to predistort a signal in the digital domain. This is because of the lower frequency of work with respect to RF or IF predistortion. For these reason this type of predistortion is easier to implement on DSP or FPGA board. Another important advantage of this technique lies in the possibility of a simple extension to an adaptive form. The only problem in the adaptive form is that in the feedback path the signal has to be demodulated back into baseband.

Basically, baseband predistortion algorithms can be divided into two main categories, on the base of the position of the predistorter in the transmission system.

8.1 DATA PREDISTORTION

These systems try to compensate the PA distortion on the constellation diagram, working with complex baseband symbols. They are simpler to implement, but the big problem is that they are modulation dependent, since the predistortion is applied before the modulation in the transmission system. Also, since the signal is predistorted before sampling and filtering, this technique is not able to compensate for the Adjacent Channel Power Ratio.

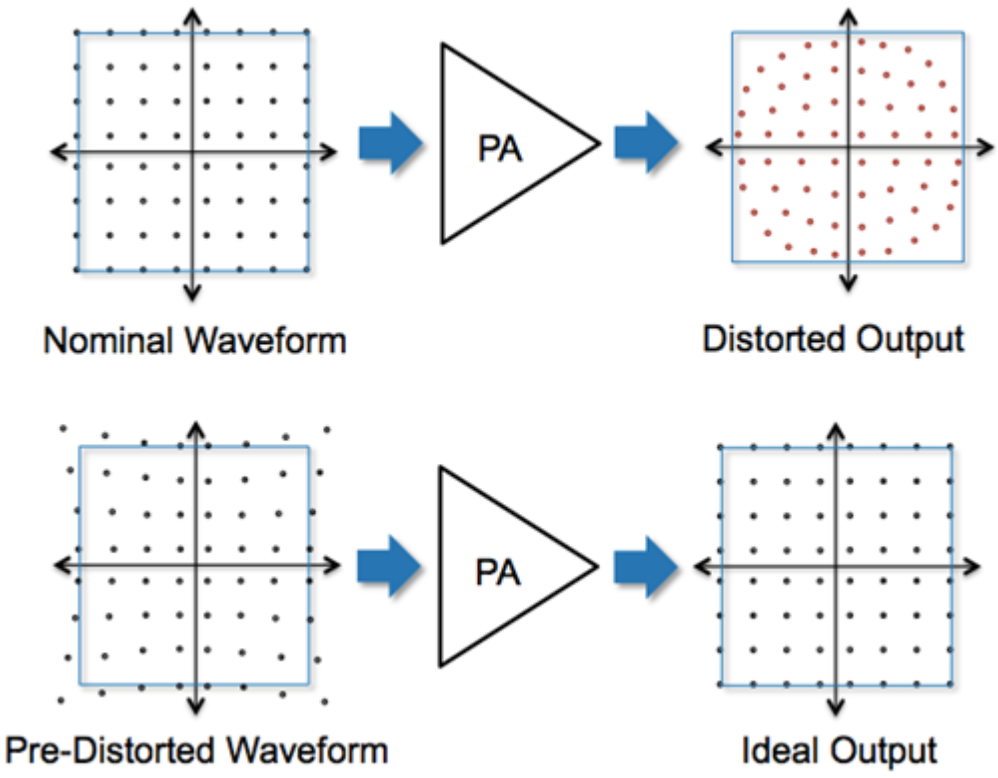

Figure 39 - Data Predistortion

An example for this technique can be found in [30], and in [14] another implementation is studied for the particular case of OFDM input signal.

8.2 SIGNAL PREDISTORTION

These systems generally work on the signal, after modulation and the pulse shaping filter. The advantage is that they are independent on modulation format, but the problem is that the large dynamic of signal amplitude slows down the adaptation speed.

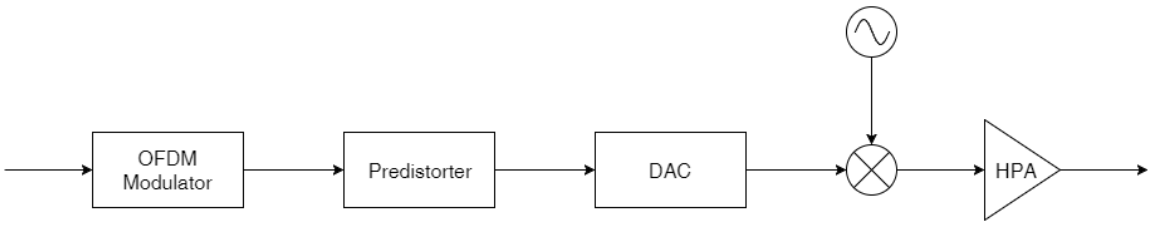

Figure 40 - OFDM signal predistortion

In case of OFDM signal, the data predistortion is really difficult, because the *IFFT* made by the modulator completely transforms the data symbols in a noise-like signal, therefore the predistortion on the constellation symbols is useless. For this reason, with input signals having these modulation schemes, most of the developed predistortion systems are based on signal predistortion, like [11,12].

Another classification of baseband predistorter can be given on the base of the form of the predistorter characteristic. In particular, we can find two main categories.

8.3 PARAMETRIC PREDISTORTION

This type of predistortion approximates the curve of the amplifier with a nonlinear function (polynomial, spline, Volterra series etc.). It is a bit imprecise, however this is acceptable for quite linear amplifiers because of the small number of parameters required [31]. When using more distorting amplifiers the nonlinear function becomes very complicated (it needs higher orders for the polynomial function) and the computational cost increases, discouraging the use of this type of predistortion.

8.4 BASEBAND LUT PREDISTORTION

This predistortion system is based on a **Look Up Table** (LUT) addressed by input signal amplitude or power. The number of parameters is high compared to parametric predistortion, because the parameters are the LUT entries, which have to be a lot to have good performances, but the computational cost does not increase with the nonlinearity order of the PA characteristic, and good results can be obtained for every kind of nonlinearity. Implementation examples of this approach can be found in [11,12].

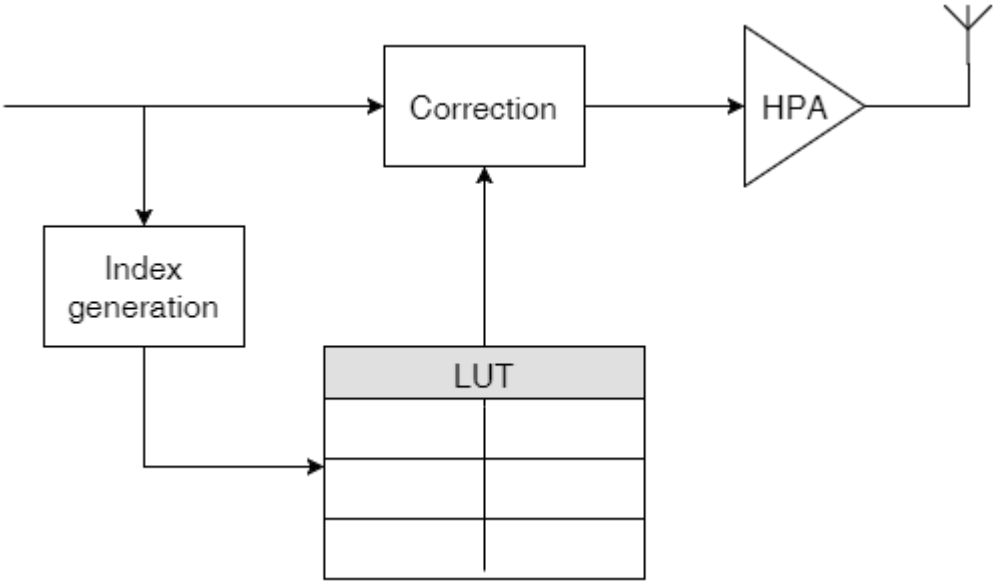

Figure 41 - LUT predistortion basic scheme

Our proposed algorithm is based on this last type of predistortion, so it will be further described in the next chapters.

9 BASEBAND LUT PREDISTORTION

The proposed algorithm that will be further discussed after in this thesis is a baseband LUT predistorter. This choice was naturally given because of the architecture on which the predistorter is based. A software predistorter of course cannot operate analogically, and this excluded RF and IF predistortion.

LUT predistortion was chosen for this thesis because of the easier hardware implementation compared to the parametric one.

There are two types of LUT predistortion we can find in literature: mapping LUT predistortion and complex gain LUT predistortion.

9.1 MAPPING LUT PREDISTORTION

This technique was first introduced by Nagata [11] when LUT predistortion was developed. With this approach the correction values in the LUT are complex numbers to add to the input sample, again complex. This means the algorithm maps each input complex input sample in a corresponding complex output sample. The LUT so is 2-dimensional, and it is addressed by two indexes: the I component and the Q component of the input sample.

The main drawbacks of this approach are the large LUT size, which leads to slow adaptation, and the need for a phase recovery in the feedback path. This is necessary since the LUT values to be updated are addressed by real and imaginary part of the amplifier output sample, so amplitude and phase are needed.

9.2 COMPLEX GAIN LUT PREDISTORTION

This second group of LUT based predistortion methods is more recent, and it was proposed by Cavers in [12]. In this approach the predistorter output is obtained by multiplication of the input signal and a specific gain factor, representing the LUT correction value. As the PA characteristic distorts generally both amplitude and phase of the input samples, these gain factors have to be complex.

Thanks to the fact the phase and amplitude distortion on the output signal both depends only on amplitude of the input signal, the LUT can be addressed by the amplitude of the input signal only, or by its square in most cases. This means reduced size of the LUT compared to mapping predistortion. This leads also to more speed in the adaptation process, and makes the adaptation algorithm also easier to implement, because the phase recovery is no more necessary.

Complex values in the LUT can be expressed both in Cartesian and Polar coordinates, leading to two different predistortion schemes. The difference is only either the presence or absence of coordinates converter.

9.3 ADAPTIVE SCHEMES

Different strategies can be adopted to make the predistortion algorithm adaptive. The parameters which defines the goodness of an approach are the adaptation time, that we want to be the lowest possible, and the hardware complexity to implement the method.

Here are some schemes typically adopted in predistortion systems:

- Linear iteration method
- Secant method
- RLS (Recursive Least Squares)
- LMS (Least Mean Squares)

9.3.1 Linear iteration method

This is the simplest method to design an adaptive predistorter. The LUT values are updated one at a time when each value is indexed by the input signal. A simple error is computed and, after being scaled by a certain parameter, the result is added to the LUT value to be updated. The iterative formula can be derived as [33]:

$$LUT_{n+1} = LUT_n \left(1 + a\left(\frac{V_{out}(n) - V_{in}(n)}{V_{out}(n)}\right)\right) \tag{9.1}$$

Where *n* is the index of the current iteration, LUT_n is the value of the LUT entry corresponding to the input amplitude value $V_{in}(n)$ and $V_{out}(n)$ is the PA output envelope. The parameter *a* is the constant that determines the convergence speed of the algorithm.

The main advantage is the easy hardware implementation, but on the other hand the adaptation is really slow. This method is used in the Nagata predistorter [11], without the division by $V_{out}(n)$.

9.3.2 Secant method

With this approach the computed error takes into account not only the current input sample and LUT value, but also information about the previous values. This method is faster than the linear method, but the hardware complexity is increased by the necessity to know past values of input signal and LUT entries. Secant method formula can be expressed as [34]:

$$LUT_{n+1} = LUT_n - a\,\Delta V(n)\left(\frac{LUT_n - LUT_{n-1}}{\Delta V(n) - \Delta V(n-1)}\right) \tag{9.2}$$

In (9.2), $\Delta V(n) = V_{out}(n) - V_{in}(n)$ and *a* assumes the same meaning it had for linear iteration method. This is the LUT update technique adopted by Cavers in [12].

9.3.3 RLS and LMS

Differently from the two methods described above, both RLS and LMS techniques update the whole LUT at once. This operation requires more computational power and the complexity increases rapidly as the number of LUT entries increases. However, they are more suitable for compensation of PA memory effects which require several codependent functions to be updated simultaneously [35].

The difference between RLS and LMS is that the first has a faster convergence with increased computational complexity, the second is easier to implement but with slower convergence. An example for RLS technique is found in [36], while LMS is the adopted algorithm in the system presented in [37]

10 PROPOSED ALGORITHM

For this thesis a software predistorter has been implemented. Basically, it performs a digital predistortion (DPD) on the baseband OFDM signal, then feeds the signal to the power amplifier. This predistorter needs to know the characteristic of the HPA to work, despite an alternative MATLAB script has been implemented which can adaptively find the characteristic simply feeding the HPA with a training signal specifically developed.

The developed linearization system is memoryless. This is not the optimal choice for an input signal like the OFDM one, because the very wide bandwidth of these signals generates memory effects when passed through power amplifiers. However, the loss of performance given by this effect should be irrelevant compared to the increase of computational power needed, so a simpler predistortion scheme like the memoryless predistortion was chosen.

10.1 SIMULATION BLOCK DIAGRAM

In Figure 42 the block diagram relevant to the MATLAB environment used to obtain the predistorted transmission file is presented.

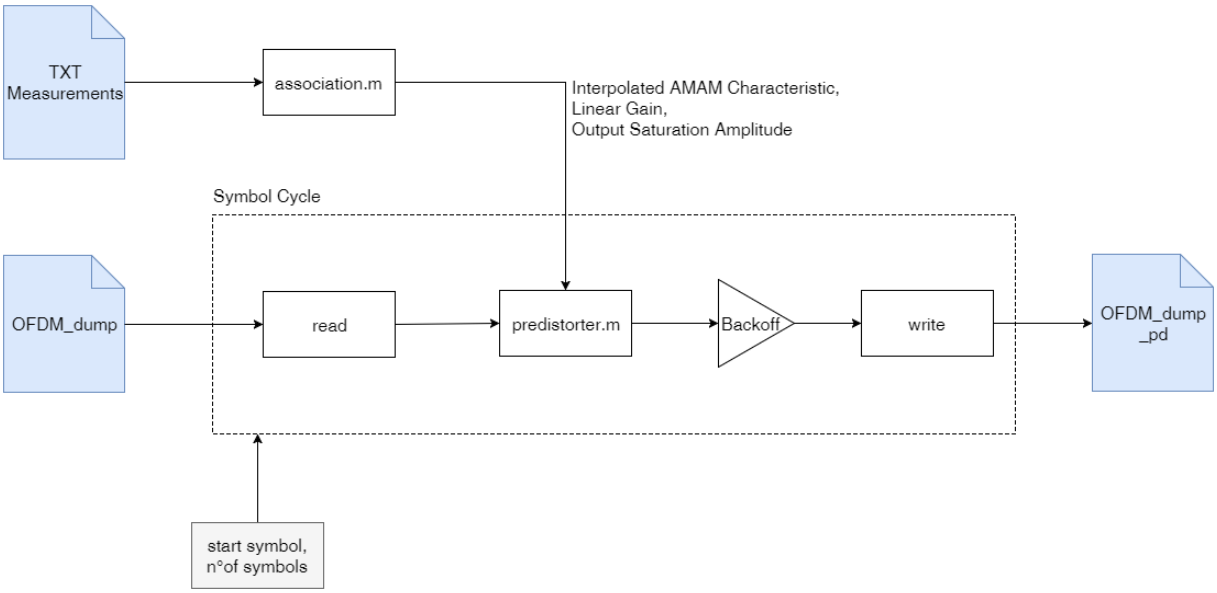

Figure 42 – Simulaton environment description

10.2 BASIC OPERATING MODE

In its basic configuration, the algorithm performs the following operations. Once measured the AM-AM characteristic, the algorithm creates the LUT starting from the given points and then linear interpolates the latter to have a higher number of entries, to obtain more accuracy. The predistorter logic block simply takes the amplitude of the input sample, calculates the ideal amplitude of the output sample, and search the PA characteristic for the input value that gives the desired output

amplitude. Since there are a limited number of entries in the LUT, the algorithm chooses the best approximation of the desired output amplitude and returns the correspondent amplifier input value.

To improve the accuracy, linear interpolation between the entries has been implemented. The software finds the two entries which are the nearest to the desired value, then calculates the angular coefficient *m* and the constant value of the straight line between them. Finally, it uses these parameters to calculate the value the amplitude of the predistorter output should have. Of course this additional block of signal elaboration is paid with more powerful hardware required for a hardware implementation.

The number of points of the LUT is fixed to 500. This number is very important, because the accuracy of the predistortion depends on it; furthermore, increasing this number also leads to increased computational cost for the hardware implementation.

10.2.1 LUT indexing

LUT predistortion schemes performances depend especially on LUT parameters, such as dimension, indexing function, and update algorithm.

The proposed system uses power indexing, this means that the input signal power is calculated and used to index the LUT. In practice the square amplitude of the current sample, converted in dB, is computed. The dB conversion is very important, because the OFDM signal has a power histogram that is too concentrated near the zero if we consider the linear power, but it is more uniform when we use the dB representation. In other words, a typical OFDM signal has a lot of samples with low amplitude, and few samples with large amplitude, so it is better to use a logarithmic uniform distributed LUT instead of a linear one. This can be further explained by Figure 43 and Figure 44.

10.2.2 LUT generation

Regarding LUT generation, this simpler basic operation mode creates the LUT starting from the measured AM-AM characteristic of the power amplifier. This means a previous measure of this characteristic is required to apply the predistortion. If the amplifier behavior is easily obtainable and if its characteristics do not change excessively with time, this operation scheme is reasonably applicable and it is more than sufficient to obtain good results.

Once obtained the AM-AM characteristic, the measured data are elaborated to extrapolate an analytic model that better approximate the behavior of the power amplifier. For this predistorter, Rapp model has been chosen, because it is a simple analytic approximation which however fits very well a lot of power amplifiers, included those used in this thesis.

Other analytic model can be easily used to predistort the signal. Also Saleh model and Memoryless polynomial model have been implemented by simple MATLAB functions. This is the great advantage using software predistortion, that is the ability to change the amplifier model quickly according to the power amplifier to linearize.

10.3 ADVANCED OPERATING MODE

As written before, an adaptive version of the predistorter also has been developed. This algorithm is very different from the non-adaptive ones, because it does not need to know the AM-AM characteristic of the PA. The algorithm has a feedback that compare the input signal and the scaled output signal, calculating an error. This error then is used to correct the LUT value indexed by the input signal.

10.3.1 LUT indexing

For the LUT indexing the same approach of basic operating mode has been used. In adaptive predistortion the LUT indexing is important not only for the precision of the predistorter but also for the adaptation speed. Because of the chosen adaptation algorithm, which is based on linear iteration method, LUT values are updated only when indexed. This means that if the access probability for a certain LUT value is not uniformly distributed, the adaptation process requested time increases. Also for this reason the best indexing function would be the one which gives equal access probability for each LUT entry.

10.3.2 LUT generation

The LUT generation, in adaptive predistortion techniques, can be done without the knowledge of the PA characteristics. This is a very important advantage, because sometimes the AM-AM characteristic of the PA used in a communication system is very difficult to obtain. In the developed algorithm, the LUT values are first initialized to ones, then a training signal has been generated and sent as input signal to the amplifier. The training signal that we used consists of a power sweep covering the entire range of power reached by the LUT, with a length of 1200 samples. Every LUT entry first is initialized to one, then the training signal spans more times the input power of the power amplifier, letting the adaptation algorithm update the LUT values each time. The time domain signal amplitude can be seen in Figure 45.

10.3.3 LUT update

Regarding LUT update, the procedure simply consists of an update of the current indexed LUT entry. The error between HPA output sample and the ideal scaled input sample is multiplied by a scaling factor and then added to the indexed LUT value. In this way, LUT values are updated one at a time, every time that value is indexed.

An alternative method to update the LUT would be to update the entire table in one single time, once every specific time interval, which of course will control adaptation speed. Anyway, for this particular algorithm, the first described method has been used.

Of course LUT update is useless if we do a single test with the predistorter and HPA to compare results, but if we imagine to use this algorithm in real application, thus operating in real time, it becomes a very important feature. In the simulation results this feature will not be used, because the amplifier's characteristics do not change during one single transmission of the signal.

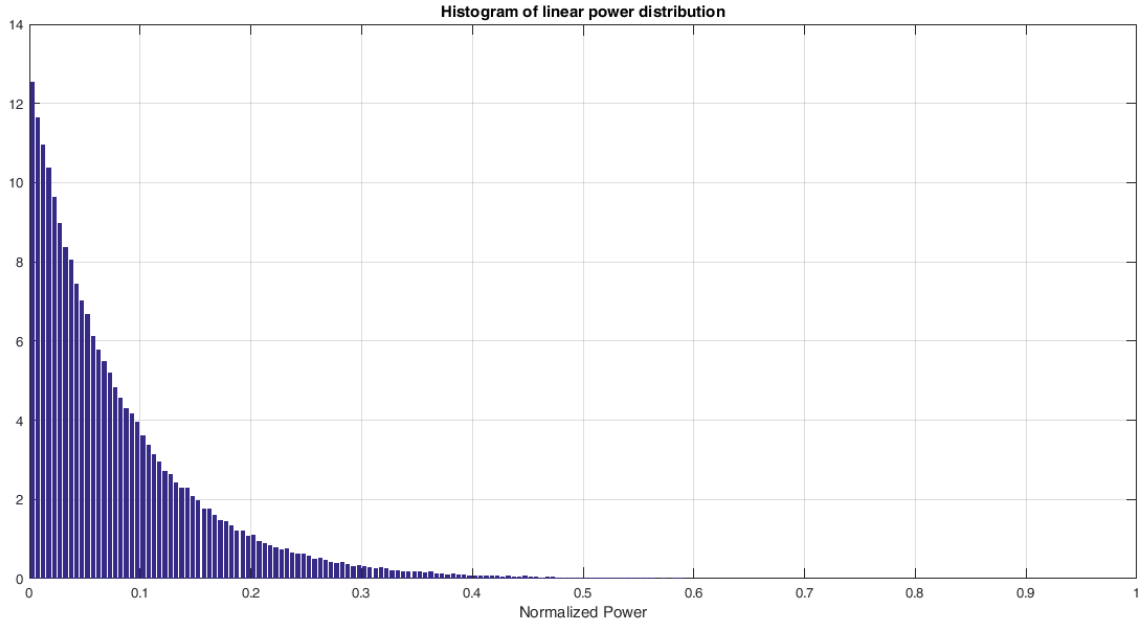

Figure 43 – PDF of linear values of signal power relevant to symbols 500-600

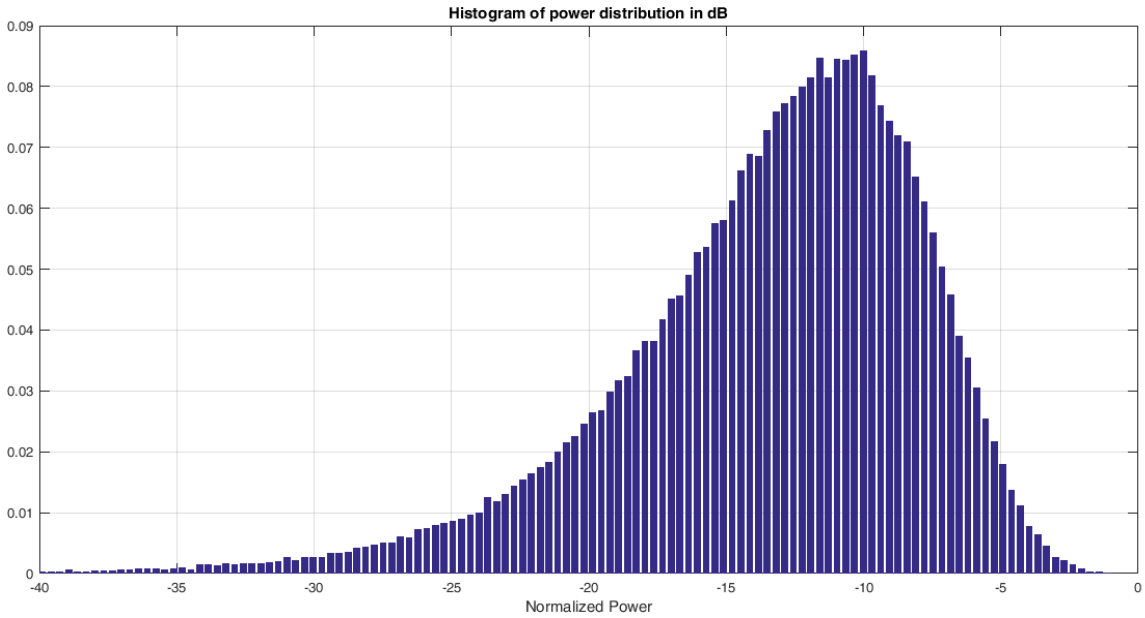

Figure 44 - Logarithmic representation of the PDF of signal power relevant to symbols 500-600

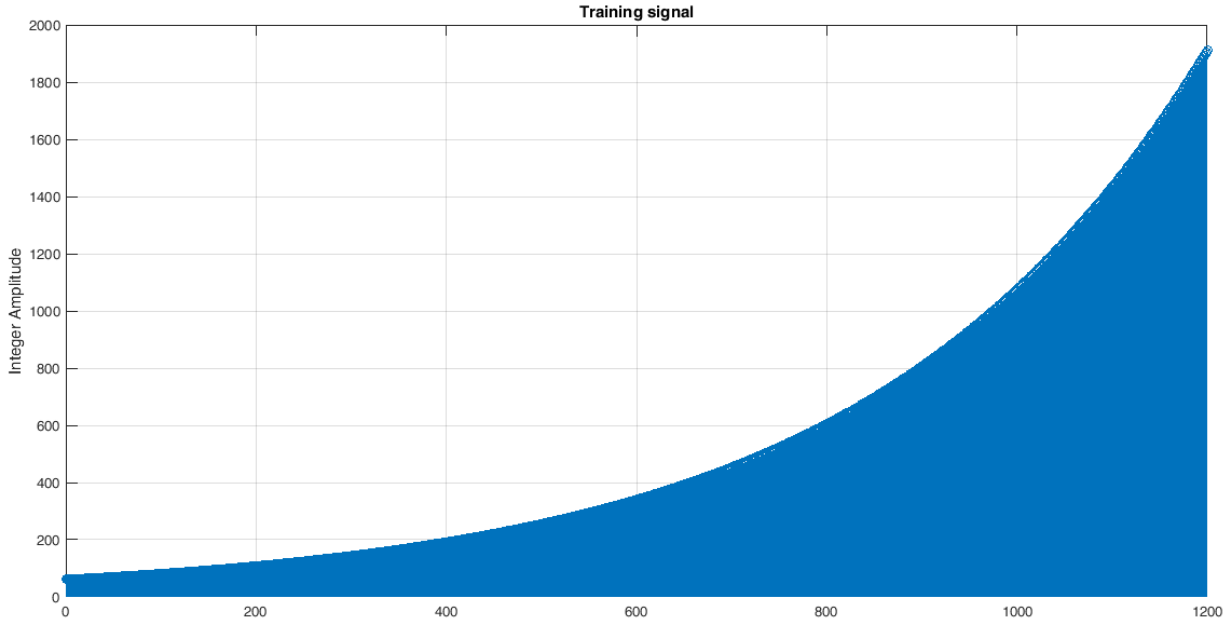

Figure 45 - Amplitude of training signal discrete values

The behavior is not linear since the plot is relevant to linear values of amplitude. If logarithmic amplitude was plotted, this would be a linear ramp. This choice was made to correctly fill the LUT, because the table entries are uniformly distributed when expressed in dB.

Adaptation speed could be calculated on the basis of the number of spans of the training signal required to reach the convergence of the LUT values.

11 SIMULATIONS

11.1 SIMULATION WITH ANALYTIC MODEL OF PA

In this first simulation the implemented predistorter has been tested through a number of MATLAB scripts, using either an amplifier described by an analytic function or by interpolating measurements made before.

11.1.1 Amplifier modeling

Rapp model has been chosen to give an analytic model to the PA, since it typically describes very well a solid state power amplifier behavior. A MATLAB function that associates measured data to the correct Rapp model has been implemented. This function calculates the parameters of the Rapp model (smoothness factor, gain, output saturation power) which best fit the measured AM-AM characteristic, read by a TXT file containing input and output power expressed as dB.

Each amplifier has been characterized through Rapp model, obtaining three sets of parameters used in the simulation.

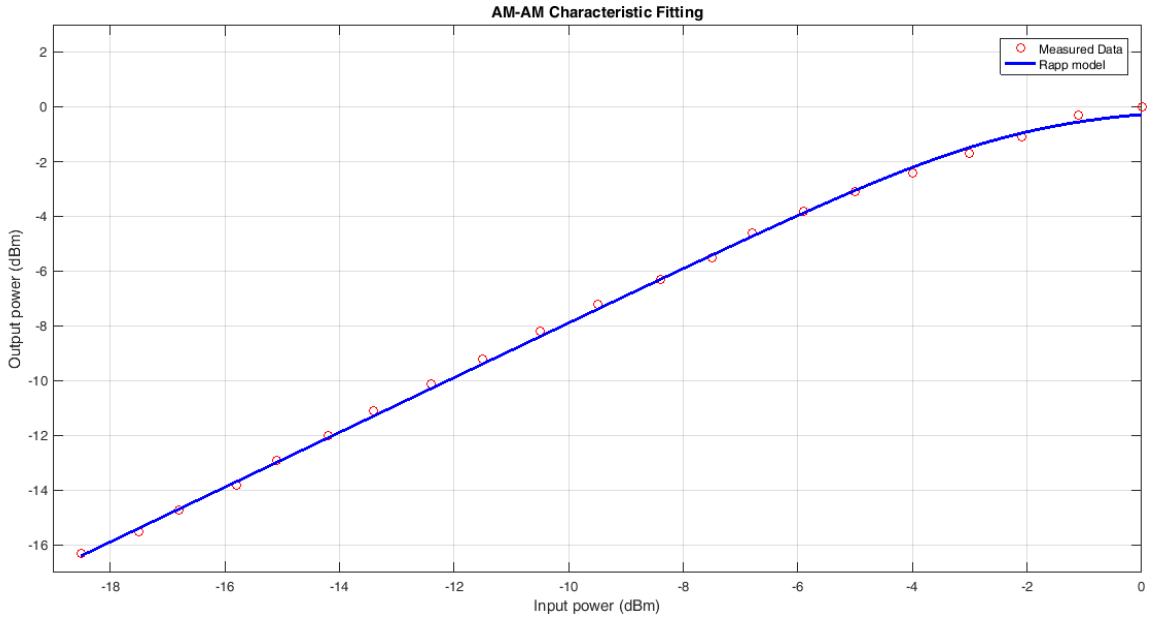

Figure 46 - Kuhne AM-AM characteristic fitting with Rapp model

For the second amplifier, the OvisLink, Rapp model has been chosen again, even if the fitting isn't so good. We can note from Figure 47 that the Rapp approximation does not follow very well the non-linearity at low input power values, but fits reasonably good the PA behavior near the saturation, which is the region we are more interested to represent.

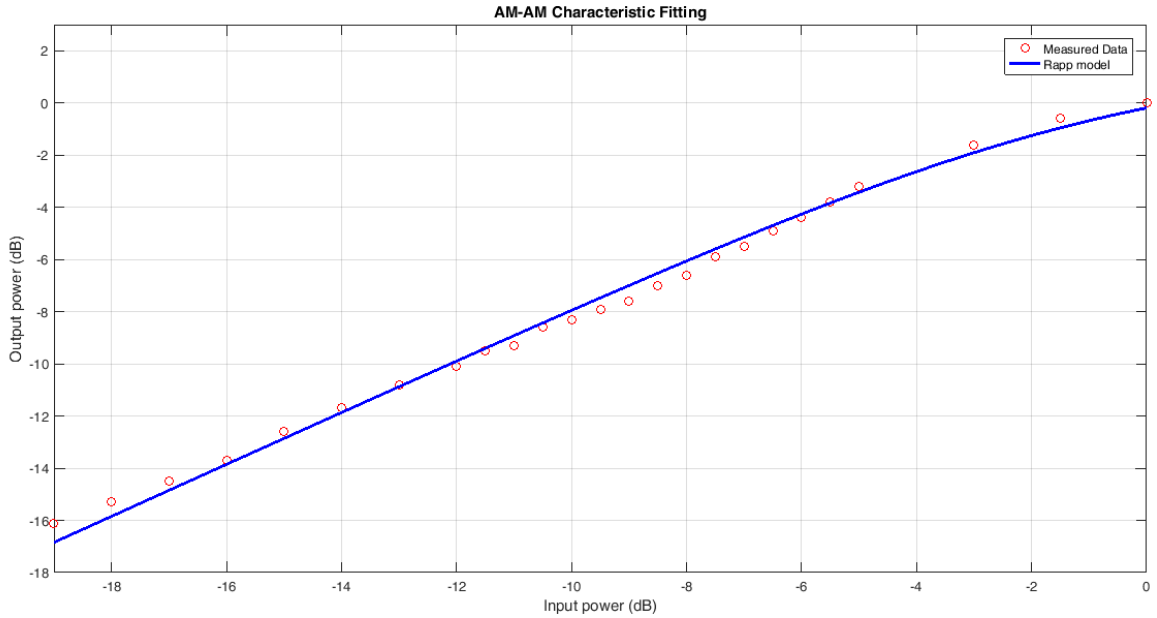

Figure 47 - OvisLink AM-AM characteristic fitting with Rapp model

It can be noted from Figure 48 that for the Fujitsu amplifier, a second curve fitting has been made. This is due to the strong non-linearity of the amplifier, that does not fit very well with Rapp model. To characterize this amplifier so it was used a memoryless polynomial model, which is a far better approximation, but requires more computational power.

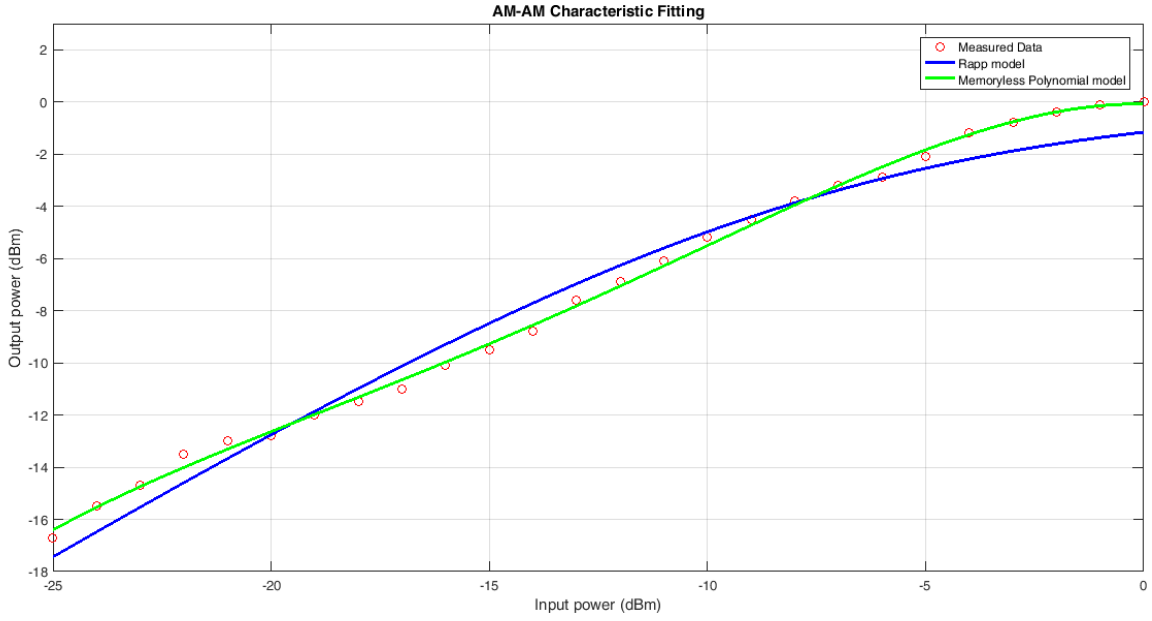

Figure 48 - Fujitsu AM-AM characteristic fitting with Rapp and memoryless polynomial model

Concerning the AM-PM characteristic, as written before, Rapp model does not take it into account. For this reason, it has not been considered also for the simulation. However, the MATLAB script

has the possibility of considering also AM-PM characteristic, simply using a fifth-order polynomial approximation that fits the measured data.

In Table 1 the parameters obtained by this fitting are presented, relevant to the two amplifiers represented with Rapp model.

	ρ	Linear gain (dB)	Output saturation power(dBm)
Kuhne KU PA 242 TX	1.8	20.7	38
OvisLink Airlive WPA-2400IG	2.1	10	31

Table 1 - Parameters fitting for the amplifiers

11.1.2 Predistortion

The next step to obtain the numerical results is to predistort the file coherently with the previously measured AM-AM characteristic. The procedure is similar to the one described previous: for a certain predistorter input value, the algorithm finds the value that, given to amplifier input, produces the desired output value with a linear behavior. Also AM-PM correction is possible. To compensate the phase distortion, the algorithm searches the value of the phase deviation introduced by the amplifier corresponding to the predistorted amplitude, then reverts this value and applies the resulting phase to the input sample.

In Figure 49, a block diagram shows the logic procedure followed to run the simulation. Also, before writing the predistorted CUT file, a MATLAB script has been run to check the correct operation of the various MATLAB functions used in accessing the CUT file, in both reading and writing mode.

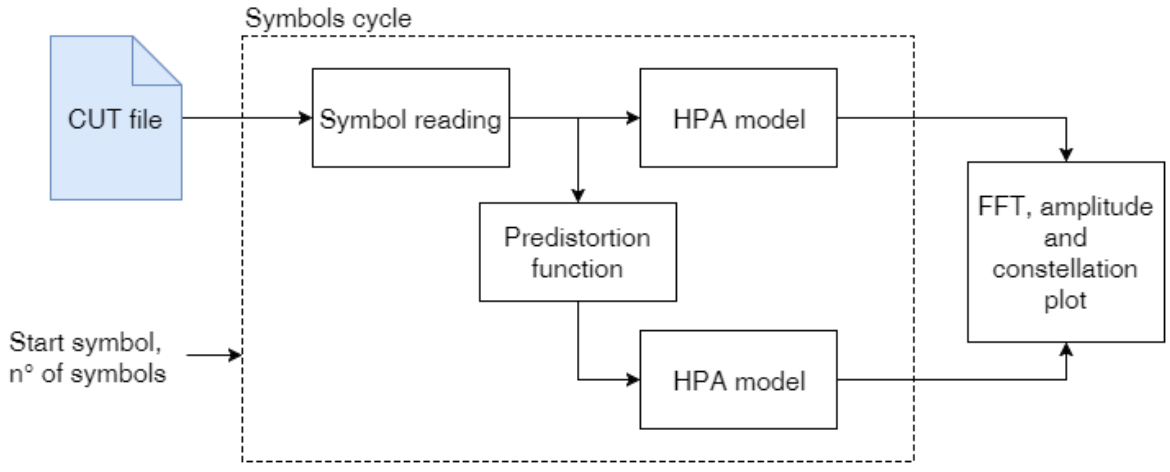

Figure 49 – Block diagram of adopted simulation procedure

11.1.3 Description of the input signal

In this section the input signal used experimentally is fully described. Instead of using a random generated signal to run the simulation, we preferred a real DVB-T transmission, because of the better approximation of a real communication system. In this way, we were able to consider every aspect

of the OFDM modulation, such as virtual subcarriers, guard intervals, etc. This real transmission is offline-elaborated, because of the high speed required by a real time predistortion, especially when using high bandwidth signals. However, the implemented predistortion algorithm can be easily modified to work real time, and the performance should be similar to the following.

The input OFDM signal consists of a DVB-T transmission with 2048 subcarriers, 343 of them virtual, formed by 68000 OFDM symbols with 16QAM modulation. The parameters of the OFDM modulation are shown in Table 2.

	T_g/T_u	N	N_v	T_u (μs)	$1/T_u$ (Hz)	B (MHz)	T_g (μs)	$T_g + T_u$ (μs)
2K	1/4	1705	343	224	4464	7.61	56	280
	1/8	"	"	"	"	"	28	252
	1/16	"	"	"	"	"	14	238
	1/32	"	"	"	"	"	7	231
8K	1/4	6817	1375	896	1116	7.61	224	1120
	1/8	"	"	"	"	"	112	1008
	1/16	"	"	"	"	"	56	952
	1/32	"	"	"	"	"	28	924

Table 2 - DVB-T 2k and 8k OFDM parameters

In particular, T_g is the time duration of the guard interval, which is typically chosen as a certain fraction of the time duration of the entire OFDM symbol T_u, N is the number of data subcarrier, N_v is the number of virtual subcarriers, and B represents the frequency spacing between the first and the last subcarrier, and is strictly correlated with the bandwidth of the signal, which in this case is approximately 8 MHz for both 2K and 8K mode.

The complex baseband samples are stored in a CUT file as 16 bit short integers for phase component and 16 bit short integers for quadrature component. In Figure 51 the histogram of these samples is presented. We can note the maximum integer value for the real or imaginary part of the samples (they have the same distribution) is about 1000, but there are isolated samples with values above 1500. Furthermore, the distribution of samples is perfectly symmetric.

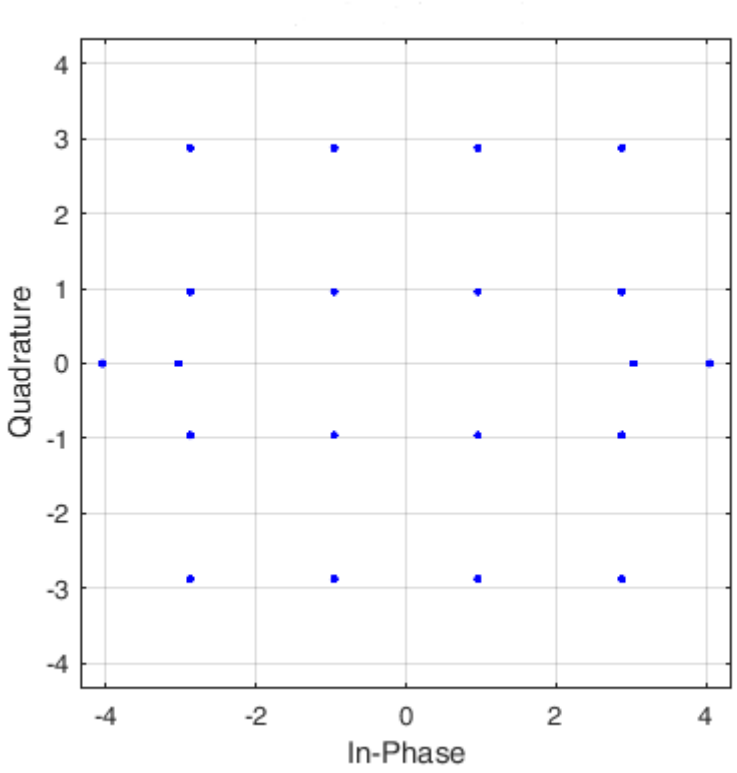

Figure 50 - IQ diagram of the 16QAM transmitted constellation

In the baseband constellation it can be noticed the presence of only real symbols out of the typical 16QAM position. The more external ones are the pilot subcarriers of the OFDM modulation, while the others are given by the coding used in DVB-T signals.

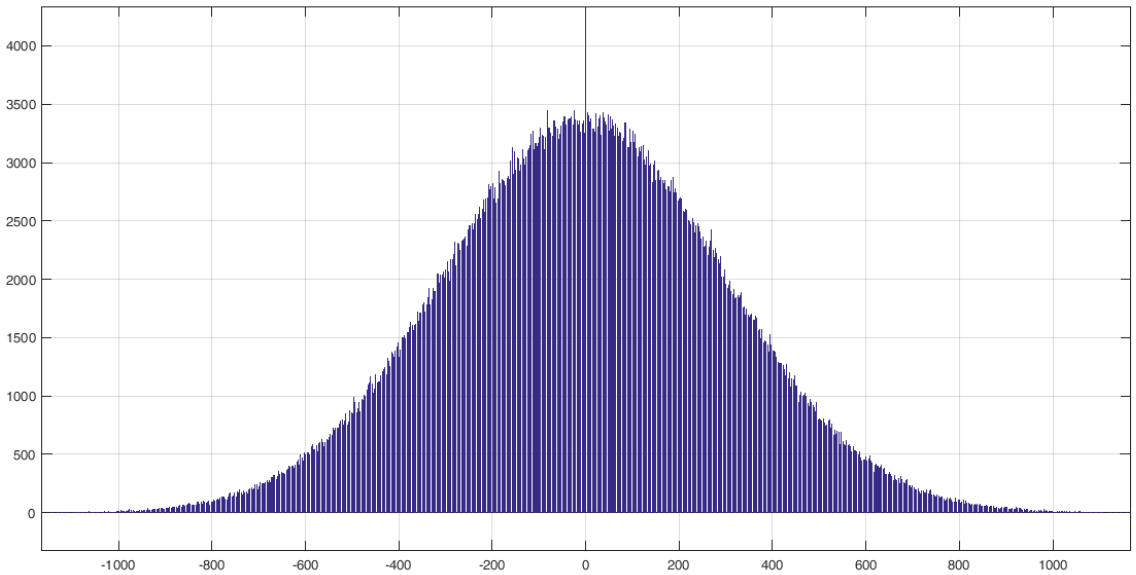

Figure 51 - Distribution of I-Q samples

To read the CUT file containing the input signal a set of MATLAB functions has been created, being able to extrapolate every symbol one by one from the file, that is 2560 samples for every iteration (2048 subcarriers plus 512 samples representing the guard interval). These functions can read the file starting from a specific number of symbol, and read a specific number of symbols. This is very useful since it is very difficult to store the entire number of symbols contained in the file without saturating the RAM of the device where MATLAB is running.

Thanks to these functions the input signal has been examined to plot a histogram representing the Probability Density Function (PDF) of the instantaneous power of the samples, and to plot the Power Spectral Density (PSD). In particular, the histogram is relevant to symbol numbers from 871 to 900, while the spectrum is relevant to OFDM symbol number 895.

First symbols of the signal could not be used to obtain these plots because it has been noted that they had a higher power compared to the average power of the entire signal.

11.1.4 Input Backoff

Subsequently, a signal with an instantaneous squared amplitude spanning the entire input signal power range has been used as input signal for the system formed by predistorter and analytically modeled amplifier. In this way the threshold representing the saturation input power of the linearized amplifier (hard saturation) has been calculated. Given the threshold and the percentage of symbols above hard saturation, the necessary input backoff (IBO) has been calculated, with respect to input saturation power of the single amplifier. Those samples whose power is higher than the threshold are above the saturation of the amplifier, thus being affected by clipping.

These results have been combined in a plot showing how many samples are clipped by the amplifier after predistortion and amplification.

The input OFDM signal then has been amplified with the resulting input backoff; the PSD has been also calculated, comparing it with the one of the original non-predistorted signal, and finally the resulting AM-AM characteristic has been plotted to verify the linearity gain obtained.

Subsequently, the input OFDM signal has been first predistorted and then amplified, and the measurements described above have been repeated and compared with the previous ones to verify the performances of the linearization system. These operations are performed in a single MATLAB cycle, that reads each OFDM symbol contained in the CUT file and memorizes three sequences of symbols that are necessary to compare the results: original input symbols, amplified symbols without predistortion, and the final symbols after predistortion and amplification. Of course for simulation purposes we have examined only a small part of the signal, otherwise the required RAM on the device running MATLAB would be too high.

Amplification and predistortion have been realized with two functions that work on a single OFDM symbol at a time and so they return a vector representing the entire OFDM symbol amplified or predistorted.

11.1.5 Implementation of the Receiver

Finally, to show the received symbols constellation and consequently to calculate performance parameters, the receiver has been implemented. Here the demodulation of the signal is made, both the non-linearized one, and the one passed through predistortion and amplification, to visualize the symbols constellation and make a MER measurement. Also the BER (Bit Error Rate) is calculated to better understand the good performances achieved by this system.

Initially, the thermal noise has not been considered in the communication system, calculating the performance only regarding the distortion generated by the amplifier non-linearity. Figures explaining the results obtained by the described procedure are shown below.

11.2 RESULTS OF SIMULATIONS

Here are showed the histogram and the baseband symbols constellation relevant to 30 OFDM symbols (from 871 to 900). The spectrum is relevant to symbol number 895. All of these results are obtained under the hypothesis of absence of thermal noise. The results obtained for each run of the simulation are presented in Figures and Tables below.

Different simulations were run with different backoff values. To choose these backoff values, first the percent of the clipped samples has been set, then the corresponding backoff, with respect to the hard saturation of the HPA, has been calculated. Different histograms have been plotted, for different values of the percentage value described above: 40%, 20%, 10%, 5%, 1%, 0.01%.

11.2.1 Kuhne KU PA 242 TX

In the following section the simulation results for Kuhne amplifier are presented. For every value of the clipped samples threshold a set of figures and a table describe the results in terms of MER gain obtained with the predistorted file.

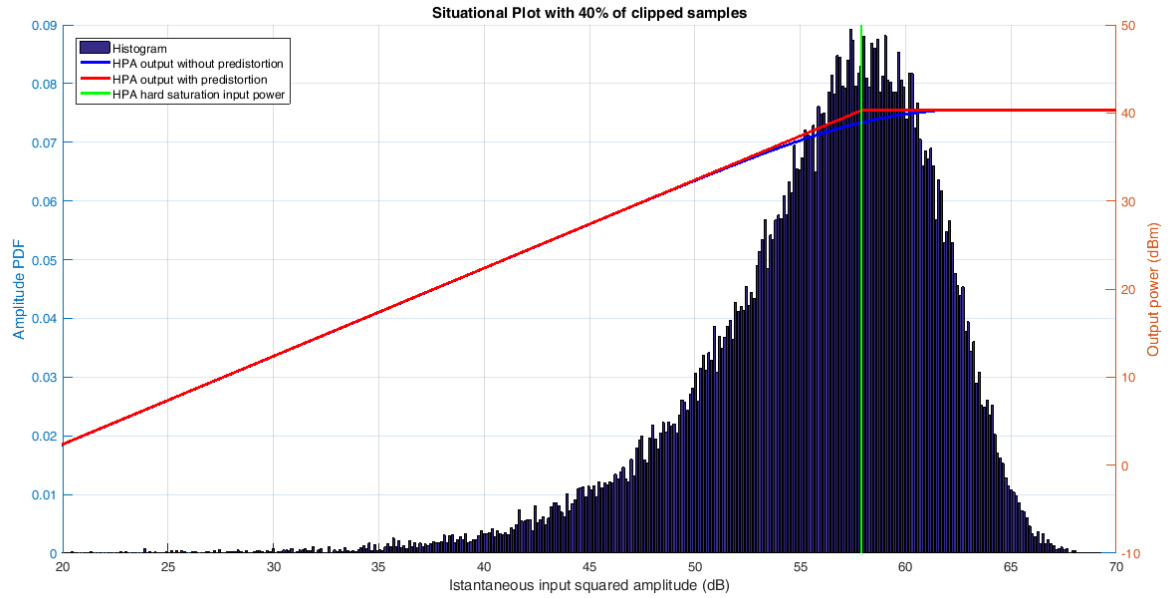

Figure 52 – Amplitude distribution with 40% clipped samples

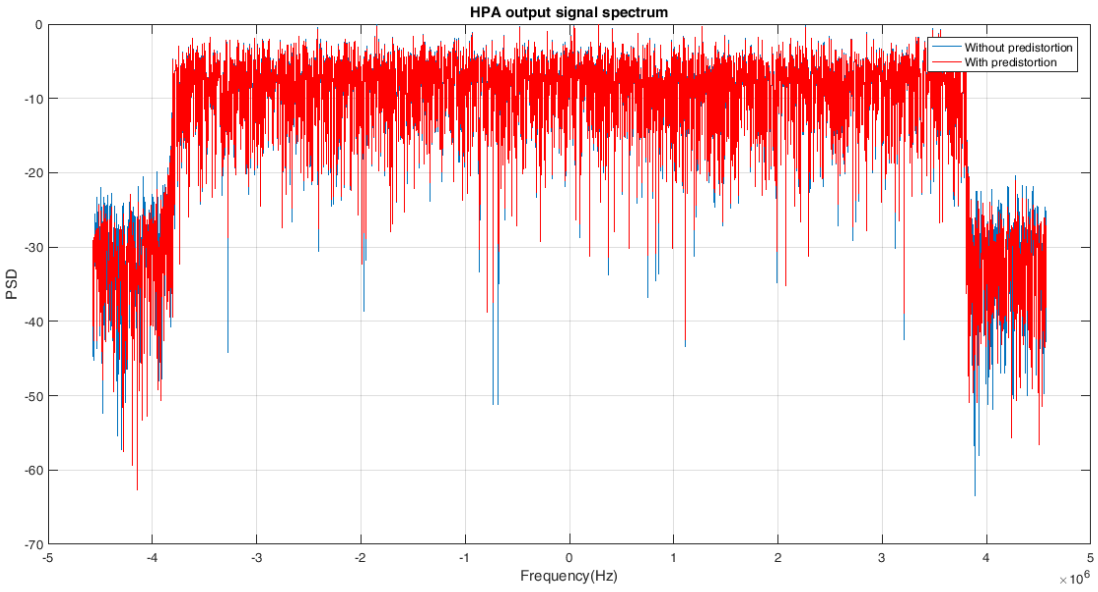

Figure 53 - HPA output spectrum comparison

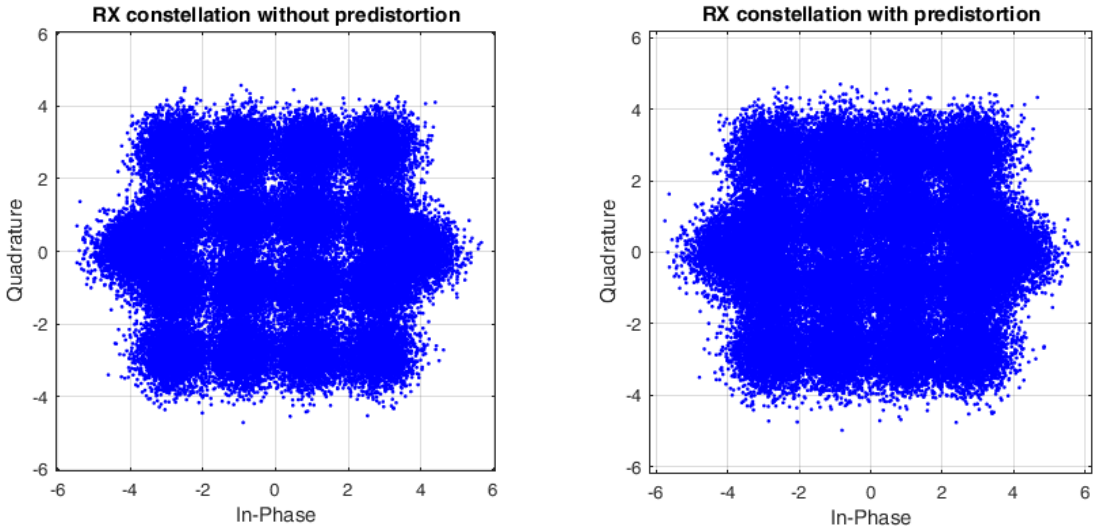

Figure 54 - Comparison between baseband symbol constellation with 40% clipped samples

Clipped samples percentage	Input Backoff	MER without predistortion	MER with predistortion
40%	9.2 dB	12.7801 dB	12.3364 dB

Table 3 - MER gain with 40% clipped samples

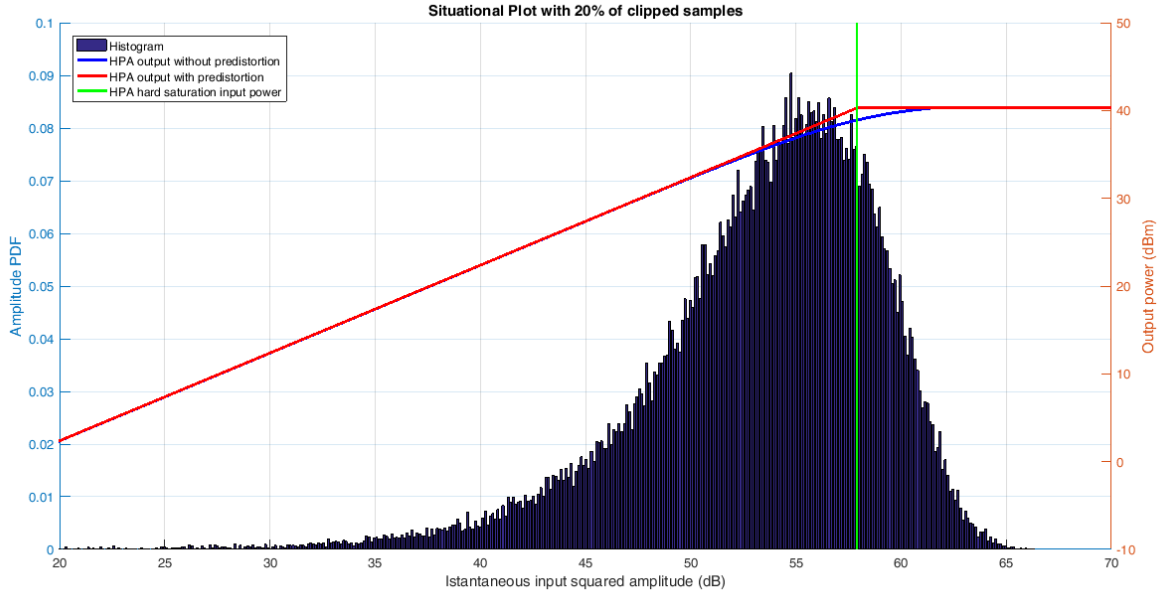

Figure 55 - Amplitude distribution with 20% clipped samples

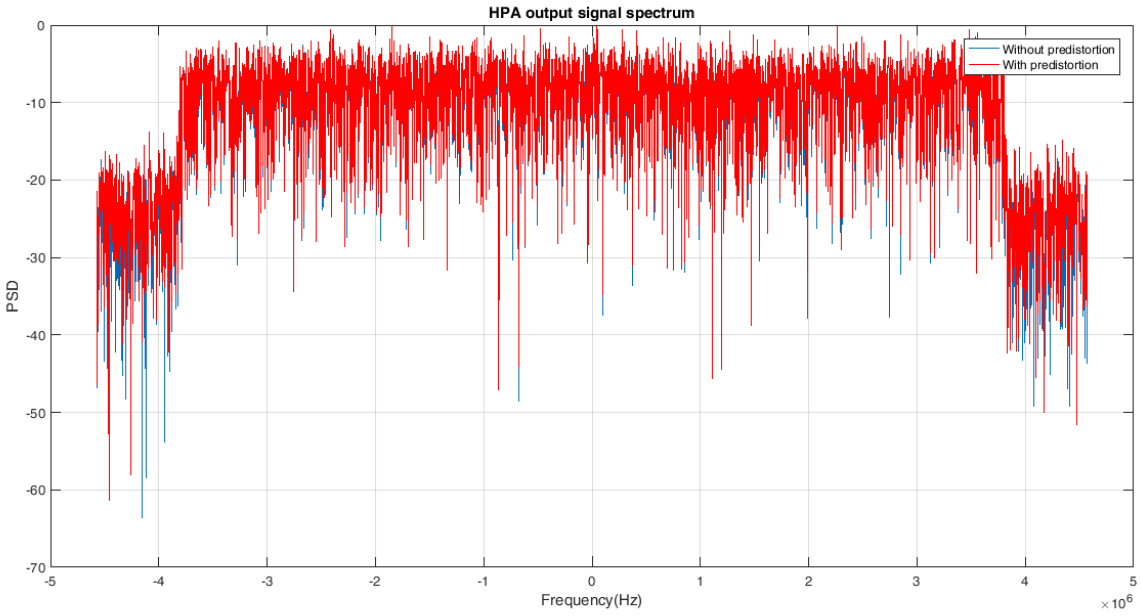

Figure 56 - HPA output spectrum comparison with 20% clipped samples

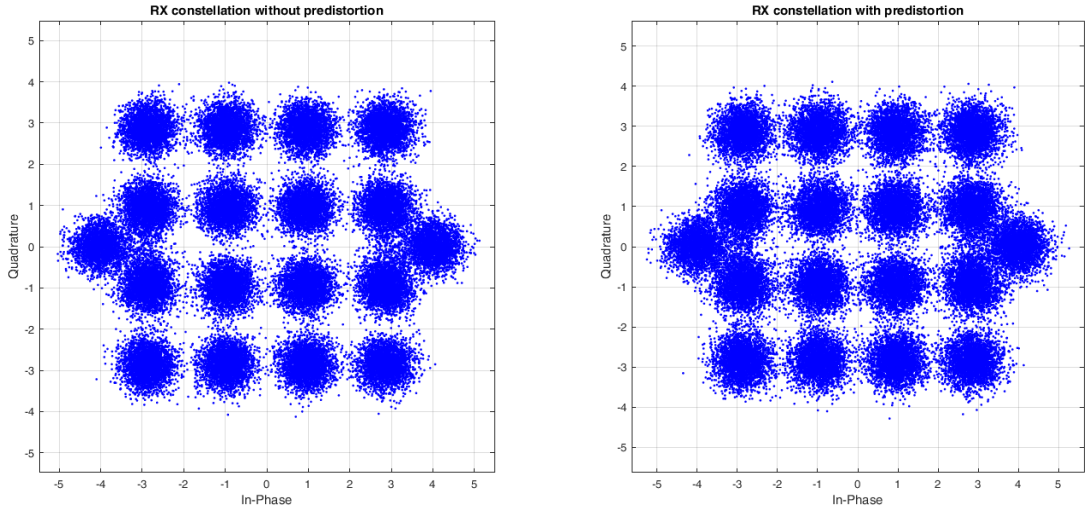

Figure 57 - Comparison between baseband symbol constellation with 20% clipped samples

Clipped samples percentage	Input Backoff	MER without predistortion	MER with predistortion
20%	11.59 dB	15.2977 dB	15.8992 dB

Table 4 - MER gain with 20% clipped samples

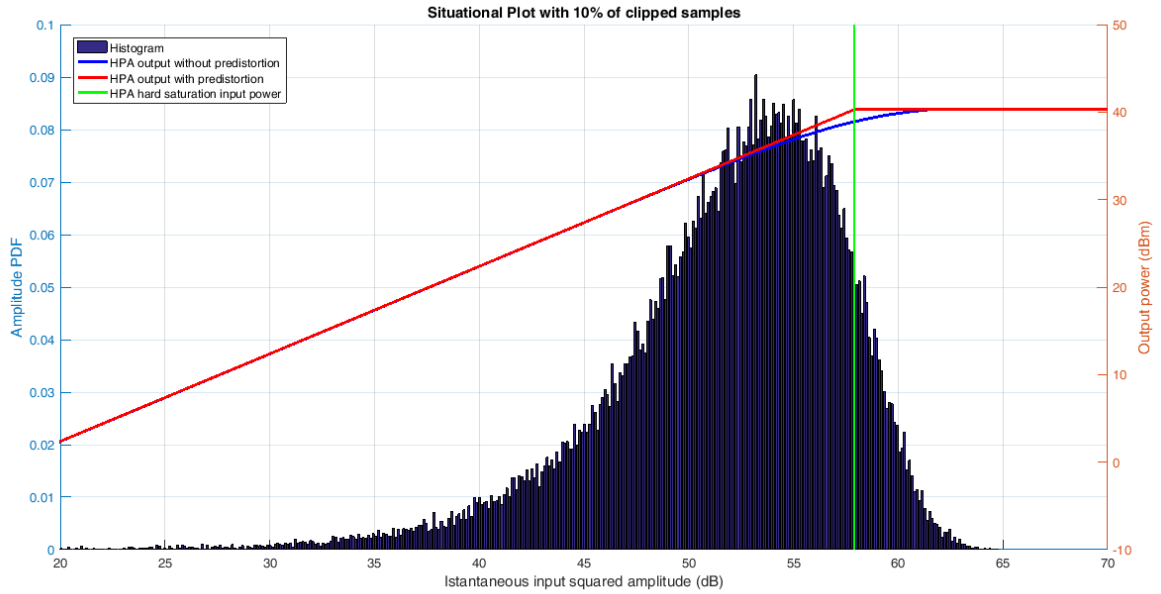

Figure 58 - Amplitude distribution with 10% clipped samples

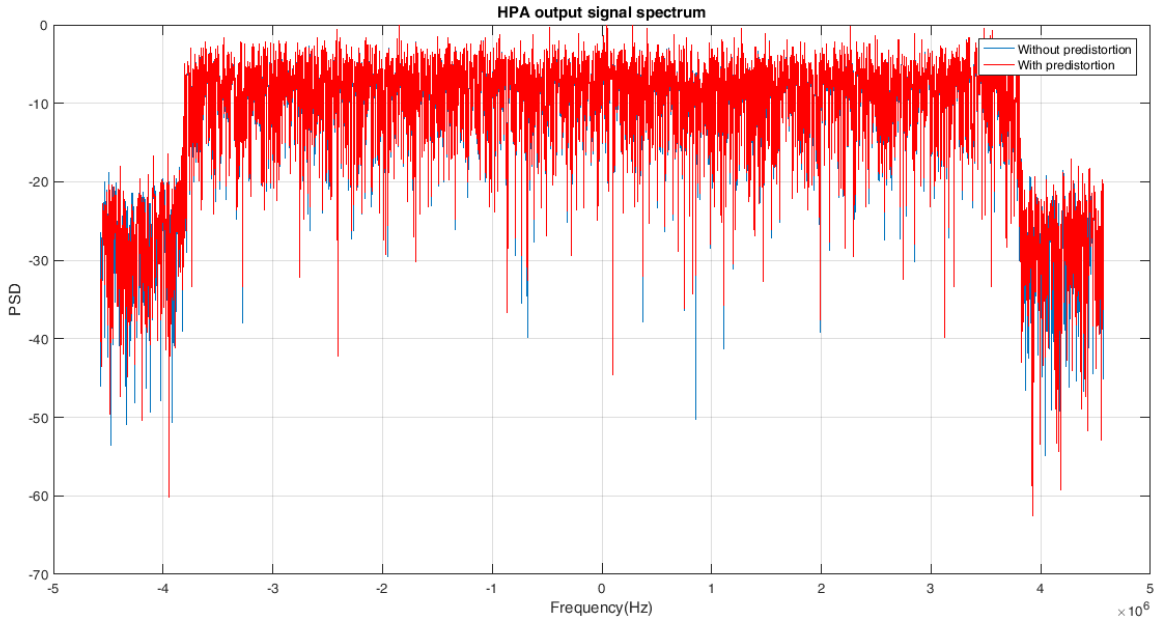

Figure 59 - HPA output spectrum comparison with 10% clipped samples

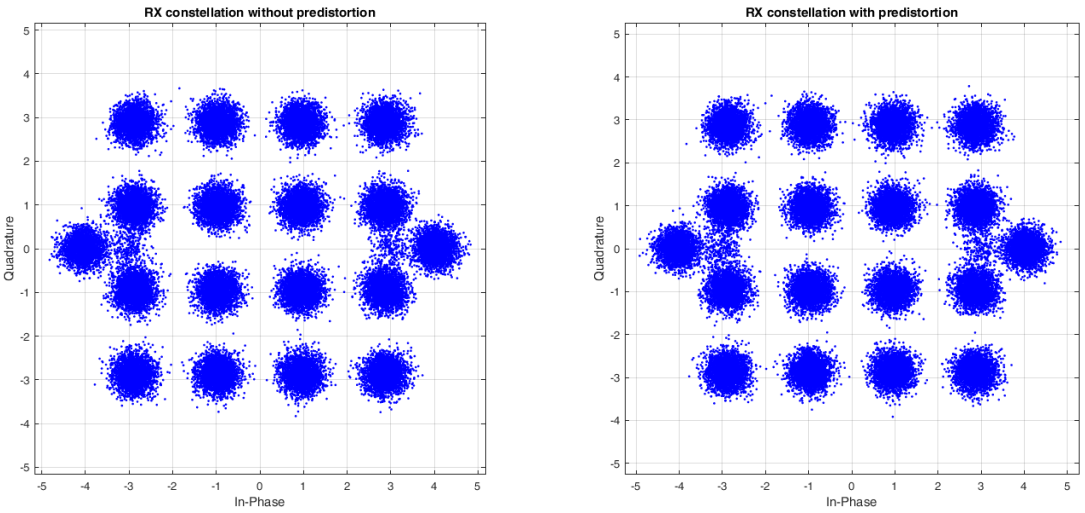

Figure 60 - Comparison between baseband symbol constellation with 10% clipped samples

Clipped samples percentage	Input Backoff	MER without predistortion	MER with predistortion
10%	13.19 dB	16.7991 dB	19.2122 dB

Table 5 - MER gain with 10% clipped samples

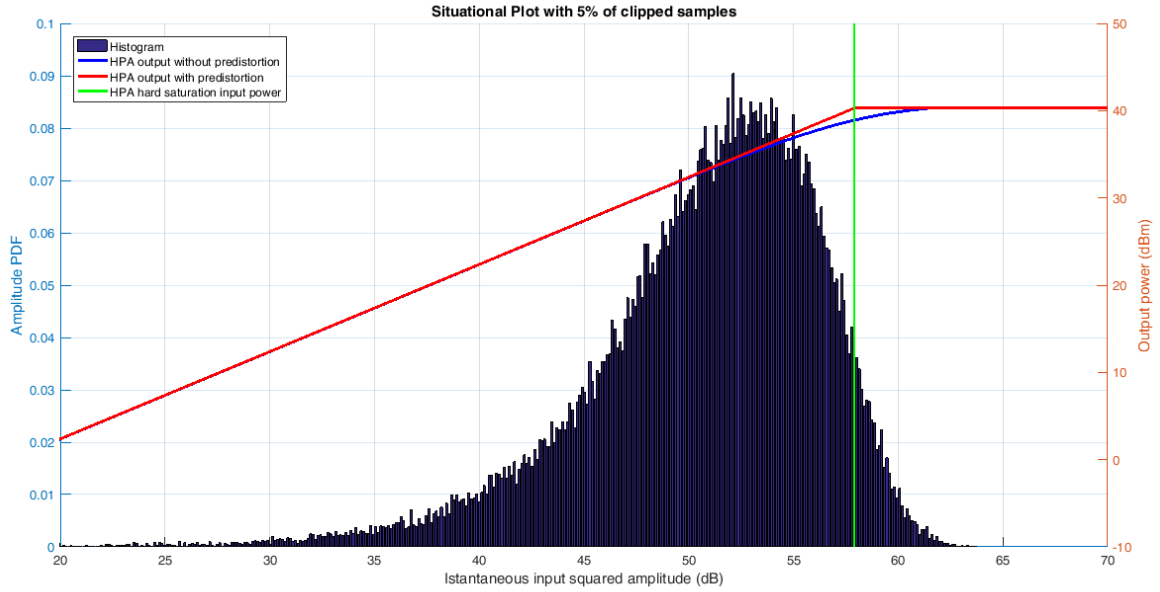

Figure 61 - Amplitude distribution with 5% clipped samples

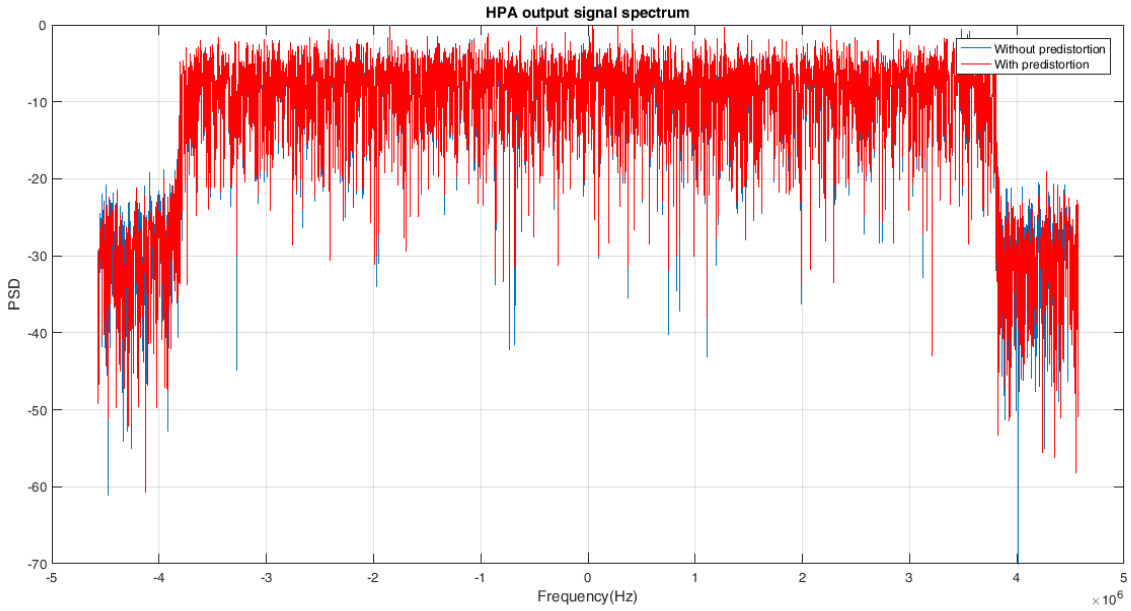

Figure 62 - HPA output spectrum comparison with 5% clipped samples

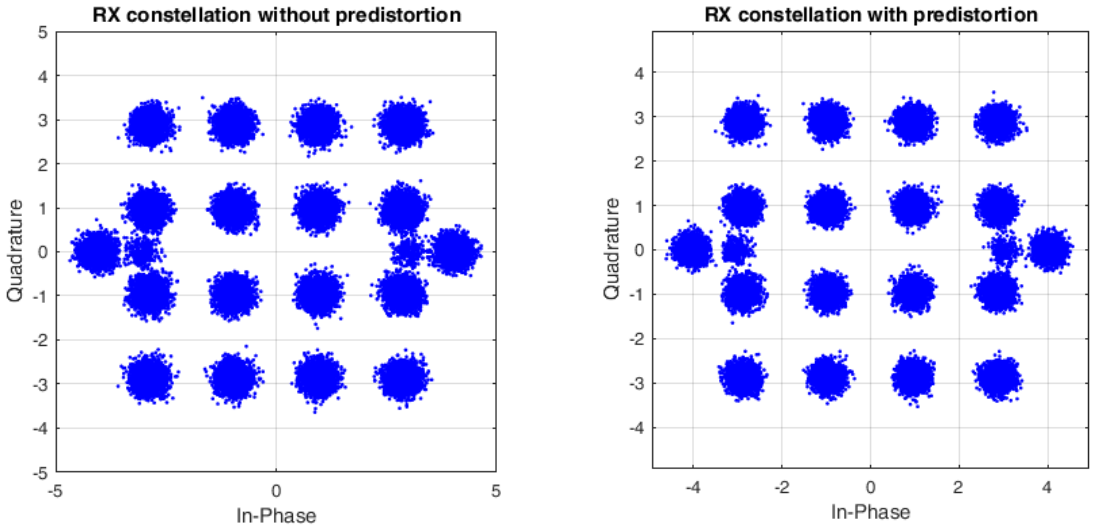

Figure 63 - Comparison between baseband symbol constellation with 5% clipped samples

Clipped samples percentage	Input Backoff	MER without predistortion	MER with predistortion
5%	14.33 dB	17.9740 dB	22.5497 dB

Table 6 - MER gain with 5% clipped samples

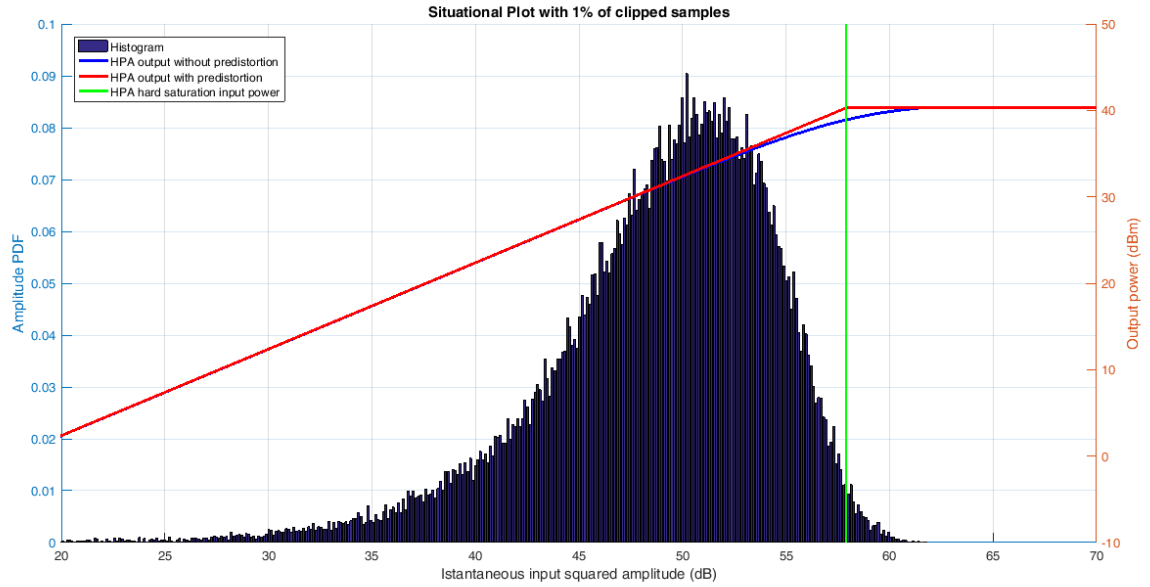

Figure 64 - Amplitude distribution with 1% clipped samples

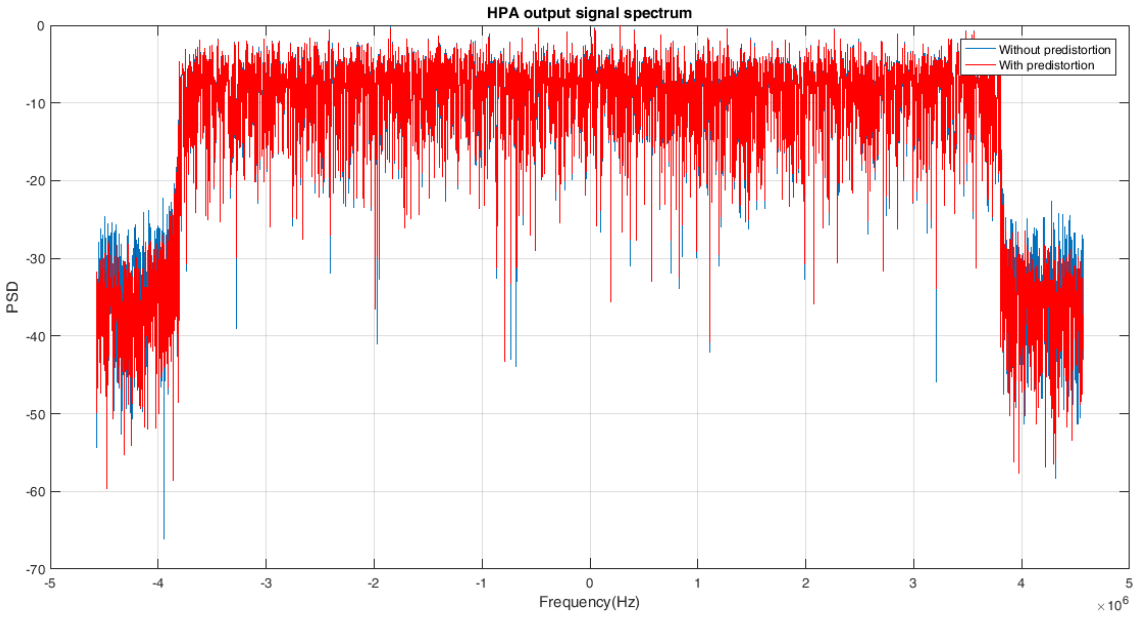

Figure 65 - HPA output spectrum comparison with 1% clipped samples

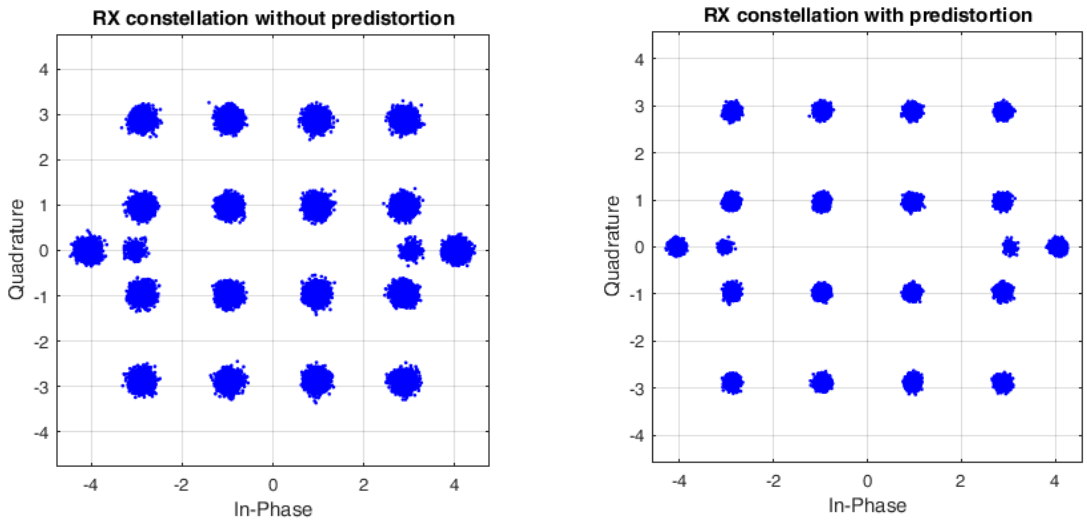

Figure 66 - Comparison between baseband symbol constellation with 1% clipped samples

Clipped samples percentage	Input Backoff	MER without predistortion	MER with predistortion
1%	16.15 dB	19.8665 dB	30.0482 dB

Table 7 - MER gain with 1% clipped samples

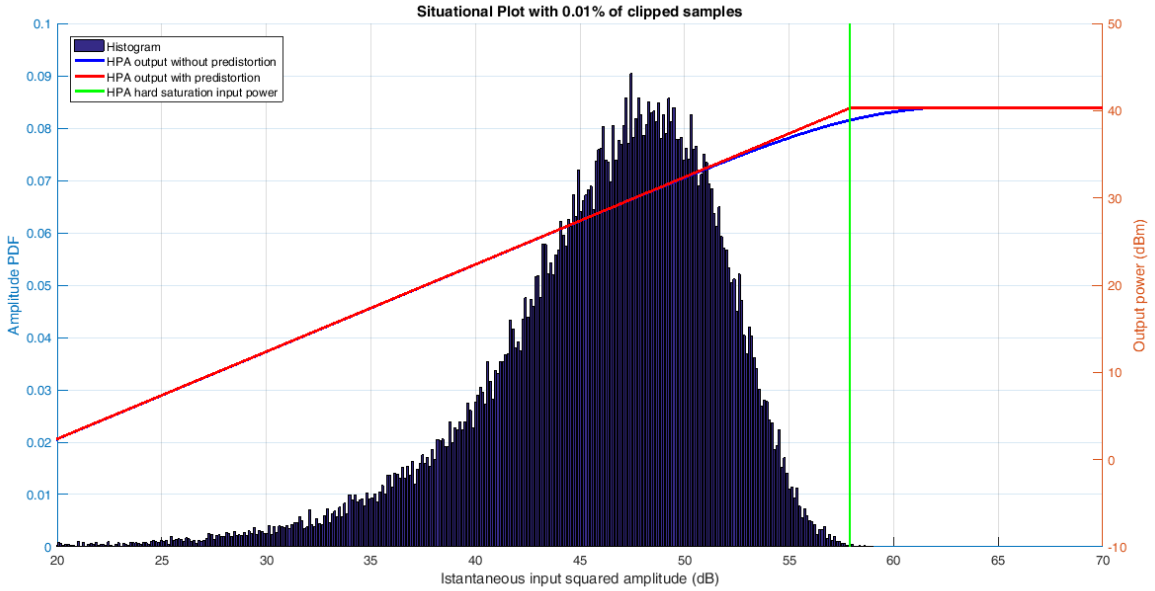

Figure 67 - Amplitude distribution with 0.01% clipped samples

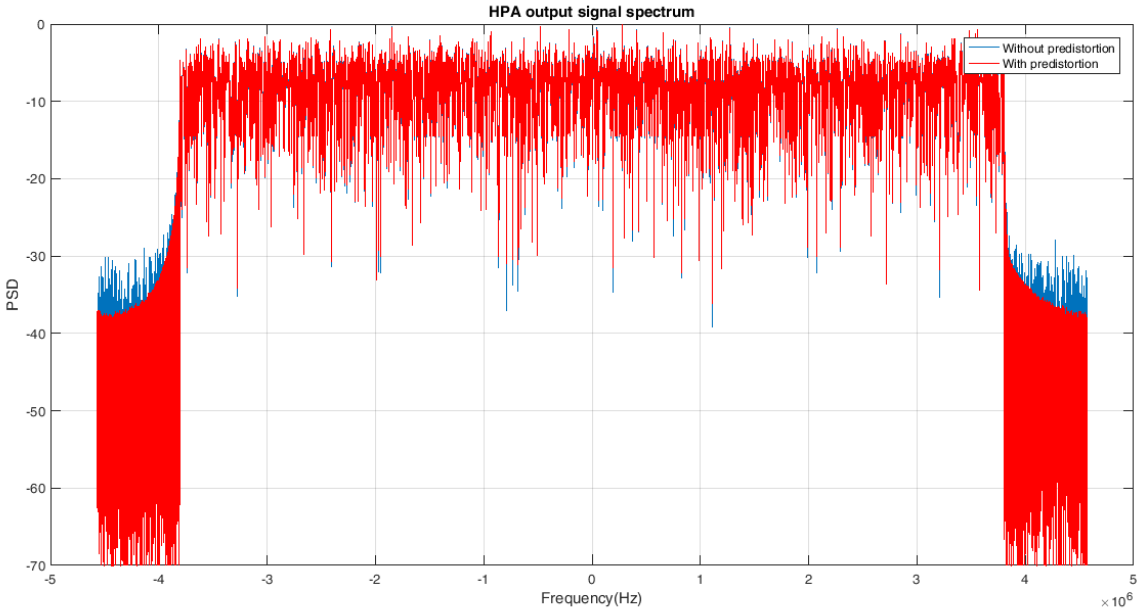

Figure 68 - HPA output spectrum comparison with 0.01% clipped samples

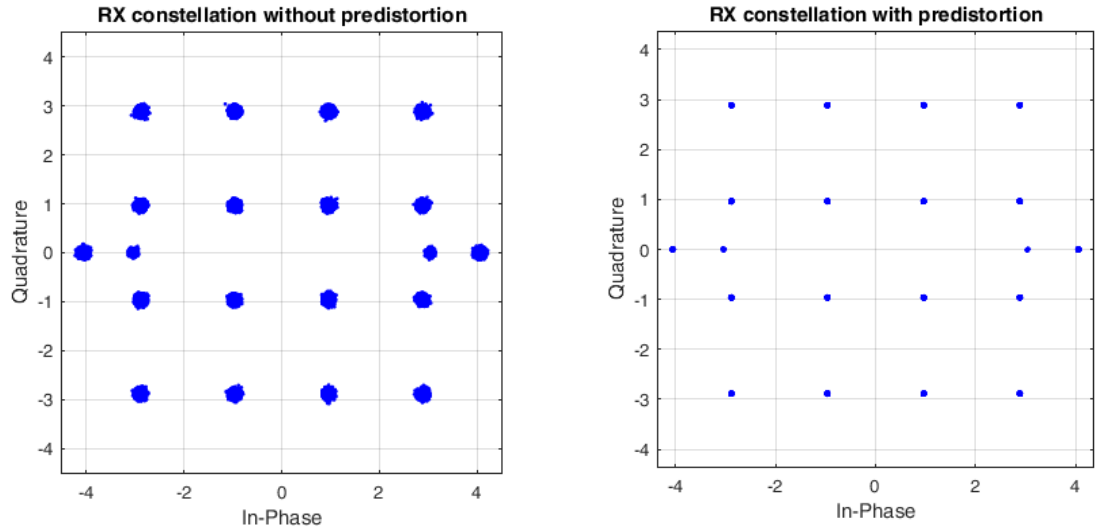

Figure 69 - Comparison between baseband symbol constellation with 0.01% clipped samples

Clipped samples percentage	Input Backoff	MER without predistortion	MER with predistortion
0.01%	19.12 dB	23.3283 dB	49.3136 dB

Table 8 - MER gain with 0.01% clipped samples

Results show that the performances of this predistorter vary greatly depending principally on the percentage set, thus to the corresponding input backoff. In particular, for the first value of threshold (40%), the predistortion does not provide improvements in terms of OFDM shoulder, and worsens the MER after the modulation. With 20% of samples that are clipped, there are no significant differences between the system with predistortion and the one without predistortion. For lower values of clipped samples percentage instead the situation improves both from the point of view of

the spectrum and with the constellation of the 16QAM symbols. Finally, with the 0.01% values of clipped samples, the spectrum of the original signal and that of the signal predistorted and amplified are virtually identical and the constellation is very close to the ideal constellation.

To better understand the behavior of the predistorter, also a plot has been realized in which the obtained MER gain (between non-predistorted and predistorted signal) with respect to the smoothness factor of the Rapp modeled amplifier. The backoff has been fixed to a value equal to 8 dB.

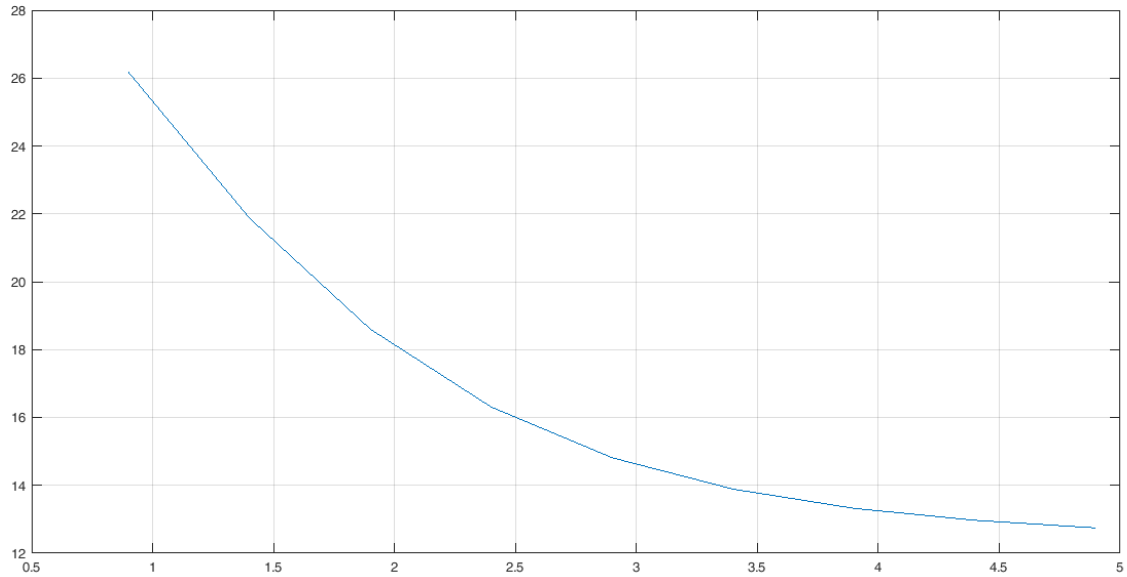

Figure 70 - MER gain with predistortion vs smoothness factor of Rapp model

From the graph we can see that with low smoothness factor values, the MER gain is more consistent. To explain this, we can see the smoothness factor as a linearity parameter. When it is high, the hard saturation is reached abruptly, in an almost linear manner, so the predistortion can only slightly improve the MER. Instead, when the smoothness factor is low, the characteristic has a softer approach to saturation, and the predistorter can obtain good results.

In Figure 71 instead the MER gain has been examined on varying the input backoff, thus with fixed smoothness factor (the one obtained for the Kuhne amplifier).

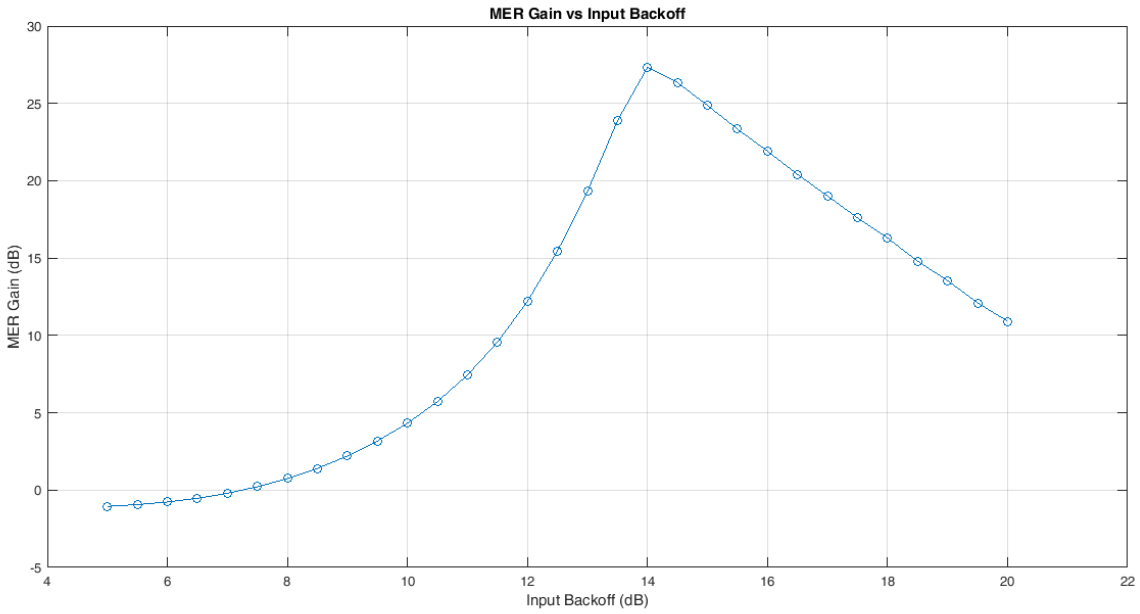

Figure 71 - MER gain vs input backoff for Kuhne amplifier

The plot shows that a backoff increase leads to a better MER gain, and this was predictable since even the predistorter can't linearize the samples whose power are above the hard saturation. If we increase the backoff, these samples will be less numerous and the performance will be better. Another important effect that is shown in the plot is that the MER gain reach a maximum value before start decreasing. This happens because if we work with low input power, the HPA is already linear, and the predistorter can't improve the linearity. For very high backoff values, the predistorter simply does not modify the signal, and this of course generates a MER gain equal to zero.

11.2.2 OvisLink Airlive WPA-2400IG and Fujitsu FMC1616L1015

The same simulation has been run also for the OvisLink and Fujitsu HPAs, using different analytic models (Rapp for OvisLink, memoryless polynomial for Fujitsu).

Results are presented in Table 9 and Table 10.

	Backoff	MER (no predistortion)	MER(predistortion)
40% clipped samples	3.2240 dB	12.8119 dB	12.4740 dB
20% clipped samples	5.6181 dB	16.2172 dB	16.0148 dB
10% clipped samples	7.2142 dB	19.2395 dB	19.6458 dB
5% clipped samples	8.3543 dB	21.8858 dB	23.1660 dB
1% clipped samples	10.1784 dB	27.2742 dB	31.0137 dB
0.01% clipped samples	13.1425 dB	39.4172 dB	48.4473 dB

Table 9 - Results for OvisLink HPA simulation

	Backoff	MER (no predistortion)	MER(predistortion)
40% clipped samples	4.1559 dB	13.0085 dB	11.9602 dB
20% clipped samples	6.5413 dB	16.6216 dB	15.3983 dB
10% clipped samples	8.0138 dB	19.5631 dB	18.6763 dB
5% clipped samples	9.1281 dB	21.8361 dB	21.7095 dB
1% clipped samples	10.8359 dB	26.1476 dB	29.2135 dB
0.01% clipped samples	13.7811 dB	32.7492 dB	49.0969 dB

Table 10 - Results for Fujitsu HPA simulation

12 EXPERIMENTAL RESULTS

The results shown above are relevant to the simulation run with MATLAB. After simulation, the developed predistorter has been tested experimentally, using real power amplifiers and a real transmission system. Both the Kuhne and the Fujitsu power amplifier have been tested, and the results have been compared to the ones obtained by simulation.

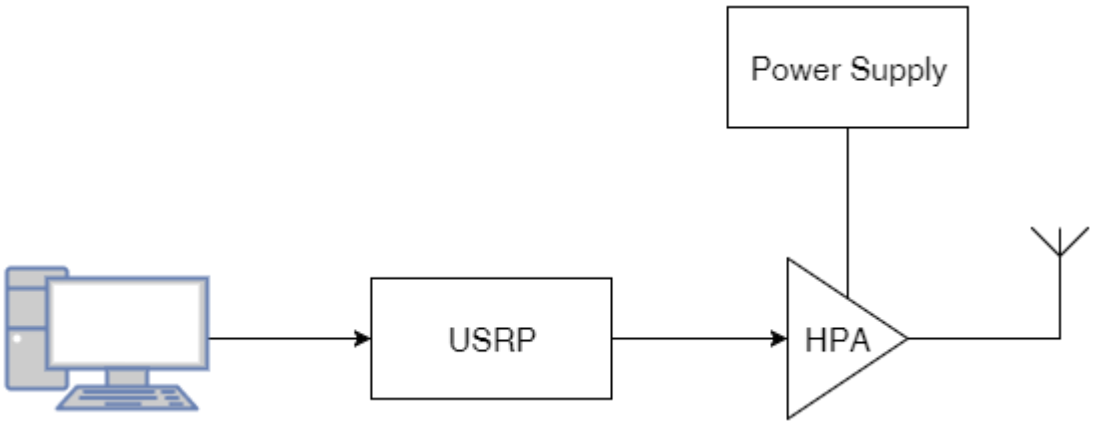

Figure 72 - TX setup for experimental results

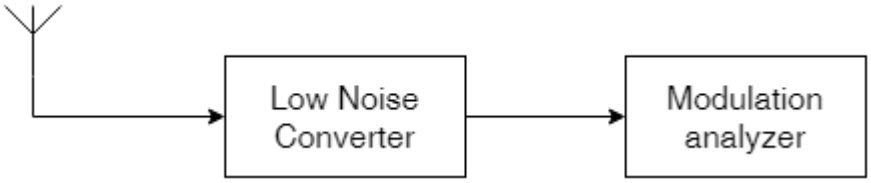

Figure 73 - RX setup for experimental results

In Figure 72 and Figure 73 the logic links between the instruments are showed. As we can see, the MER is calculated and displayed by the modulation analyzer, which can also show the baseband constellation and the demodulated video stream.

It is important to notice that the final goal of this predistorter is to achieve the maximum possible transmitted power, without losing signal quality by distortion generated by amplifier's non-linearities. This means fixing a quality parameter, such as a MER threshold, and find what output power is needed to reach that value of MER, both with and without predistortion system. Obviously, the more output power we have, the more distortion the amplifier generates, the less MER we obtain. In this way, we can discover the power gain that the predistorter gives us with respect to the system without predistortion. Having more transmitted power leads to a more robust RF signal.

12.1 KUHNE AMPLIFIER

For this amplifier the experiment showed that the best results are achieved with the USRP gain set to 22, which means an average output power from the USRP equal to 11 dBm, and an output power from the amplifier of 31.5 dBm.

In particular, with the output power fixed, we obtain a MER gain equal to 2.5 dB, while if we fix a target MER, in particular 27.5 dB, the power gain obtained is equal to 3 dB.

	Non-predistorted	Predistorted
MER @ 11 dBm	25 dB	27.5 dB
Output power @ 27.5 dB MER	28.5 dBm	31.5 dBm

Table 11 - Experimental results for Kuhne HPA

12.2 OVISLINK AMPLIFIER

The OvisLink amplifier presents similar characteristic to the Kuhne one. For this reason, results are similar, with a 1.7 dB MER gain obtained with 20.5 dBm. The main difference from both Kuhne and Fujitsu is the irregular characteristic and the lower output power, since the theoretical gain is about 10 dB.

	Non-predistorted	Predistorted
MER @ 11.7 dBm	25.3 dB	27 dB
Output power @ 27 dB MER	20.5 dBm	22.4 dBm

Table 12 - Experimental results for OvisLink HPA

12.3 FUJITSU AMPLIFIER

This amplifier is really different from both Kuhne and OvisLink. First, it has bad linearity properties, giving the fact it is a Class A amplifier. Second, it presents a remarkable memory effect. This is problematic if we use a PA model that does not take into account this effect. To solve this problem, a modified version of the algorithm has been developed. While the standard version modifies the current sample only watching the current input amplitude, the advanced version calculates the predistortion gain after operating an average on the current and a number of past values of the input amplitude. Every sample in the averaging window then is scaled by the same predistortion factor.

	Non-predistorted	Predistorted
MER @ 77dB (USRP B200 gain)	23.4 dB	24.7 dB

Table 13 - Experimental results for Fujitsu HPA

The results are presented in Table 13. They show a MER gain equal to 1.4 dB, with an output power of 25.9 dBm, which is less than the gain obtained with Kuhne, but this was predictable since the presence of memory effect.

As we can see, these results do not match exactly with the simulations run before. This incongruence however was expected, because the designed predistortion system does not take into account every possible distortion source. The most important is the memory effect, which has already been described, that with wideband signals such as OFDM should be considered, but also other effects generate distortions on the symbols of the received constellation. For example, the filters in the communication system, whose effect on the signal is not seen by the predistorter, which works before the signal filtering and the digital to analog conversion.

There is also another important fact to consider. In the simulation, we found the maximum MER gain value varying the input backoff; however, in experimental environment, the IBO should not be too large, because this would mean very low output power. The first aim of the predistorter is to increase the output power from the amplifier without ruining the signal. Thus, finding the maximum IBO decrease obtainable with a fixed target MER. For this reason we could not choose the backoff which maximize the MER, and a tradeoff between MER gain and input backoff was needed.

13 CONCLUSIONS

After the experimental results, we can conclude that this predistortion system achieves good results for already quite linear amplifiers. In particular, results underline that this solution is not optimal for amplifier with memory like the Fujitsu one, but a simple change on the predistortion can handle also this effect. Also, the best MER improvement was obtained with the limiter, meaning the predistorter works better when the non-linearity is strong but also regular (there are not "jumps" in the characteristic). Regarding amplifiers with memory, the predistorter in its basic version cannot handle the memory effect, lowering the MER instead of increasing it, but with a small modification good results can be obtained also in this case. The modified algorithm indexes the LUT with the average amplitude of a temporal window of 256 samples instead of using the current sample, then applies the indexed coefficient to all of these samples.

The main advantages of the described technique are the portability, because it is a software oriented solution, and the flexibility. Having the possibility to switch between different analytic models for the amplifier is a great advantage, because always the best solution can be chosen. Rapp model for SSPAs, Saleh model for TWTs, and every other model can be easily implemented, the only change to do in the software is the associating function that generates the LUT. Clearly there is the necessity of the knowledge of the PA characteristic, but this is often necessary also to develop a good hardware predistorter, since different power amplifier have different optimal solutions.

Regarding possible future work for this thesis, one interesting possibility would be the porting of the source code on a low-level programming language with the purpose of building a software defined predistorter based on DSP or FPGA. Another possible project would be the design of a hardware predistorter taking idea from the code developed for this thesis. Of course this specific algorithm is software oriented, but it can be easily modified to work well on hardware platform. In fact, this is also a possible future work on this thesis, examining the possibility of a hardware predistorter based on the presented algorithm. This should be easy to implement, given the simplicity of the LUT predistortion approach. A possible improvement in the algorithm could be the implementation of the AM-PM correction, since in this thesis the phase distortion was not considered (SSPA typically introduce very low phase distortion).

BIBLIOGRAPHY

[1] Dardari D., Tralli V., Vaccari A., *"A Theoretical characterization of Nonlinear Distortion Effects in OFDM systems"*, IEEE Transactions on Communications, Vol.48 No.10, October 2000, pp. 1755-1763.

[2] Stapleton S., Cavers J., *"A new technique for adaptation of linearizing predistorters"*, Proceedings of IEEE 41nd Vehicular Technology Conference, May 1991, pp. 753-758.

[3] Saleh A., *"Frequency-independent and frequency-dependent nonlinear models of TWT amplifiers"*, IEEE Transactions on Communications, Vol.29, 1981, pp. 1715-1720.

[4] R.C., *"Effects of HPA-nonlinearity on an 4-DPSK/OFDM-signal for a digital sound broadcasting system"*.

[5] G.A. and S.M, *"The effect of solid state power amplifiers (SSPAs) nonlinearities on MPSK and M-QAM signal transmission"*, Proceedings of 6th International Conference on Digital Processing of Signals in Communications, 1991, pp. 193-197.

[6] Morgan D., Ma Z., Kim J., Zierdt M., Pastalan J., "A generalized memory polynomial model for digital predistortion of RF power amplifiers", IEEE Transactions on Signal Processing, Vol.54, 2006, pp. 3852-3860.

[7] Crama P., Schoukens J., *"Hammerstein-Wiener System Estimation Initialization"*, ISMA 2002, Noise and Vibration Engineering, Leuven, September 2002, pp. 1169.1176.

[8] Kim J., Konstantinou K., *"Digital predistortion of wideband signals based on power amplifier model with memory"*, Electronics Letters, Vol.37, 2001, pp. 1417-1418.

[9] Vaananen O., *"Digital modulators with crest factor reduction techniques"*, Ph.D. dissertation, Helsinki University of Technology, 2006.

[10] Tellado J., *"Multicarrier Modulation with Low PAR"*, Kluwer Academic Publishers, 2000.

[11] Nagata Y., *"Linear amplification technique for digital mobile communications"*, Proceedings of IEEE Vehicular Technology Conference, May 1989, pp. 159-164.

[12] Cavers J., *"Amplifier linearization using a digital predistorter with fast adaptation and low memory requirements"*, IEEE Transactions on Vehicular Technology, Vol.39, November 1990, pp. 374-382.

[13] He Z., Ge J., Geng S., Wang G., *"An improved Look-Up Table Predistortion Technique for HPA With Memory Effects in OFDM Systems"*, IEEE Transactions on Broadcasting, Vol.52, March 2006, pp. 87-91.

[14] Jeon W., Chang K., Cho Y., *"An adaptive Data Predistorter for Compensation of Nonlinear Distortion in OFDM Systems"*, IEEE Transactions on Communications, Vol.45, October 2007, pp. 1167-1171.

[15] Tarek H., Richard D., Mohamed T., *"BER Performance of OFDM Signals in Presence of Nonlinear Distortion due to SSPA"*, Wireless Pers Commun (2012).

[16] Américo B., Antoine C., *"Compensation of nonlinear distortions for orthogonal multicarrier schemes using predistortion"*.

[17] Rahul G., Saad A., Reinhold L., John M., *"Adaptive Digital Baseband Predistortion for RF Power Amplifier Linearization"*, High Frequency Electronics, September 2006.

[18] Krzysztof W., *"A Novel Fast HPA Predistorter for High PAPR Signals"*, IEEE 16th International Symposium on Personal, Indoor and Mobile Radio Communications, 2005, pp. 863-867.

[19] Giannetti F., Lottici V., Stupia I., *"Iterative Multi-User Data Predistortion for MC-CDMA Communications"*, IEEE Transactions on Wireless Communications, Vol.7, October 2008, pp. 3823-3833.

[20] Rishad S., Shahriar R., Razibul I., *"On the Extended Relationships Among EVM, BER and SNR as Performance Metrics"*, 4th International Conference on Electrical and Computer Engineering, December 2006, pp. 408-411.

[21] Kennington P.B., *"High-linearity RF amplifier design"*, Artech House, 2000.

[22] Black H., *"Translating system"*, U.S. Patent 1,686,792, October 1928.

[23] Black H., *"Wave translation system"*, U.S. Patent 2,102,671, October 1937.

[24] Cox D., *"Linear amplification with nonlinear components"*, IEEE Transactions on Communications, Vol.22, 1974, pp. 1942-1945.

[25] Azirar A., Robertson I., *"OFDM LINC transmitter with digital I/Q imbalance compensation"*, IEEE MTT-S International Microwave Symposium Digest 2004, Vol.2, 2004, pp. 743-746.

[26] Kahn L., *"Single-sideband transmission by envelope elimination and restoration"*, Proceedings of the IRE, Vol.40, 1952, pp. 803-806.

[27] Chen J.-H., Fedorenko P., Kenney J., *"A low voltage W-CDMA polar transmitter with digital envelope path gain compensation"*, IEEE Microwave and Wireless Components Letters, Vol.16, 2006, pp. 428-430.

[28] Egger A., Horn M., Vien T., *"Broadband linearization of microwave power amplifiers"*, Proceedings of 10th European Microwave Conference, 1980, pp. 490-494.

[29] Woo W., Park E., U-yen K., Kenney S., *"Wideband predistortion linearization system for RF power amplifiers using an envelope modulation technique"*, Proceedings of Radio and Wireless Conference, August 2003, pp. 401-404.

[30] Saleh A., Salz J., *"Adaptive linearization of power amplifiers in digital radio systems"*, The Bell System Technical Journal, Vol.62, April 1983, pp. 1019-1033.

[31] Cripps S., *"Advanced techniques in RF power amplifier design"*, Boston, USA, Artech House, 2002.

[32] Aracely F., Roberto R., Peter H., Joseph B., Paul D., *"Adaptive Digital Post Distortion Reduction"*, U.S. Patent 2011/0103455 A1, May 2011.

[33] Cavers J., *"The effect of quadrature modulator and demodulator errors on adaptive digital predistorters for amplifier linearization"*, IEEE Transactions on Vehicular Technology, Vol.46, May 1997, pp.456-466.

[34] Weisstein E., *"Secant method"*, MathWorld-A Wolfram Web Resource, http://mathworld.wolfram.com/SecantMethod.html.

[35] Diniz P., *"Adaptive filtering"*, Boston, USA, Kluver Academic Publishers, 1997.

[36] Eun C., Powers E., *"A new Volterra predistorter based on the indirect learning architecture"*, IEEE Transactions on Signal Processing, Vol.45, 1997, pp. 223-227.

[37] Zhou D., Debrunner V., *"A simplified adaptive nonlinear predistorter for high power amplifiers based on the direct learning algorithm"*, Proceedings of IEEE International Conference on Acoustics, Speech, and Signal Processing, Vol.4, 2004, pp. 1037-1040.

[38] Nee R., Prasad R., *"OFDM for wireless multimedia communications"*, Artech House Publishers, 2000.

[39] Muller H. S., Huber J.B., *"A novel peak power reduction scheme for OFDM"*, Proc. of the Int. Symposium on Personal, Indoor and Mobile Radio Communications PIMRC'97, September 1997, pp. 1090-1094.

[40] WA5VJB, LP8565, http://www.wa5vjb.com/pcb-pdfs/LP8565.pdf.

[41] Ettus Research USRP B100, https://www.ettus.com/content/files/07495_Ettus_B100_DS_Flyer_HR.pdf.

[42] Kuhne Electronic KU PA 242 TX, http://shop.kuhne-electronic.de/kuhne/en/.

[43] Fujitsu FMC1616L1015, http://www.rf-microwave.com/datasheets/4255_Fujitsu_FMC1616L1015_01.pdf.

[44] OvisLink corp. Airlive WPA-2400IG, http://www.airlive.com/products/WPA-2400IG/wpa_2400ig.shtml.

[45] Hassan Z., Vahid T.V., *"Analytical EVM, BER, and TD performances of the OFDM systems in the presence of jointly nonlinear distortion and IQ imbalance"*, Ann. Telecommun. (2009), May 2009, pp. 753-762.

Vorrei ringraziare tutti coloro che mi hanno seguito nello svolgimento della tesi, aiutandomi a raggiungere questo importante traguardo, e coloro che hanno riposto fiducia in me.

Ringrazio il Professor Filippo Giannetti, per la sua disponibilità, i suoi consigli e per l'indispensabile aiuto fornitomi durante il lavoro di tesi.

Ringrazio la mia famiglia, per avermi permesso di raggiungere questo importante risultato e per la fiducia incondizionata che hanno avuto nei miei confronti.

Ringrazio Ivan per il suo aiuto e per il sostegno che mi ha dato anche e soprattutto nei momenti più difficili, e con lui tutti i miei amici.

Un grazie infine a Vincenzo per il tempo che mi ha dedicato durante il lavoro svolto per questa tesi.